



universität
wien

DIPLOMARBEIT

Titel der Diplomarbeit

**„Illuminating the gut: Design and application of
fluorescence *in situ* hybridization probes targeting health
state-associated intestinal bacteria for quantification and
single cell analysis“**

Verfasser

Jochen Reichert

angestrebter akademischer Grad

Magister der Naturwissenschaften (Mag. rer. nat.)

Studienkennzahl lt. Studienblatt:	A441
Studienrichtung lt. Studienblatt:	Genetik - Mikrobiologie
Betreuer/Betreuerin:	Prof. Dr. Michael Wagner

Wien, 2012

Table of Contents

A Introduction.....	1
A.1 Fluorescence in situ hybridization.....	1
A.2 Shifts in microbial community upon induced colitis.....	2
A.3 Nano secondary ion mass spectrometry.....	3
A.4 Aims of this study.....	5
B Materials and Methods.....	7
B.1 Materials.....	7
B.1.1 Chemicals.....	7
B.1.2 Disposable items.....	7
B.1.3 Software.....	8
B.1.4 Technical equipment.....	9
B.1.5 Buffers.....	10
B.1.6 Probes.....	11
B.2 Methods.....	13
B.2.1 Fluorescence in situ hybridization.....	13
B.2.2 FISH analysis.....	14
B.2.2.1 Analysis of formamide series.....	14
B.2.2.2 Quantification.....	14
B.2.3 Design and optimization of probes.....	15
B.2.3.1 Optimization of probe Akk1437 targeting Akkermansia spp.....	15
B.2.3.2 Design of 16S rRNA-targeted FISH probes.....	15
B.2.4 Sampling, fixation and FISH of samples from colitis development at different time points.....	16
B.2.4.1 Comparative analysis on healthy and DSS-treated mice concerning distinct microbial community members (Trial A).....	16
B.2.4.2 Detection of bacterial shifts in colitis development and multiple colitis induction (Trial C and G).....	17
B.2.5 FISH and NanoSIMS.....	20
B.2.5.1 Stable isotope labeling of mice colon.....	20
B.2.5.2 Preparation of London resin (LR)-White sections.....	20
B.2.5.3 Si (Silicon) wafer pieces vs. ITO (Indium tin oxide) coated glass slides.....	21
B.2.5.4 FISH on wafers for NanoSIMS.....	21
B.2.5.5 Recording images and marking samples with the LMD for NanoSIMS.....	21

B.2.5.6 Performance of LR-White: FISH signal intensity and re-use of sections.....	22
C Results.....	23
C.1 Design and optimization of probes.....	23
C.1.1 Akkermansia spp. (Probe Akk1437).....	23
C.1.2 Design and evaluation of 16S rRNA-targeted FISH probes.....	24
C.1.2.1 Probes for identification of members of the genus Mucispirillum (Probe Mcs487 and Mcs547).....	26
C.1.2.2 Evaluation of the probe Dsp158 targeting Desulfovibrio piger.....	27
C.1.2.3 Lachnospiraceae OTU_11021 (Probes Ctl11021a-1127 and Ctl11021b-1448).....	28
C.1.2.4 Lachnospiraceae OTU_9468 (Probe DSS9468a-999 and DSS9468b-1259).....	30
C.1.2.5 Bacteroides OTU_9164 (Probe 9164a-1000 and 9164b-177).....	32
C.1.2.6 Ruminococcaceae OTU_5807 (Probe 5807a-431, 5807b-986 and 5807c-1202).....	35
C.2 Abundance of specific gut bacteria in healthy and DSS-treated mice.....	41
C.2.1 Akkermansia muciniphila.....	41
C.2.2 Mucispirillum schaedleri.....	42
C.2.3 Lachnospiraceae OTU_11021	43
C.2.4 Lachnospiraceae OTU_9468.....	44
C.3 Comparison of bacterial shifts in colitis development.....	44
C.4 Preparation of LR-White embedded samples for NanoSIMS analysis.....	53
C.4.1 Preparation and recording of sections from LR-White on CLSM and LMD.....	53
C.4.2 Preparation of whole cell samples on NanoSIMS wafers.....	59
C.4.3 Performance of LR-White: FISH signal intensity and re-use of sections.....	61
D Discussion.....	65
D.1 Design and optimization of probes.....	65
D.1.1 Akkermansia spp. (Probe AKK1437).....	65
D.1.2 16S rRNA-targeted FISH probes for Mucispirillum schaedleri.....	65
D.1.3 Desulfovibrio piger (Probe Dsp158).....	66
D.1.4 Lachnospiraceae OTU_11021 (Probes Ctl11021a-1127 and Ctl11021b-1448).....	66
D.1.5 Lachnospiraceae OTU_9468 (Probe DSS9468a-999 and DSS9468b-1259).....	67
D.1.6 Bacteroides OTU_9164 (Probe 9164a-1000 and 9164b-177).....	67
D.1.7 Ruminococcaceae OTU_5807 (Probe 5807a-431, 5807b-986 and 5807c-1202).....	67
D.2 Abundance of specific gut bacteria in healthy and DSS-treated mice.....	68
D.3 LR-White sections for NanoSIMS analysis.....	70
D.3.1 FISH signal intensity and re-hybridization capacity of LR-White sections.....	71
E Summary.....	73

E.1 Zusammenfassung.....	75
F Appendix.....	77
F.1 IRMS sample preparation.....	85
F.1.1 Chemicals used.....	85
F.1.2 Disposable items.....	85
F.1.3 Technical Equipment.....	86
F.1.4 Buffers and solutions.....	86
F.1.5 Isopycnic fractionation of secreted mucosa (Davies and Carlstedt, 2000).....	88
F.1.6 SDS-PAGE.....	88
F.1.7 Trypsin digest.....	88
F.1.7.1 Destaining of gel.....	88
F.1.7.2 Reduction and Alcylation.....	88
F.1.7.3 Trypsin Gold digest.....	89
F.1.8 Preparation for IRMS.....	89
F.2 Creating a 16S-rRNA amplicon library for 454-pyrosequencing.....	94
F.2.1 Chemicals and disposable items.....	94
F.2.2 Technical equipment.....	95
F.2.3 Buffers and solutions.....	95
F.2.4 Extraction and Purification Procedure for RNA and DNA (adapted from Griffiths et al., 2000).....	97
F.2.5 Amplification of 16S rRNA-genes via 2-step bcPCR (Berry et al., 2011).....	98
G List of abbreviations.....	107
H References.....	113
I Acknowledgement.....	121
J Curriculum Vitae.....	123

A Introduction

A.1 Fluorescence *in situ* hybridization

Fluorescence *in situ* hybridization (FISH) is an identification method for microorganisms. It is not dependent on cultivation, which is error-prone and leads to false microbial patterns in environmental samples (Schleifer, 2004). Only a small percentage of bacteria is cultivable. Using cultivation methods results in some microorganisms showing a higher relative abundance in the environmental sample and consequently causing a wrong impression of the microbial composition (Staley and Konopka, 1985). Cultivable microorganisms only show a viable state and do not undergo cell division (Roszak and Colwell, 1987). The instant use of a sample without cultivation allows a more detailed and realistic analysis and also targets organisms, which cannot be cultured *in vitro*.

FISH (DeLong et al., 1989) is a method for phylogenetic identification of microorganisms in environmental samples (Amann et al., 1995). It has become a widespread and popular method due to its straight-forward, culture-independent and quick protocol. What is more, it allows direct identification of microorganisms in environmental samples by microscopy. FISH can detect eukaryotes as well as bacterial 16S and 23S rRNA by using complementary 5'-fluorescent dye labeled oligonucleotides probes with a typical length of 15 to 25 nucleotides (Wagner et al., 2003). Bacterial cells in environmental samples are fixed with paraformaldehyde (PFA) or ethanol and hybridized with fluorescently-labeled probes, which have different characteristics in forming a stable duplex with their complementary rRNA. The stability of this duplex is dependent on the stringency of the hybridization. Hybridization stringency can be adjusted by changing the temperature, the formamide concentration or the salt concentration. rRNA is highly abundant in microbial cells. It consists of highly conserved and highly variable regions and can be used as an evolutionary marker (Ludwig et al., 1998). Being a central part of protein synthesis in cells, rRNA is present in all domains of life and less affected by horizontal gene transfers or environmental changes. rRNA is a perfect candidate to serve as a phylogenetic fingerprint to identify microorganisms (Rossello-Mora and Amann, 2001) but is limited to differentiate between strains of one species (Daims et al., 2005). The huge amount of data for 16S rRNA sequences makes it possible to design proper

oligonucleotide probes *in silico* in order to detect the desired target organism. For this purpose the software ARB is used as a commonly used tool that is updated regularly (Ludwig et al., 2004). A probe cannot be designed without knowledge of the 16S rRNA sequence, database entries have to be created by modern sequencing techniques by using the full cycle 16S rRNA approach (Amann et al., 1995). With this approach, database entries increase exponentially each year and enable new insights in the diversity of bacteria, that are not cultivable and only known by their 16S rRNA sequence (Fry, 2000).

A.2 Shifts in microbial community upon induced colitis

The mammalian gut is a nutrient-rich habitat for many bacteria and can be seen as an ecosystem cooperating with its surrounding, the host. This interaction is mostly beneficial for both partners (Backhed et al., 2007). It is regulated by the mucosal epithelial tissue and immune cells (Macdonald et al. 2005). Shifts in this community can lead to an exaggerated immune response in the intestinal lumen and in further consequences to severe diseases, such as inflammatory bowel disease (IBD) (Braun, Wei, 2007). Studies including patients with IBD showed a change in microbial community (Reiff and Kelly, 2010) and that microorganisms play an important role in colitis development (Dianda et al., 1997) (Kühn et al., 1993) (Sartor, 2004) (Egan et al., 2004) (Xavier and Podolsky, 2007).

Most of known facts are derived from animal models. Inflammation can be induced and controlled (Strober et al., 2002) (Elson et al., 2005) (Nell et al., 2010) by orally administering dextran sodium sulfate (DSS) (Okayasu et al 1990). DSS salt is a polyanionic derivative of dextran. It causes severe inflammation, manifested by shortened colons in mice (Lee et al., 2010) and also increases the expression of the proinflammatory cytokines, IL-1 β , TNF- α and IL-6, in the colon (Romagnani et al., 1997) (Johansson et al., 2010) (Kitakima et al., 1999) (Mueller and Macpherson 2006). In further studies, sequencing results from 16S rRNA clone libraries derived from DSS-treated mice revealed a shift in the composition of the microbial community and decreased species variety (Nagalingam et al 2011).

A.3 Nano secondary ion mass spectrometry

Nano secondary ion mass spectrometry is a mass-spectrometry based topochemical analysis instrument. It enables semi-quantitative, element specific or isotope selective analysis of a solid sample at high spatial resolution. Under ultra high vacuum (UHV, $p < 1\text{E-}9$ mbar), atoms from one to three atomic layers are ejected from the sample through bombardment by the highly energetic primary ion beam and $<5\%$ are ionized, which can be analyzed by means of an electrostatic field and reduces the thickness of the sample by several nm (Kuypers and Jorgensen, 2007). The primary ion beam features a depth resolution of 10 nm and its lateral resolution is under standard operating conditions 75-100 nm, but can be focused down to 35 nm. Parameters for sensitivity are the ionization yield of the secondary ion species, which is in further case affected by the sample topography) and the transmission of the spectrometer. Depending on the analyzed element, the detection limit can vary from ppt (e.g. Na or F) to far beyond ppm level.

The use of multiple detector screens enables detection of up to seven secondary ion species from which isotope deviation maps and elemental distribution images can be obtained. Isotope deviation maps rely on the variation of the secondary ion intensity distribution of two distinct isotopic species. The maximum number of isotope deviation maps by using seven detector screens is 3. For elemental distribution images the maximum number is 6, since one species is required for normalization. With a lateral resolution of 50 x 50 nm, detailed images of single cells and their relative elemental or isotopic composition can be made.

Incorporation of isotopes in cells can be used to detect a further uptake and a possible distribution of isotope labeled substrate within the microbial community (Wagner, 2009). FISH can be used for phylogenetic identification of microorganisms (Orphan et al., 2001) in addition to analysis of the atomic composition by using NanoSIMS. SIMS *in situ* hybridization (SIMSISH) or enhanced labeling elemental FISH (EL-FISH) enable the simultaneous analysis by the use of halogen labeled probes (Li et al., 2008) In case of EL-FISH halogen (fluorine or bromine) labeled tyramides are used (Behrens et al., 2008) (Musat et al. 2008) as SIMS is highly sensitive towards halogens if primary ions formed by ionization of highly electropositive elements, such as Cs, are applied. This halogen needs to be rarely abundant in samples to obtain minimal natural background. However, if samples show a high halogen background and halogen labeled probes do not work in FISH, the combination of fluorescence microscopy and subsequent SIMS on the same field of view is preferable.

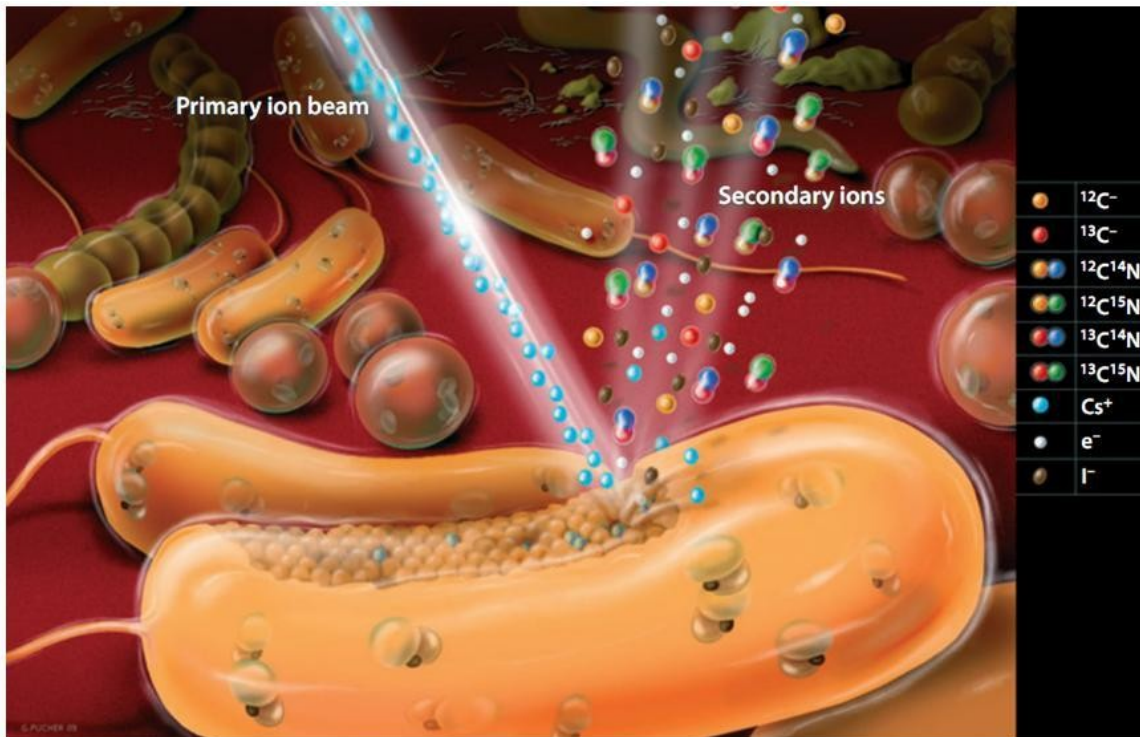


Figure A.1. The principle of NanoSIMS. Primary ion beam sputters the cell and produces secondary ions, which are analyzed via mass spectrometry. Figure by Gerhard Pucher (Wagner, 2009).

A.4 Aims of this study

One of the main aims of this study was the design and optimization of probes detecting *Ruminococcaceae*, *Bacteroidaceae*, *Enterobacteriaceae*, *Deferribacteraceae*, and *Verrucomicrobiaceae* and re-evaluation of the probe Akk1437, which targets *Akkermansia muciniphila* (Derrien et al., 2008). These probes were used for quantitative analysis in DSS-treated STAT1^{-/-}, Tyk2^{-/-} and wild type (wt) C57BL/6 mice (Meraz et al., 1996) to detect shifts in the microbial community and confirm possible indicators of DSS-induced colitis. Tyk2^{-/-} is responsible for signaling interferons by viral or bacterial infection (Decker et al., 2005) and can be crucial in acute murine colitis (Bandyopadhyay et al., 2008).

In addition to the design of probes, a comprehensive list of already designed and evaluated FISH probes targeting members of the gut microbiota was compiled based on published peer-reviewed literature.

Another main aim was to improve the combination of FISH and NanoSIMS and include sections from colon embedded in LR-White-Resin. This study deals with sample preparation, adherence to sample carriers, properties of this resin concerning signal intensities and probe uptake in FISH compared to whole cell samples. For further spectrometric analysis, multiple use of sample carriers was required and methods to mark the spot of particular interest had to be developed.

In addition to the primary aims, two supplementary projects were completed: (1) a library of bacterial 16S rRNA cDNA amplicons for 454 pyrosequencing was prepared using 2-step bcPCR (Berry et al., 2011) for a more detailed phylogenetic analysis of the microbial community, and (2). mucosa proteins from mice were purified and prepared for isotope-ratio mass spectrometry (IRMS) to detect an uptake of injected ¹⁵N- and ¹³C-labeled threonine into epithelial tissue. Possible mucin degraders, such as *Akkermansia muciniphila*, feed from ¹⁵N- and ¹³C-labeled mucus and can be analyzed on NanoSIMS.

B Materials and Methods

B.1 Materials

B.1.1 Chemicals

Table B.1. Chemicals used

Chemicals	Manufacturer
	Biozym Scientific GmbH, Hessisch Oldendorf, Germany
Agarose	
Citifluor AF1	Agar Scientific Ltd., Stansted, UK
Disodiumhydrogenphosphate (Na_2HPO_4)	Carl Roth GmbH & Co., Karlsruhe, Germany
Ethanol, absolute (EtOH)	Merck KGaA, Darmstadt, Germany
Ethylenediamine-tetraaceticacid (EDTA)	Carl Roth GmbH & Co., Karlsruhe, Germany
Formamide deionized (FA)	Carl Roth GmbH & Co., Karlsruhe, Germany
Hydrochloric acid 37% (w/w) (HCl)	Carl Roth GmbH & Co., Karlsruhe, Germany
Isopropanol (2-propanol)	Carl Roth GmbH & Co., Karlsruhe, Germany
LR (London Resin)-White, Hard	Ing.-Büro für Prozesstechnik und instr. Analytik, Unterföhring, Germany
Paraformaldehyde (PFA) 37%	Carl Roth GmbH & Co., Karlsruhe, Germany
Sodium chloride (NaCl)	Carl Roth GmbH & Co., Karlsruhe, Germany
Sodium dihydrogen phosphate (NaH_2PO_4)	Carl Roth GmbH & Co., Karlsruhe, Germany
Sodium dodecyl sulfate (SDS)	Carl Roth GmbH & Co., Karlsruhe, Germany
Sodium hydroxide (NaOH)	Carl Roth GmbH & Co., Karlsruhe, Germany
Tris	Carl Roth GmbH & Co., Karlsruhe, Germany

B.1.2 Disposable items

Table B.2. Disposable items used

Disposable item	Manufacturer
	Marienfeld Laboratory Glassware, Lauda-Königshofen, Germany
Cover glasses 24 x 60 mm	

Eppendorf reaction tubes, various sizes	Eppendorf AG, Hamburg, Germany
Glass strips, 400 x 25 x 6,4 mm	Leica Microsystems GmbH, Wetzlar, Germany
Greiner tubes 50 ml	Greiner Bio-One GmbH, Frickenhausen, Germany
Pipette tips (various sizes)	Carl Roth GmbH & Co. KG, Karlsruhe, Germany
PCR tubes (0.2 ml)	Biozym Scientific GmbH, Hessisch Oldendorf, Germany
SafeSeal-Tips® Premium (various sizes)	Biozym Scientific GmbH, Hessisch Oldendorf, Germany
Teflon coated microscope slides, 10 wells	Marienfeld Laboratory Glassware, Lauda-Königshofen, Germany

B.1.3 Software

Table B.3. Software used

Software	Manufacturer / Reference
ARB software-package	http://www.arb-home.de/ (Ludwig et al., 2004)
Axio Vision 4.8	Carl Zeiss Microimaging GmbH, Jena, Germany
DAIME	(Daims et al., 2006)
GNU Image Manipulation Program (GIMP)	http://www.gimp.org/ (Kimball et al., 2010)
LSM Image Browser	Carl Zeiss Microimaging GmbH, Jena, Germany
OpenOffice.org 3.2	http://www.openoffice.org/welcome/credits
probeBase	http://www.microbial-ecology.net/probebase/ (Loy et al., 2003)

probeCheck	http://www.microbial-ecology.net/probecheck/ (Loy et al., 2008)
Ribosomal Database Project	http://rdp.cme.msu.edu/ (Cole et al., 2003)
SigmaPlot 11.0	Systat Software Inc., Chicago IL, USA

B.1.4 Technical equipment

Table B.4. Technical equipment used

Instrument	Manufacturer
Boron doped 8" silicon wafer platelets, <100>, SSP, 0,1 – 0,3 Ω m, 7 x 7 mm	Active Business Company GmbH, München, Germany
Centrifuge 5804 R	Eppendorf AG, Hamburg, Germany
Confocal Laser Scanning Microscope LSM 510 Meta	Carl Zeiss MicroImaging GmbH, Jena, Germany
DC10 Thermo waterbath	Haake, Karlsruhe, Germany
Eppendorf research pipettes 1 – 1000 μ l	Eppendorf AG, Hamburg, Germany
GFL Typ 1004 waterbath	Gesellschaft für Labortechnik GmbH, Burgwedel, Germany
Hybridisation oven UE-500	Memmert GmbH, Schwabach, Germany
ITO coated float glass slides (7 Ω /sq.), 7,1 x 7,1 x 1,1 mm	Präzisions Glas & Optik GmbH, Iserlohn, Germany
Laser micro dissection LMD 7000	Leica Microsystems GmbH, Wetzlar, Germany
Leica EM KMR3 glass knifemaker	Leica Microsystems GmbH, Wetzlar, Germany
MILLI-Q water purification system	Millipore GmbH, Vienna, Austria
Minicentrifuge Galaxy Mini	VWR, Darmstadt, Germany
NanoSIMS 50L	CAMECA, Gennevilliers Cedex, France
OHAUS Analytical Plus balance	Ohaus Corporation, Pine Brook, NJ, USA
pH-Meter WTW inoLab Level 1	Wissenschaftlich-Technische Werkstätten

	GmbH, Weilheim, Germany
PocketBloc® Thermomixer	Biozym Scientific GmbH, Hessisch Oldendorf, Germany
Sartorius BL 3100 balance	Sartorius AG, Göttingen, Germany
Ultracut Microtome	Reichert-Jung Optische Werke AG, Austria
Ultrasonic Cleaner SC100T	VWR International, Leuven, Belgium
Variomag Maxi magnetic stirrer	Variomag, Dayton Beach, FL, USA
Vortex Genie 2	Scientific Industries, New York, USA

B.1.5 Buffers

Table B.5. Phosphate buffered saline (PBS) stock solution 10x. pH was adjusted to 7,2 with HCl and NaOH and autoclaved.

Ingredient	Concentration	Quantity
NaH ₂ PO ₄	200 mM	35,6 g/l
Na ₂ HPO ₄	200 mM	27,6 g/l

Table B.6. 1x Phosphate buffered saline (PBS) with pH of 7,2. Pure culture strains used

Ingredient	Concentration	Quantity
NaCl	130 mM	7,6 g
PBS stock solution	10 mM	50 ml
MQ		ad 1000 ml

Table B.7. Organisms used

Name	DSM No.	Fixation
<i>Akkermansia muciniphila</i>	22959	PFA
<i>Desulfovibrio piger</i>	749	PFA
<i>Mucispirillum schaedleri</i>		PFA

B.1.6 Probes

The following table shows all probes used in this study as well as fluorescence dyes for FISH-oligonucleotide probes.

Table B.8. List of probes used in this study

Probe name	Specificity	Sequence (5' - 3')	Formamide [%] ²	Reference
EUB338I ¹		GCTGCCTCCCGTAGGAGT	0-50	Amann et al. 1990
EUB338II ¹	all <i>Bacteria</i>	GCAGCCACCCGTAGGTGT	0-50	Daims et al. 1999
EUB338III ¹		GCTGCCACCCGTAGGTGT	0-50	Daims et al. 1999
NonEUB	Complementary to EUBI	ACTCCTACGGGAGGCAGC	0-50	Wallner et al. 1993
Akk1437	<i>Akkermansia</i> spp.	CCTTGCGGTTGGCTTCAGAT	25-35 [30]	Derrien et al. 2008
MCS487	<i>Mucispirillum</i> spp.	GCCGGGGCTGCTTATACAGGT	25-35 [30]	this study
MCS547	<i>Mucispirillum</i> spp.	CAGTCACTCCGAACAACGCT	25-35 [30]	this study
Bac303	most <i>Bacteroidaceae</i>	CCAATGTGGGGGACCTT	10	Manz et al., 1996
Dsp158	<i>Desulfovibrio piger</i>	CCACCCUCUCCCGGAUUC	30-35 [30]	this study
Ctl11021a-1127	<i>Lachnospiraceae</i> OTU_11021	TTCCCATCTTTCTTGCTGGC	30	this study
Ctl11021b-1448	<i>Lachnospiraceae</i> OTU_11021	GCAGCTCCCTCCTCTCGG	30	this study
DSS9468a-999	<i>Lachnospiraceae</i> OTU_9468	CTTTGCCCATACGGCGTCCG	10	this study
DSS9468b-1259	<i>Lachnospiraceae</i> OTU_9468	TGCTCAACGTCACCGTCTCG	10	this study
Erec482	<i>Eubacterium rectale</i> , <i>Clostridium</i> <i>coccoides</i>	GCTTCTTAGTCARGTACCG	0	Franks et al., 1998
9164a-1000	<i>Bacteroides</i> OTU_9164	AACATGTTTCCACATTATTCAGG	25	this study
9164b-177	<i>Bacteroides</i> OTU_9164	CATGCGGTAGGACTATGACATCG	25	this study

5807a-431	<i>Ruminococcaceae</i> OTU_5807	TTATCGTCCCCCTCCACAGAGGT	25	this study
5807b-986	<i>Ruminococcaceae</i> OTU_5807	CCTTTCACTCGATGTCAAGACC	25-30 [30]	this study
5807c-1202	<i>Ruminococcaceae</i> OTU_5807	AGCCCGGGTCATAAAGGGCATG	25-35	this study

¹ EUBmix: EUBI, II and III were combined to produce a general bacterial probe mixture at equimolar concentrations. The final concentration was 8 pmol/μl for the FLUOS-labeled and 5 pmol/μl for the CY3-labeled and CY5-labeled probes.

² Formamide concentration with high stringency. Values in brackets show the formamide concentration used for FISH analysis in this study.

Table B.9. Fluorescence dyes for oligonucleotides used for FISH.

Fluorescence Dye	Absorption maxima [nm]	Emission maxima [nm]	Molar factor of extinction ϵ [1/mol x cm]
FLUOS	494	518	$7,5 \times 10^4$
CY3	554	570	$1,3 \times 10^5$
CY5	650	667	2×10^5

All fluorescence-labeled probes were ordered HPLC-purified and freeze-dried from Thermo Scientific, Germany. A mother stock was created by diluting the freeze-dried probe with MQ to a concentration of 100 pmol/μl. Working stocks were diluted to a final concentration of 5 pmol/μl and stored at -20 °C.

B.2 Methods

B.2.1 Fluorescence in situ hybridization

For immobilization, 1 μ l of sample was pipetted on each well and dehydrated by dipping the slide into 50%, 80% and 96% ethanol for three minutes each. Next the dried samples were hybridized by adding 10 μ l hybridization buffer and 1 μ l of each probe and put into a hybridization chamber for 90 minutes at 46 °C. This chamber was made by folding a paper towel soaked up with hybridization buffer put into a 50 ml conical centrifuge tube. Meanwhile a tube with Milli-Q water (MQ) was cooled on ice and all wash buffers were preheated in a water bath to 48 °C. After hybridization the slides were transferred under the fume hood into the preheated wash buffer and put into the water bath for 10 minutes. This treatment was followed by the slides being dipped into ice-cold MQ for approximately three seconds and dried under an air-jet. All slides were stored in a box impermeable to light at -20 °C. For analysis on the confocal laser microscope (CLSM) the slides were embedded with CitiFluor.

Table B.10. Hybridization buffer for FISH

FA [%]	0	10	20	25	30	35	40	50	60
NaCL 5M [μ l]	180	180	180	180	180	180	180	180	180
Tris Hcl 1M pH 8 [μ l]	20	20	20	20	20	20	20	20	20
MQ [μ l]	800	700	600	550	500	450	400	300	200
FA [μ l]	0	100	200	250	300	350	400	500	600
SDS 10% [μ l]	1	1	1	1	1	1	1	1	1

Table B.11. Wash buffer for FISH

FA [%]	0	10	20	25	30	35	40	50	60
NaCL 5M [ml]	9	4,5	2,15	1,49	1,02	0,7	0,46	0,18	0,04
Tris Hcl 1M pH 8 [ml]	1	1	1	1	1	1	1	1	1
EDTA 0,5 M [ml]	0	0	0,5	0,5	0,5	0,5	0,5	0,5	0,5
MQ [μ l]	ad 50	ad 50	ad 50	ad 50	ad 50	ad 50	ad 50	ad 50	ad 50

B.2.2 FISH analysis

Hybridized slides were analyzed with a confocal laser scanning microscope (CLSM) (Carl Zeiss GmbH, Germany) and corresponding software Axio Vision 4.8 (Carl Zeiss GmbH, Germany). The microscope was equipped with an Ar-laser (430-514 nm) for excitation of the FLUOS-dyes and two He-Ne-lasers (543 nm and 633 nm) for excitation of CY3 and CY5. Pictures were recorded with a 63x Plan-Neoflar objective. The pinhole size was set to 1 μm and resolution of all images was 1024 x 1024 pixels with a depth of 12 bits. A digital zoom was not used. The images were exported in tiff format, which is a requirement for the software DAIME.

B.2.2.1 Analysis of formamide series

In case of formamide series, all laser settings (amplifier offset, amplifier gain and detector gain) for recording refer to the fluorescence intensity at 10% formamide and remained static for whole series. A total cell count of 100-500 cells was recorded per formamide concentration. Samples were diluted to avoid clustering of bacteria. The mean intensities for each used formamide concentration (0, 10, 20, 25, 30, 35, 40, 50 and 60%) were calculated with DAIME, exported as text file (.txt) and transferred to SigmaPlot 11.0. For proper visualization a sigmoid curve was added to each graph with its function $y=f(x)$:

$$y = \frac{a}{1 + e^{-\left(\frac{x - x_0}{b}\right)}}$$

Parameters a, b, x_0 and e refer to the difference between minimum asymptote and maximum asymptote, the slope, the inflection point (center) and Euler's number.

B.2.2.2 Quantification

For quantification of desired bacteria compared to the total cell count, 3-5 images per environmental sample were taken randomly and analyzed with DAIME (Daims et al., 2006). To calculate the abundance of specific bacteria it is necessary to exclude autofluorescence background from analysis, which was done with the tool 'Object editor' for each fluorescence dye. With the tool 'Biovolume fraction' raw data was exported as a text file and transferred into OpenOffice Spreadsheet to calculate intensities, mean intensities and standard deviations

in order to plot them in SigmaPlot.

B.2.3 Design and optimization of probes

B.2.3.1 Optimization of probe Akk1437 targeting *Akkermansia* spp.

The probe Akk1437 is an already designed probe (Derrien et al., 2008) and the optimal formamide concentration is described to be 20%. A formamide series as described in B.2.2.1 with a pure culture of *Akkermansia muciniphila* (DSM No. 22959) was performed to re-evaluate this probe and analyzed as described above.

B.2.3.2 Design of 16S rRNA-targeted FISH probes

For a proper analysis of the gut microbiota from inflamed tissue over a period of time, it is necessary to detect specific bacteria. Probes were designed *in silico*, by using the non-redundant ARB-SILVA database version 102Ref (<http://www.arb-silva.de/documentation/background/release-102/>) in ARB (Ludwig et al., 2004) and probeCheck (Loy et al., 2008). To detect the genus *Mucispirillum* probe Mcs487 was designed and ordered in CY3 and Mcs547 in CY5 and evaluated by using a formamide series on a PFA-fixed pure culture. Slides were analyzed as described above.

Data from 454 pyrosequencing of cDNA from a previous study (Berry et al., 2012) revealed, that some operational taxonomic units (OTUs) can be correlated with colitis development. An OTU describes a data set under examination, in our case a species-level designation. Probes Ctl11021a-1127 and Ctl11021b-1448 were designed to aim for the specific operational taxonomic unit OTU_11021 and DSS9468a-999 and DSS9468b-1259 target the OTU_9468. Ctl11021a-1127 and DSS9468a-999 were 5'-FLUOS-labeled and Ctl11021b-1448 and DSS9468b-1259 had a 5'-CY3-label. For each OTU, both designed probes were applied together to obtain overlapping targets. Both, OTU_11021 and OTU_9468, are member of the genus *Lachnospiraceae*. For further analysis probes targeting *Ruminococcaceae* OTU_5807 and *Bacteroides* OTU_9164 were designed and evaluated as described above.

For OTU_5807 two probes were necessary to target the desired OTU, but three – 5807a-431, 5807b-986 and 5807c-1202 – were designed and used to evaluate the best combination of two probes with highest intensities. 5807a-431 was 5'-FLUOS-labeled, whereas 5807b-986 features a CY5-label and 5807c-1202 a CY3-label on the 5'-end. Both probes 9164a-1000 and

9164b-177 also have to be applied together to obtain overlapping targets. 9164a-1000 was 5'-FLUOS- and 9164b-177 5'-CY5-labeled.

For the formamide series, probes were hybridized with mouse gut samples, which were enriched in this specific target OTU due to sequencing data (Berry et al., 2012). For evaluation of the probes targeting *Lachnospiraceae* OTU_11021 the healthy wild type mouse gut sample A6 and for *Lachnospiraceae* OTU_9468 sample A13 from a DSS-treated STAT1^{-/-} mouse was used. For probes targeting *Bacteroides* OTU_9164 sample C8 and for *Ruminococcaceae* OTU_5807 sample C14 were hybridized. Both samples C8 and C14 are from DSS-treated wt mice.

B.2.4 Sampling, fixation and FISH of samples from colitis development at different time points

B.2.4.1 Comparative analysis on healthy and DSS-treated mice concerning distinct microbial community members (Trial A)

Wt and STAT1^{-/-} mice were nourished with 2% dextran sodium sulfate (DSS, MP Biomedicals) for 7 days and sacrificed to obtain the colon and cecum. The intestine were flushed with sterile, anoxic PBS to ensure that each sample represents the whole microbial community in the mouse gut. Samples were frozen for DNA extraction or fixed in 2% PFA overnight at 4 °C and then stored in 70% ethanol / 30% PBS at -20 °C for FISH analysis. All samples were hybridized with the probes Akk1437, Mcs487 and Mcs547 to detect *Akkermansia* spp. respectively *Mucispirillum* spp.. Probes Ctl11021a-1127/Ctl11021b-1448 and DSS9468a-999/DSS9468b-1259 were also used to quantify the abundance of OTU_11021 and OTU_9468.

Table B.12. Overview of sample IDs with relevant genotypes and treatment details.

Sample ID	Genotype	Treatment	Sample ID	Genotype	Treatment
A1	C57BL/6	DSS	A11	C57BL/6 STAT1 ^{-/-}	DSS
A2	C57BL/6	DSS	A12	C57BL/6 STAT1 ^{-/-}	DSS
A3	C57BL/6	DSS	A13	C57BL/6 STAT1 ^{-/-}	DSS
A4	C57BL/6	DSS	A14	C57BL/6 STAT1 ^{-/-}	DSS

Sample ID	Genotype	Treatment	Sample ID	Genotype	Treatment
A5	C57BL/6	DSS	A15	C57BL/6 STAT1 ^{-/-}	DSS
A6	C57BL/6	Water	A16	C57BL/6 STAT1 ^{-/-}	Water
A7	C57BL/6	Water	A17	C57BL/6 STAT1 ^{-/-}	Water
A8	C57BL/6	Water	A18	C57BL/6 STAT1 ^{-/-}	Water
A9	C57BL/6	Water	A19	C57BL/6 STAT1 ^{-/-}	Water
A10	C57BL/6	Water	A20	C57BL/6 STAT1 ^{-/-}	Water

B.2.4.2 Detection of bacterial shifts in colitis development and multiple colitis induction (Trial C and G)

In additional experiments wt and Tyk2^{-/-} mice were treated as described previously, but samples were taken at time points 0, 2, 3, 4 and 7 (Trial C). In a second cohort of mice 2% DSS was given for seven days followed by a recovery step with DSS-free drinking water (Trial G). As mice recovered a second DSS-treatment was performed and mice recovered again for a third cycle of DSS induced colitis. Samples were taken as described above at time points 0, 14, 33 and 58. They were hybridized with probes specific for *Akkermansia* spp. (Akk1437), *Mucispirillum* spp. (Mcs487/Mcs547), *Lachnospiraceae* OTU_11021 (Ct11021a-1127/Ct11021b-1448) and OTU_9468 (DSS9468a-999/DSS9468b-1259), *Bacteroides* OTU_9164 (9164a-1000/9164b-177) and *Ruminococcaceae* OTU_5807 (5807a-431/5807c-1202) and FISH images were quantified as specified above.

Table B.13. Overview of sample IDs from colitis development (Trial C) relevant to genotypes and days of treatment.

Sample ID	Genotype	Treatment	Sample day
C1	C57BL/6 wt	Control	0
C2	C57BL/6 wt	Control	0
C3	C57BL/6 wt	Control	0
C4	C57BL/6 wt	DSS	2
C5	C57BL/6 wt	DSS	2
C6	C57BL/6 wt	DSS	2
C7	C57BL/6 wt	DSS	3
C8	C57BL/6 wt	DSS	3
C9	C57BL/6 wt	DSS	3

Sample ID	Genotype	Treatment	Sample day
C10	C57BL/6 wt	DSS	4
C11	C57BL/6 wt	DSS	4
C12	C57BL/6 wt	DSS	4
C13	C57BL/6 wt	DSS	7
C14	C57BL/6 wt	DSS	7
C15	C57BL/6 wt	DSS	7
C16	C57BL/6 Tyk2 ^{-/-}	Control	0
C17	C57BL/6 Tyk2 ^{-/-}	Control	0
C18	C57BL/6 Tyk2 ^{-/-}	Control	0
C19	C57BL/6 Tyk2 ^{-/-}	DSS	2
C20	C57BL/6 Tyk2 ^{-/-}	DSS	2
C21	C57BL/6 Tyk2 ^{-/-}	DSS	2
C22	C57BL/6 Tyk2 ^{-/-}	DSS	3
C23	C57BL/6 Tyk2 ^{-/-}	DSS	3
C24	C57BL/6 Tyk2 ^{-/-}	DSS	3
C25	C57BL/6 Tyk2 ^{-/-}	DSS	4
C26	C57BL/6 Tyk2 ^{-/-}	DSS	4
C27	C57BL/6 Tyk2 ^{-/-}	DSS	4
C28	C57BL/6 Tyk2 ^{-/-}	DSS	7
C29	C57BL/6 Tyk2 ^{-/-}	DSS	7
C30	C57BL/6 Tyk2 ^{-/-}	DSS	7

Table B.14. Overview of sample IDs from multiple colitis induction (Trial G).

Sample ID	Genotype	Treatment	Sample day
G1	C57BL/6 wt	Control	0
G2	C57BL/6 wt	Control	0
G3	C57BL/6 wt	Control	0
G10	C57BL/6 wt	DSS	14
G11	C57BL/6 wt	DSS	14
G12	C57BL/6 wt	DSS	14
G19	C57BL/6 wt	DSS	33
G20	C57BL/6 wt	DSS	33
G21	C57BL/6 wt	DSS	33
G27	C57BL/6 wt	DSS	58
G28	C57BL/6 wt	DSS	58

Sample ID	Genotype	Treatment	Sample day
G29	C57BL/6 wt	DSS	58
G30	C57BL/6 wt	DSS	58
G31	C57BL/6 wt	DSS	58
G32	C57BL/6 wt	Control	58
G33	C57BL/6 wt	Control	58
G34	C57BL/6 wt	Control	58

B.2.5 FISH and NanoSIMS

B.2.5.1 Stable isotope labeling of mice colon

¹⁵N- and ¹³C-labeled threonine was injected into WT and Tyk2^{-/-} mice. Colons were removed upon sacrifice after 0, 2, 3, 4, 6 and 8 hours and embedded in LR-White (see below).

B.2.5.2 Preparation of London resin (LR)-White sections

LR-white (methacrylate) is a monomeric medium with a low viscosity, which allows good infiltration of tissues. The monomers polymerize by anoxic heating, forming a sliceable block. To be able to produce such a block, the tissue has to be dehydrated through an ascending ethanol series and embedded by stepwise increasing the amount of LR-White.

Table B.15. Dehydration and embedding protocol

Treatment	Time
80% EtOH	10 min, 2x
90% EtOH	10 min, 2x
96% EtOH	10 min, 2x
100% EtOH	20 min, 3x
3:1 (EtOH:LR White)	3 h
1:1 (EtOH:LR White)	O/N
1:3 (EtOH:LR White)	O/N
100% LR White	8-16 h, 3x

After infiltration, samples were put in gel caps, making sure to exclude air bubble, and incubated at 50 °C to start polymerization. The gel cap was removed and LR-white, surrounding the sample, was gently removed by cutting thin slices with a standard razor blade. The front of the sample was trimmed to a size of 2-4 mm in square. Sections were cut with glass knives on an Ultracut microtome with a thickness of 0,3 / 0,5 / 0,7 µm and deposited on microscope slides or NanoSIMS sample carriers to test, which thickness is best for usage in NanoSIMS. To attach the section to the slide, 5 µl of PBS containing 0,2% agarose were pipetted onto the sample, removed again with the pipette and dried at 46 °C. All hybridization parameters remain the same as with standard FISH.

B.2.5.3 Si (Silicon) wafer pieces vs. ITO (Indium tin oxide) coated glass slides

Two different sample carriers for use in NanoSIMS, prepared with environmental samples and LR-White sections, were used for further FISH analysis. The Si sample carriers were obtained from a p-type semiconducting wafer that was Boron doped, single crystalline with [100] surface orientation, single-side polished and showed a specific resistivity ρ of 0,1 – 0,3 Ωm . In contrast to Si, which is highly reflective, ITO coated glass slides are transparent due to the use of selected white float glass as substrate for the ITO layer, which features a sheet resistance R_s of 7 Ω/sq at a thickness of 260 nm. To maintain characteristics and avoid corrosion, SiO_2 is used as a passivation layer between glass substrate and ITO coating. For each wafer, 1 μl of liquid sample or a LR-White section with a thickness of 0,5 μm were deposited on the sample carriers and used for FISH.

B.2.5.4 FISH on wafers for NanoSIMS

Before use sample carriers were cleaned with an Ultrasonic Cleaner (VWR International, Leuven, Belgium) for 5 minutes in MQ and dipped in ethanol to remove residual particles. Due to the size of the wafer (7 x 7 mm), a glass slide was inserted into the hybridization chamber and the wafer was put onto it for 1,5-2 hours as with FISH. Washing buffer was filled into small glass vials containing ~ 25 ml and preheated to 48 °C. To transfer the wafer from the hybridization chamber to the washing buffer and from the washing buffer to ice-cold MQ, tweezers were used to handle the specimen.

B.2.5.5 Recording images and marking samples with the LMD for NanoSIMS

For CLSM imaging, the samples were inverted and placed onto a cover slip with a small amount of CitiFluor. Further it was weighted down with a split glass slide, small enough to fit into the specimen tray of the CLSM. The recording setup was as previously described. The Leica LMD has a CCD-camera that can record images from all three used dyes (FLUOS, CY3 and CY5), but only in greyscale. Images were taken with a 40x objective and intensity was set to 30%. Each channel was recorded in greyscale and exported in jpg format. After recording fluorescence images, samples were laser-marked. Laser intensity settings vary for each objective and were given by the software as 'factory settings'. The marked specimen was recorded with Digital Interference Contrast (DIC) and exported as jpg. To create a FISH image, the software GIMP was used. In GIMP, each file was imported as layer, colored in

green, red or blue depending of the dye. To overlay three images, layers were set 'addition' and the resulting image was exported as jpg. Whole cell samples were only recorded on LMD as described above.

B.2.5.6 Performance of LR-White: FISH signal intensity and re-use of sections

Formamide series were performed on LR-white sections and whole cells sample to compare signal intensities and a possible loss of intensity in LR-White. All samples were hybridized with EUBmix in FLUOS, CY3 and CY5 and evaluated as described above. Signal intensities were plotted with SigmaPlot 11.0 and directly compared. Probes from LR-White sections, which were hybridized with 30% formamide, were stripped off by applying preheated formamide:PBS (70:30) for 5 minutes at 60 °C. These sections were hybridized again with the same probes at 30% formamide. Eventually, images were taken, probes stripped off and hybridized a third time for final analysis.

C Results

C.1 Design and optimization of probes

C.1.1 *Akkermansia* spp. (Probe Akk1437)

The idea of re-evaluating this probe was to check, if the described formamide concentration of 20% (Derrien et al., 2008) works well for FISH and whether it can be used for our analyses. A formamide series was performed on a pure culture of *Akkermansia muciniphila* (DSM No. 22959) to monitor the highest signal intensity of this probe. Mean intensities were plotted against formamide concentration and a sigmoid curve visualizes changes of intensities.

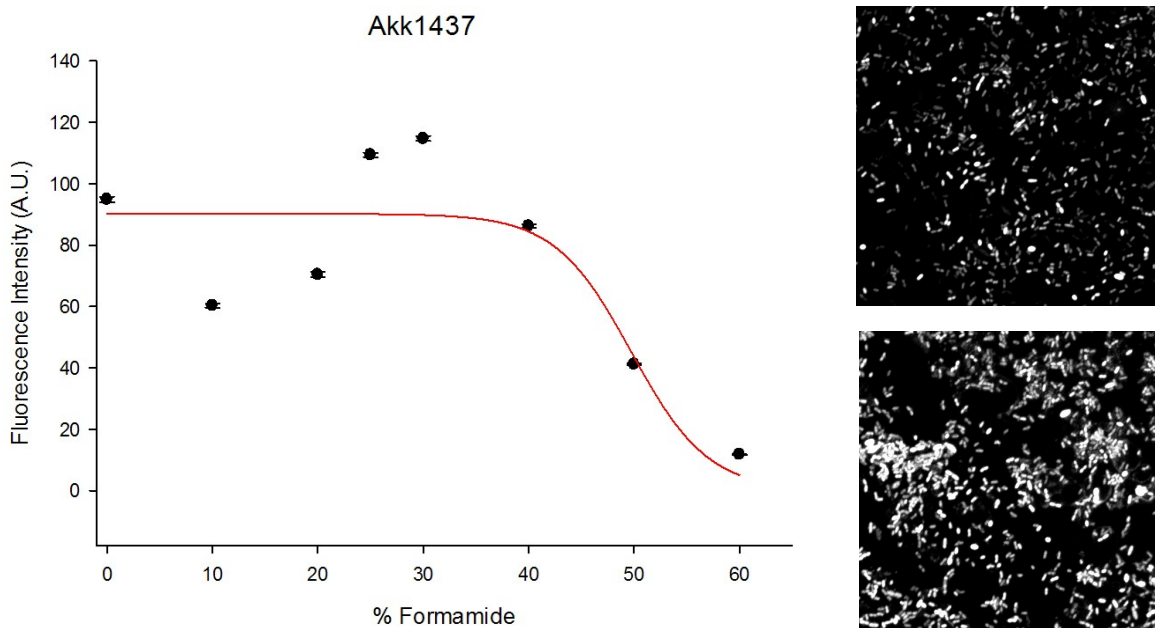


Figure C.1. Formamide curve of the probe Akk1437. The mean fluorescence intensity (y-axis) is plotted against concentration of formamide (x-axis). Black dots represent single data points and black bars show associated standard errors. The red line highlights the sigmoid curve fit. Images on the right show examples for 20% formamide (above) and 30% (below).

The graph describes the stringency of the hybridization due to formamide concentration. At 0% formamide the intensity is much higher than at 10% or 20%. The probe reaches its highest intensity at 30%, afterwards dropping significantly. At 60% almost no signal is detectable. The exemplary images show the higher intensity of using 30% formamide for hybridization compared to 20% (Derrien et al., 2008).

C.1.2 Design and evaluation of 16S rRNA-targeted FISH probes

All probes in this study were designed with the non-redundant ARB-SILVA database version 102Ref (<http://www.arb-silva.de/documentation/background/release-102/>) in ARB (Ludwig et al., 2004) and the free energy for perfect hybrid match ΔG was calculated with probeCheck (<http://www.microbial-ecology.net/probecheck>) (Loy et al., 2008). The full probe name, sequence from 5'-3', coverage and number of non-target hits for each probe are given in table C.1.

Table C.1. 16S rRNA-targeted oligonucleotide probes for fluorescence in situ hybridization.

Probe name	Full probe name (Alm et al., 1996)	Probe sequence (5' - 3')	Perfectly matched target organisms/ sequences	ΔG : Free energy for perfect match hybrid [kcal/mol] ¹	RDP II probe match ² Coverage	Non- target hits
Mcs487	S-G-Mcs-0487-a-A-21	ACCTGTATAAGCAGCCCCGGC	<i>Mucispirillum schaedleri</i>	-24.81	<i>Mucispirillum</i> 97%	0
Mcs547	S-G-Mcs-0547-a-A-20	AGCGTTGTTCGGAGTGACTG	<i>Mucispirillum schaedleri</i>	-22.39	<i>Mucispirillum</i> 96%	15
Dsp158	S-G-Dsp-0158-a-A-18	CCACCCUCUCCCGGAUUC	<i>Desulfovibrio piger</i>	-20,44	<i>Desulfovibrionaceae</i> 96,6%	15
Ctl11021a-1127	S*-Lsp-1127-a-A-20	TTCCCATCTTTCTTGCTGGC	<i>Lachnospiraceae</i> OTU_11021	-21,23	<i>Lachnospiraceae</i> 95,4%	6

Ctl11021b-1448	S-*-Lsp-1448-a-A-18	GCAGCTCCCTCCTCTCGG	<i>Lachnospiraceae</i> OTU_11021	-21,7	<i>Lachnospiraceae</i> 70,5%	25
DSS9468a-999	S-*-Lsp-999-a-A-20	CTTTGCCCATACGGCGTCCG	<i>Lachnospiraceae</i> OTU_9468	-24,29	<i>Lachnospiraceae</i> 97,6%	2
DSS9468b-1259	S-*-Lsp-1259-a-A-20	TGCTCAACGTCACCGTCTCG	<i>Lachnospiraceae</i> OTU_9468	-23,53	<i>Lachnospiraceae</i> 87,2%	27
9164a-1000	S-*-Bac-1000-a-A-23	AACATGTTTCCACATTATTCAGG	<i>Bacteroides</i> OTU_9164	-21,14	<i>Bacteroides</i> 99,4%	1
9164b-177	S-*-Bac-177-a-A-23	CATGCGGTAGGACTATGACATCG	<i>Bacteroides</i> OTU_9164	-24,23	<i>Bacteroides</i> 100%	
5807a-431	S-*-Rum-431-a-A-23	TTATCGTCCCCCTCCACAGAGGT	<i>Ruminococcaceae</i> OTU_5807	-25,67	<i>Ruminococcaceae</i> 97,00%	2
5807b-986	S-*-Rum-986-a-A-22	CCTTTCACCTCGATGTCAAGACC	<i>Ruminococcaceae</i> OTU_5807	-22,55	<i>Ruminococcaceae</i> 85,70%	3
5807c-1202	S-*-Rum-1202-a-A-22	AGCCCGGGTCATAAAGGGCATG	<i>Ruminococcaceae</i> OTU_5807	-25,57	<i>Ruminococcaceae</i> 71,40%	14

¹ Calculated using the default settings in probeCheck (<http://www.microbial-ecology.net/probecheck>).

² RDP II probe match was performed with database release 10, Update 22 (Aug 30, 2010) containing 1,418,497 bacterial and archaeal 16S rRNA sequences. The search for each probe was restricted to sequences of good quality with data in the respective probe binding region. Coverage is the percentage of sequences within the RDP II target taxon that shows a full match to the probe sequence. The number of non-target hits indicates the total number of sequences outside the respective RDP II target taxon that shows a full match to the probe sequence.

C.1.2.1 Probes for identification of members of the genus *Mucispirillum* (Probe Mcs487 and Mcs547)

Regarding 16S rRNA sequence, the target sites of the probe Mcs487 have a higher similarity (95%) than the probe Mcs547 (84,7%) which is due to 15 outliers in the genus *Leptospirillum*, with a lowest similarity of 73,7%. Both probes applied together make up a genus-level specific probe set within 5% divergence in all sequences. Evaluation of probe Mcs487 revealed that at a concentration of 20% formamide, the obtained signal is at highest intensity and decreases slowly until 35%. At a concentration of 40%, the signal intensity sharply decreases. Probe Mcs547 generally shows the same behavior. In comparison to Mcs487, a much higher signal intensity for all data points was observed.

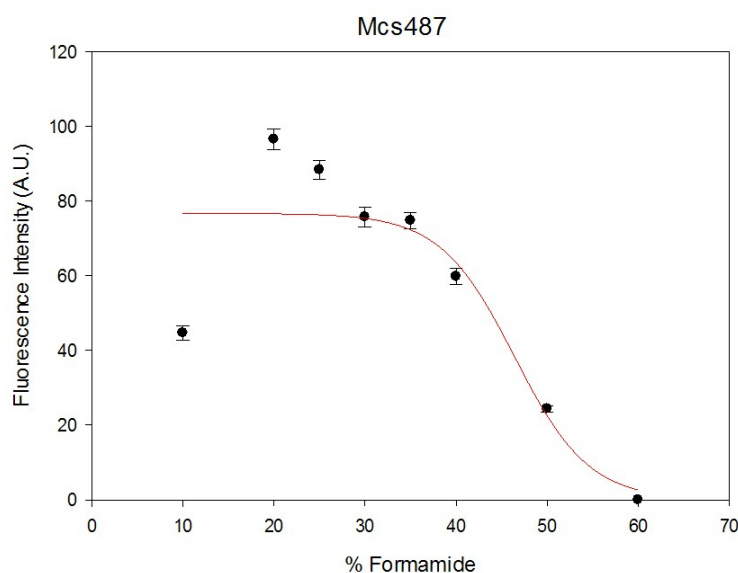


Figure C.2. Formamide curve of probe Mcs487. The mean fluorescence intensity (y-axis) is plotted against concentration of formamide (x-axis). Black dots represent single data points and black bars show associated standard errors. The red line highlights the sigmoid curve fit.

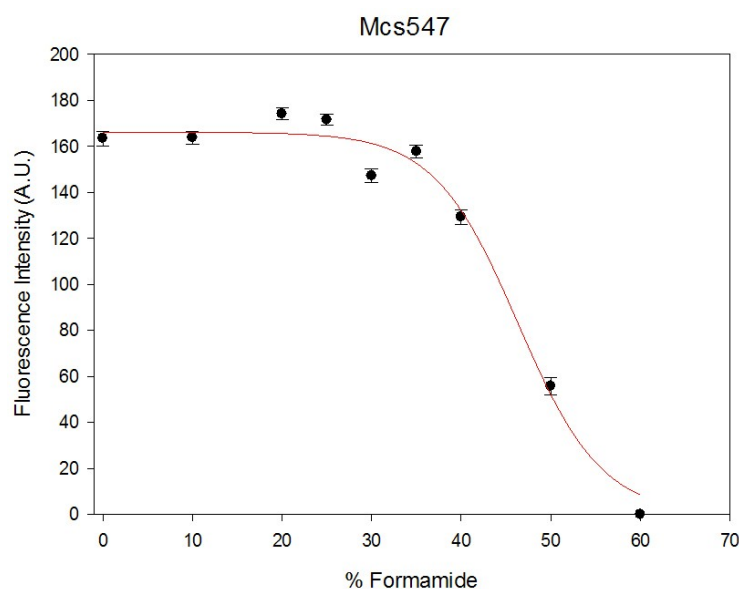


Figure C.2. Formamide curve of probe Mcs547. The mean fluorescence intensity (y-axis) is plotted against concentration of formamide (x-axis). Black dots represent single data points and black bars show associated standard errors. The red line highlights the sigmoid curve fit.

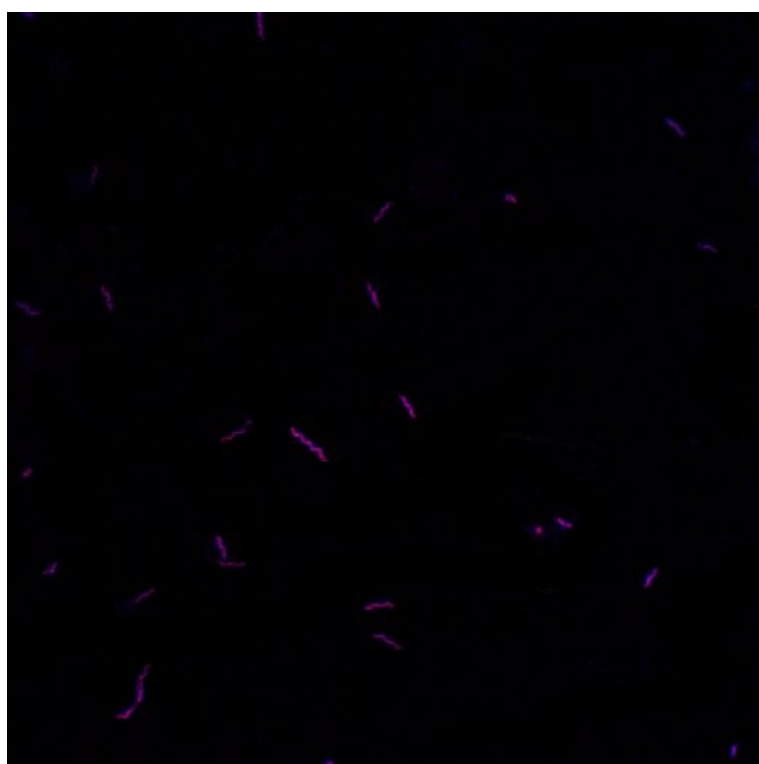


Figure C.4. FISH image recorded on CLSM with 63x objective showing the distinctive spiral-shape of *Mucispirillum schaedleri*.

C.1.2.2 Evaluation of the probe Dsp158 targeting *Desulfovibrio piger*

To detect *Desulfovibrio piger*, design of one probe was sufficient to obtain good signal intensities and discrimination against non-target hits. The sigmoid curve fit in the formamide

curve (Fig. C.5) shows a steady signal intensity up to 50% formamide. Intensities are low below 30% formamide and reached a maximum at this percentage. After having reached this maximum, intensities dropped. Compared to other probes, signal intensities from probe Dsp158 were generally very high and allow a usage from 30% up to 35% formamide.

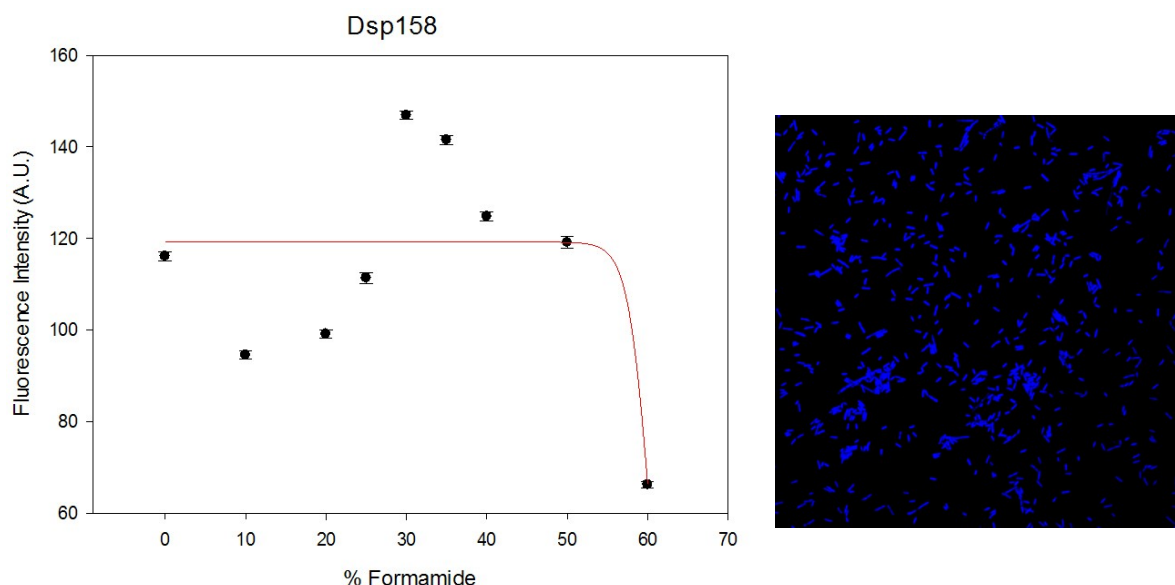


Figure C.5. Formamide curve of probe Dsp158 and exemplary image of a pure culture of *Desulfovibrio piger* hybridized with 30% formamide. The mean fluorescence intensity (y-axis) is plotted against concentration of formamide (x-axis). Black dots represent single data points and black bars show associated standard errors. The red line highlights the sigmoid curve fit.

C.1.2.3 *Lachnospiraceae* OTU_11021 (Probes Ctl11021a-1127 and Ctl11021b-1448)

For detection of the phylotype OTU_11021 from the group *Lachnospiraceae*, two probes were designed which had to be applied together. Overlapping targets of both probes were specific for OTU_11021.

For probe Ctl11021a-1127 a concentration of formamide used in hybridization of 30% had performed best and had given the best intensities in image analysis. At a concentration of 35%, signal intensities sharply decrease (Fig. C.6). Probe Ctl11021b-1448 gave steady signal intensities from 0% up to 35%. Afterwards, signal intensities were good, but simultaneous application of both probes required proper hybridization parameters and intensities for both probes to feature good contrast in images. By comparing images of each formamide concentration, a hybridization using 30% formamide gave the best result.

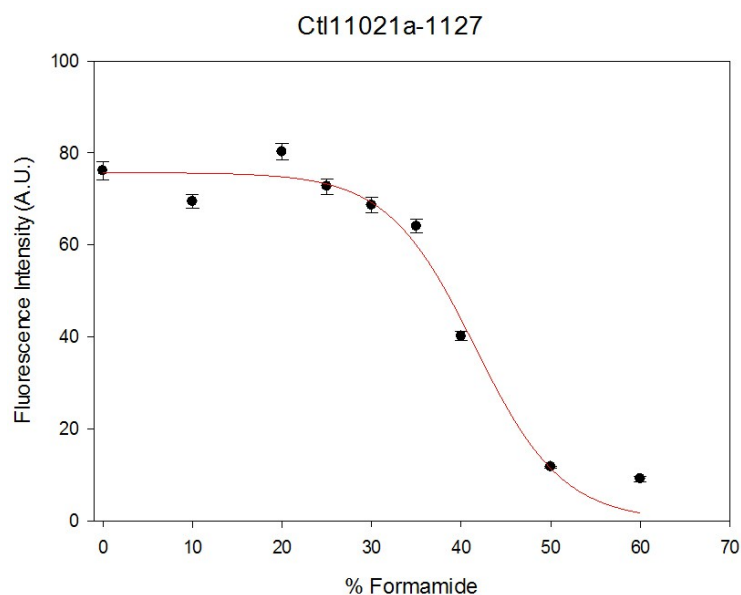


Figure C.6. Formamide curve of probe Ctl11021a-1127. The mean fluorescence intensity (y-axis) is plotted against concentration of formamide (x-axis). Black dots represent single data points and black bars show associated standard errors. The red line highlights the sigmoid curve fit.

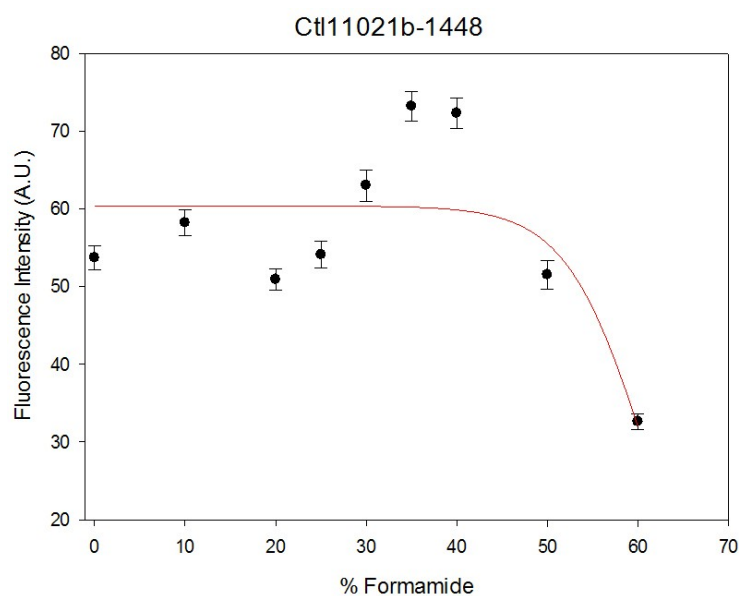


Figure C.7. Formamide curve of probe Ctl11021b-1448. The mean fluorescence intensity (y-axis) is plotted against concentration of formamide (x-axis). Black dots represent single data points and black bars show associated standard errors. The red line highlights the sigmoid curve fit.

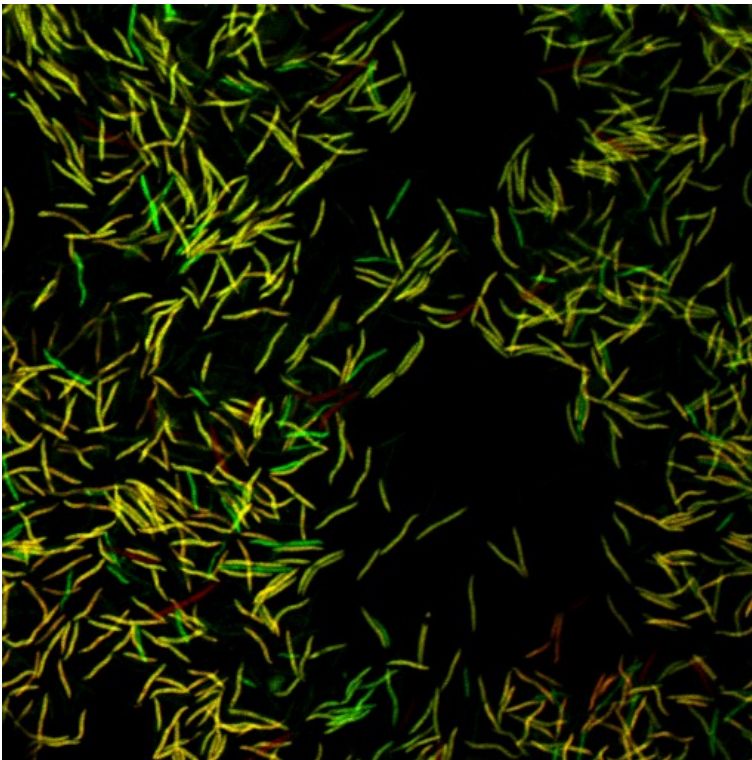


Figure C.8. Exemplary image showing probes Ctl11021a-1127 (shown in red) and Ctl11021b-1448 (shown in green) in FISH at a formamide concentration of 30% in a healthy wt mouse gut sample. Overlapping targets (shown in yellow) represent the desired target OTU_11021.

C.1.2.4 *Lachnospiraceae* OTU_9468 (Probe DSS9468a-999 and DSS9468b-1259)

For detection of the OTU 9468 from the group *Lachnospiraceae*, two overlap of two probes was necessary to specifically target this phylotype.

Probe DSS9468a-999 reached its intensity peak at 10% formamide and after this point signal intensity was lower the more formamide used (Fig. C.9). The second probe DSS9468b-1259 was characteristic in having high signal intensities over a wide range of formamide concentrations (Fig. C.10). Nevertheless, regarding the co-application of both probes, a formamide concentration of 10% gave best signal intensities in overlapping targets for both probes.

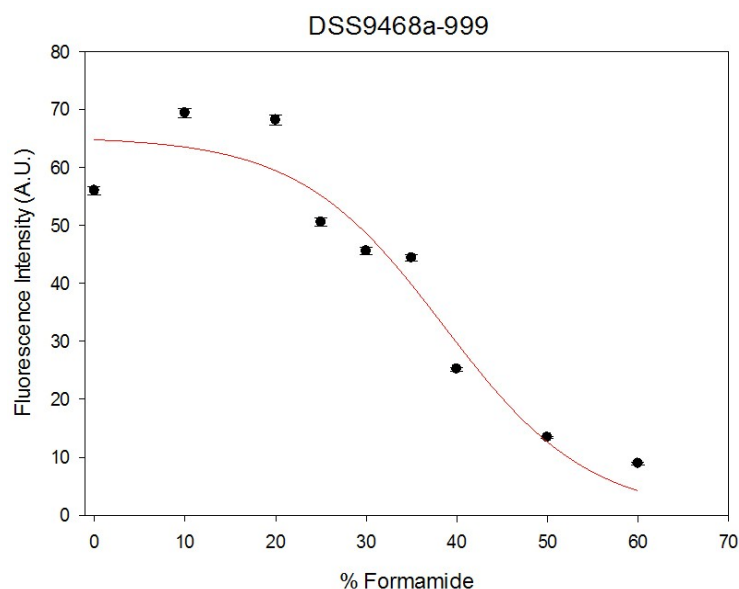


Figure C.9. Formamide curve of probe DSS9468a-999. The mean fluorescence intensity (y-axis) is plotted against concentration of formamide (x-axis). Black dots represent single data points and black bars show associated standard errors. The red line highlights the sigmoid curve fit.

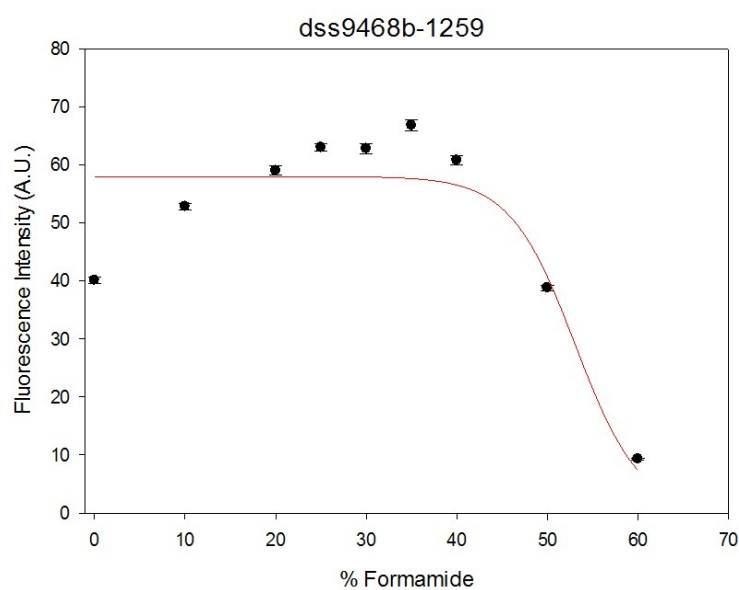


Figure C.10. Formamide curve of probe DSS9468b-1259. The mean fluorescence intensity (y-axis) is plotted against concentration of formamide (x-axis). Black dots represent single data points and black bars show associated standard errors. The red line highlights the sigmoid curve fit.

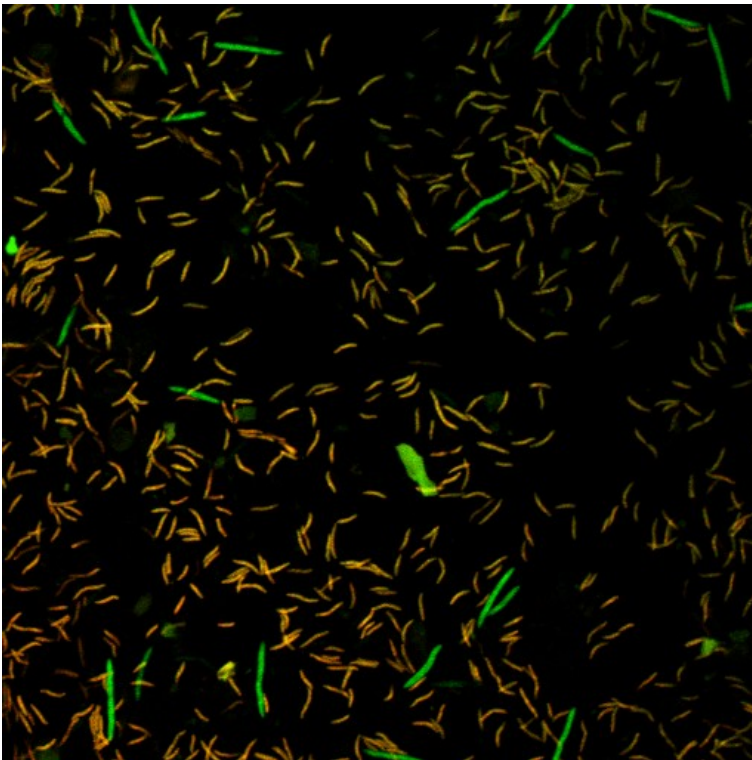


Figure C.11. Exemplary image showing overlapping targets of probes DSS9468a-999 and DSS9468b-1259 (shown in orange) in FISH at a formamide concentration of 10% in a DSS-treated STAT1^{-/-} mouse gut sample. Green signals highlight non-target hits of probe DSS9468b-1259.

C.1.2.5 *Bacteroides* OTU_9164 (Probe 9164a-1000 and 9164b-177)

Here, two probes were designed. Each probe targeted the desired OTU_9164 among several non-target hits, which differ for each probe. In co-application of both probes, overlapping targets were specific for OTU_9164.

Signal intensities of probe 9164a-1000 were highest at 10% formamide and dropped off the more formamide was used (Fig. C.12). Up to 30% formamide, signals were still intense enough to allow analysis. Further, the amount of cells targeted with probe 9164a-1000 remained at a higher level than compared to the abundance of target cells at concentrations of formamide above 30%. When it comes to the amount of target cells, probe 9164b-177 (Fig. C.15) showed the same patterns as probe 9164a-1000, but fluorescence intensities were generally much higher and sharply decreased at 40% formamide (Fig. C.14). Quantification data of target cells showed a steady decrease, the more formamide was used, allowing detection of overlapping targets up to 30% formamide (Fig. C.16). When used both probes a formamide concentration of 25% gave best results in specificity and signal intensities (Fig. C.17).

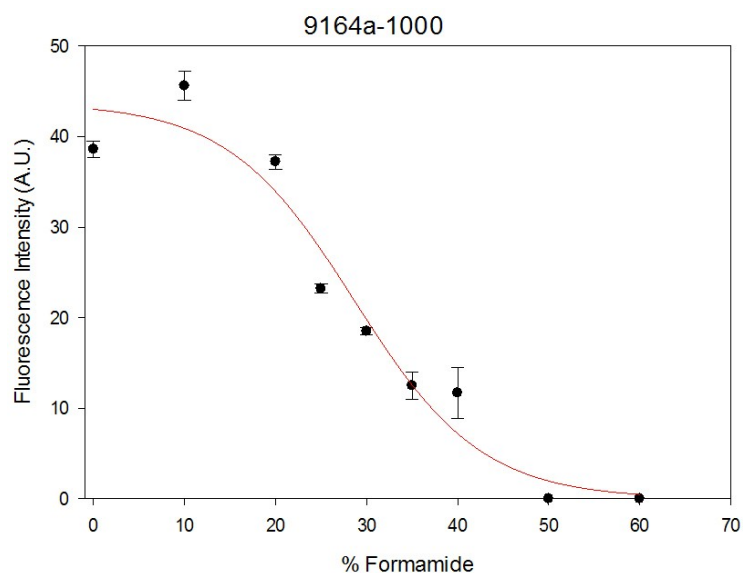


Figure C.12. Formamide curve of probe 9164a-1000. The mean fluorescence intensity (y-axis) is plotted against concentration of formamide (x-axis). Black dots represent single data points and black bars show associated standard errors. The red line highlights the sigmoid curve fit.

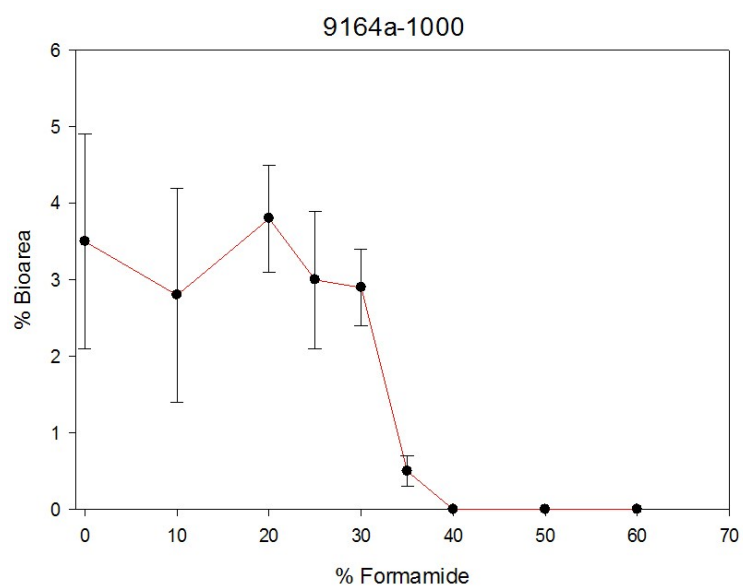


Figure C.13. Abundance of cells targeted by probe 9164a-1000 in a DSS-treated wt mouse gut sample. The percentage of bioarea (y-axis) is plotted against concentration of formamide (x-axis). Black dots represent single data points and black bars show associated standard errors.

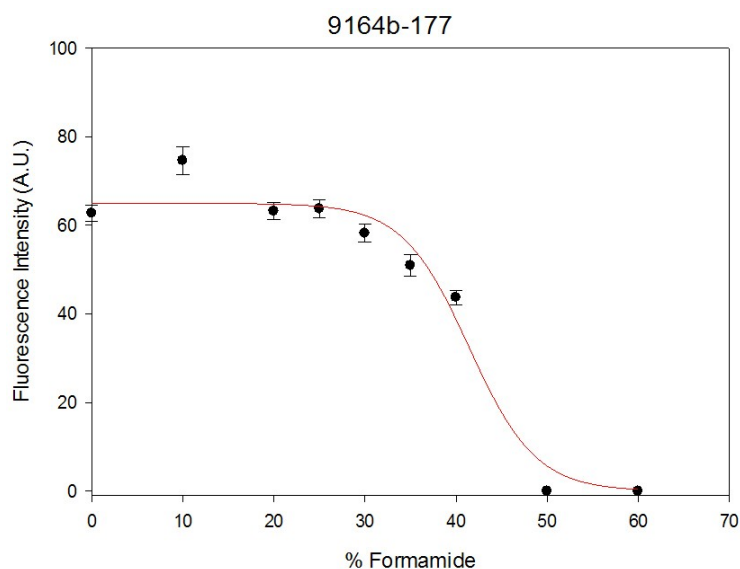


Figure C.14. Formamide curve of probe 9164b-177. The mean fluorescence intensity (y-axis) is plotted against concentration of formamide (x-axis). Black dots represent single data points and black bars show associated standard errors. The red line highlights the sigmoid curve fit.

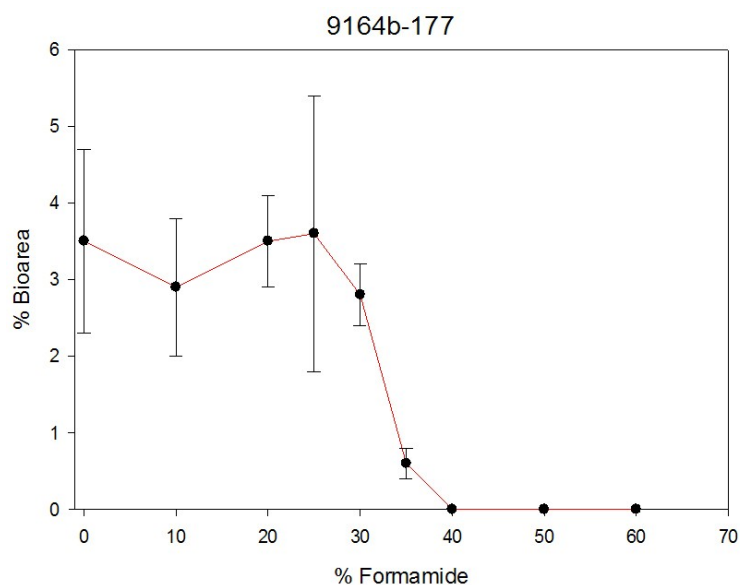


Figure C.15. Amount of cells targeted by probe 9164b-177 in a DSS-treated wt mouse gut sample. The percentage of bioarea (y-axis) is plotted against concentration of formamide (x-axis). Black dots represent single data points and black bars show associated standard errors.

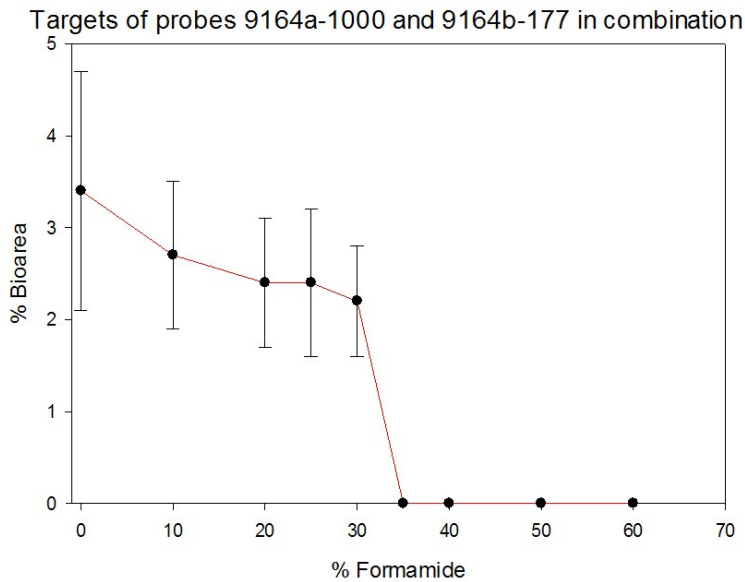


Figure C.16. Amount of overlapping targets detected by co-application of probe 9164a-1000 and 9164b-177 in a DSS-treated wt mouse gut sample. The percentage of bioarea (y-axis) is plotted against concentration of formamide (x-axis). Black dots represent single data points and black bars show associated standard errors.

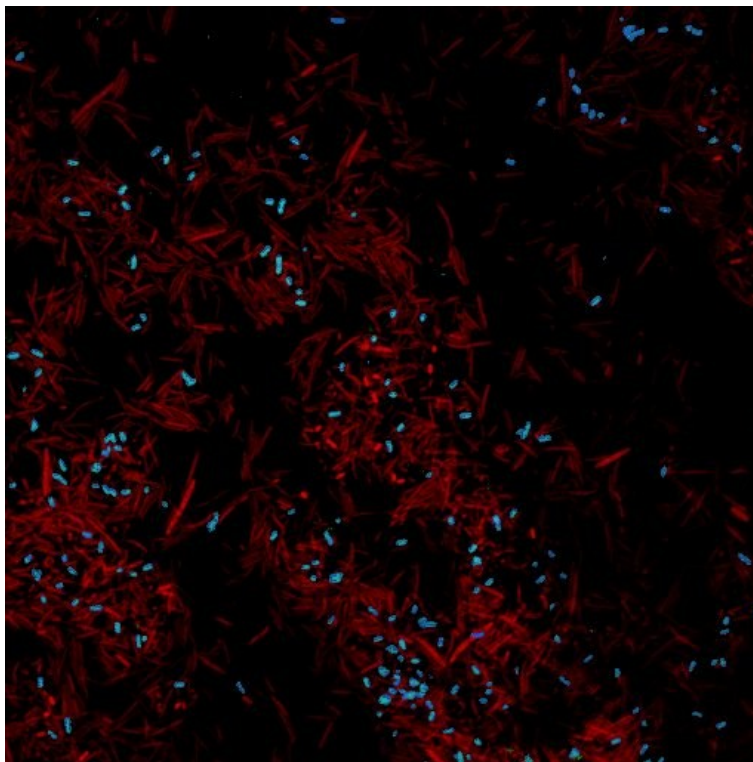


Figure C.17. Exemplary image showing overlapping targets of probes 9164a-1000 and 9164b-177 (shown in cyan) in FISH at a formamide concentration of 25% in a DSS-treated wt mouse gut sample. Red signals highlight all bacteria targeted by EUBmix probe.

C.1.2.6 *Ruminococcaceae* OTU_5807 (Probe 5807a-431, 5807b-986 and 5807c-1202)

For detection of OTU_5807 from the *Ruminococcaceae* three probes were designed and the

intersection of two of the three probes was specific for OTU_5807.

Probe 5807a-431 was always used either in combination with 5807b-986 or with 5807c-1202 to find out, which combination had best signal intensities. When looking at single probes, 5807a-431 had its highest intensity at 25%, afterwards decreasing constantly (Fig. C.18). The amount of targeted cells by this probe stayed at an elevated level up to 25%. By using 35% formamide, the amount of targeted cells decreased by 5% (Fig. C.19). The abundance of cells targeted by probe 5807b-986 slightly decreased from 0% to 35% the more formamide was used. At a concentration of 40% formamide, the amount of targeted cells dropped down from 15% to 10% compared to the data from 35% formamide. Comparing signal intensities, probe 5807b-986 reached its turning point at 20% formamide (Fig. C.21). This resulted in low signal intensities by using more than 20% formamide. However, signal intensities at a formamide concentration of 25% to 30% still allow proper analysis. For probe 5807c-1202 concentrations of formamide of 0% or 10% in hybridization gave no signals and started to increase when used 20% formamide. A concentration ranging from 25% to 40% gave highest signal intensities (Fig. C.22). When used 30% formamide the highest amount of targeted cells was detected, then the percentage of bioarea of targeted cells decreases (Fig. C.23). Due to signal intensities and the amount of targeted cells, combination of probe 5807a-431 and 5807c-1202 worked out best to detect OTU_5807 when using a formamide concentration of 25-35% (Fig. C.25).

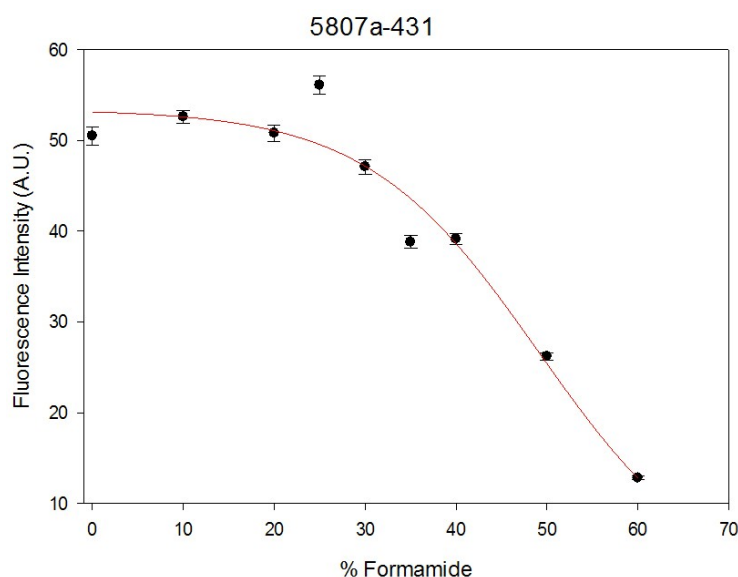


Figure C.18. Formamide curve of probe 5807a-431. The mean fluorescence intensity (y-axis) is plotted against concentration of formamide (x-axis). Black dots represent single data points and black bars show associated standard errors. The red line highlights the sigmoid curve fit.

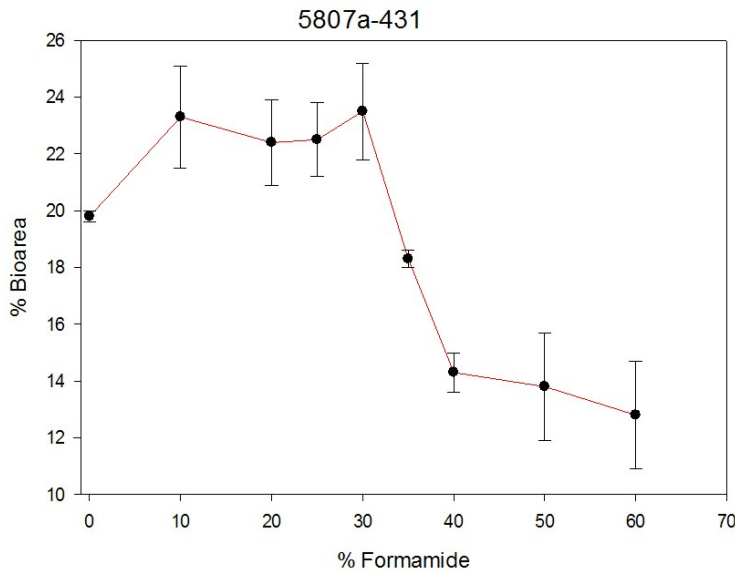


Figure C.19. Amount of cells targeted by probe 5807a-431 in a DSS-treated wt mouse gut sample. The percentage of bioarea (y-axis) is plotted against concentration of formamide (x-axis). Black dots represent single data points and black bars show associated standard errors.

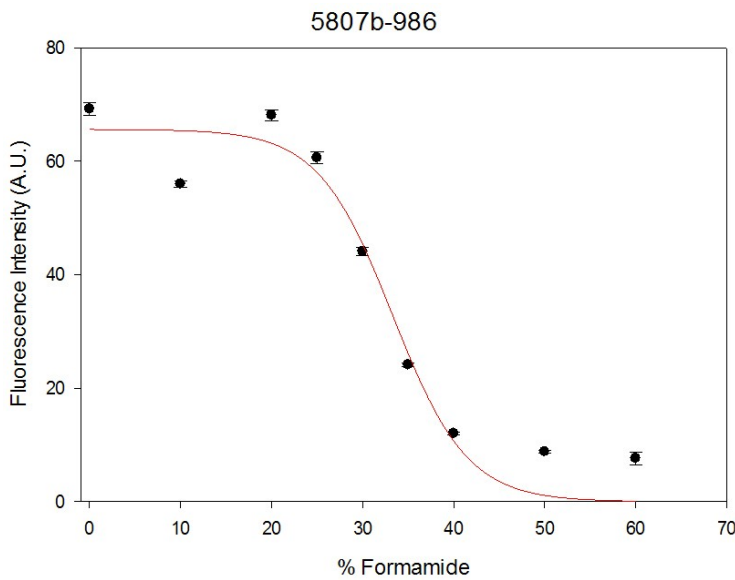


Figure C.20. Formamide curve of probe 5807b-986. The mean fluorescence intensity (y-axis) is plotted against concentration of formamide (x-axis). Black dots represent single data points and black bars show associated standard errors. The red line highlights the sigmoid curve fit.

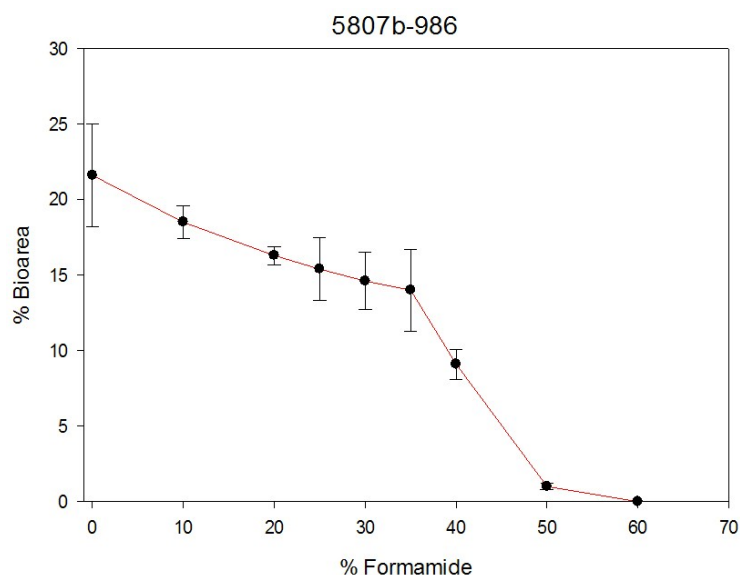


Figure C.21. Amount of cells targeted by probe 5807b-986 in a DSS-treated wt mouse gut sample. The percentage of bioarea (y-axis) is plotted against concentration of formamide (x-axis). Black dots represent single data points and black bars show associated standard errors.

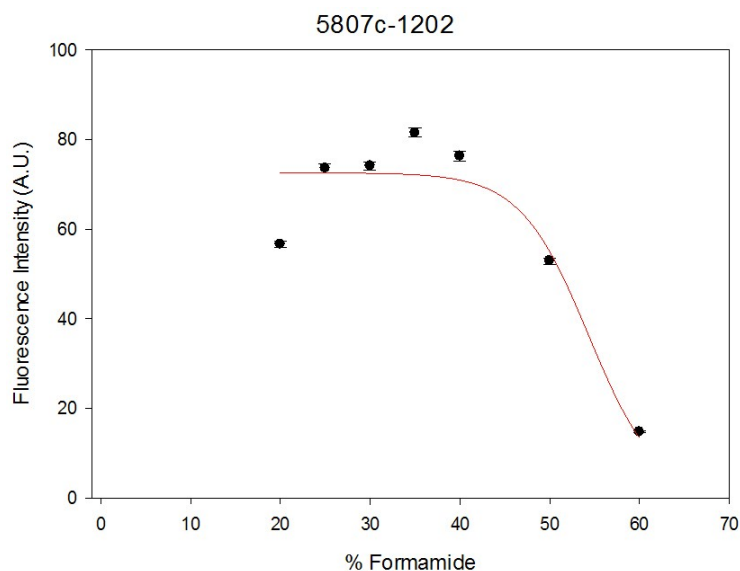


Figure C.22. Formamide curve of probe 5807c-1202. The mean fluorescence intensity (y-axis) is plotted against concentration of formamide (x-axis). Black dots represent single data points and black bars show associated standard errors. The red line highlights the sigmoid curve fit.

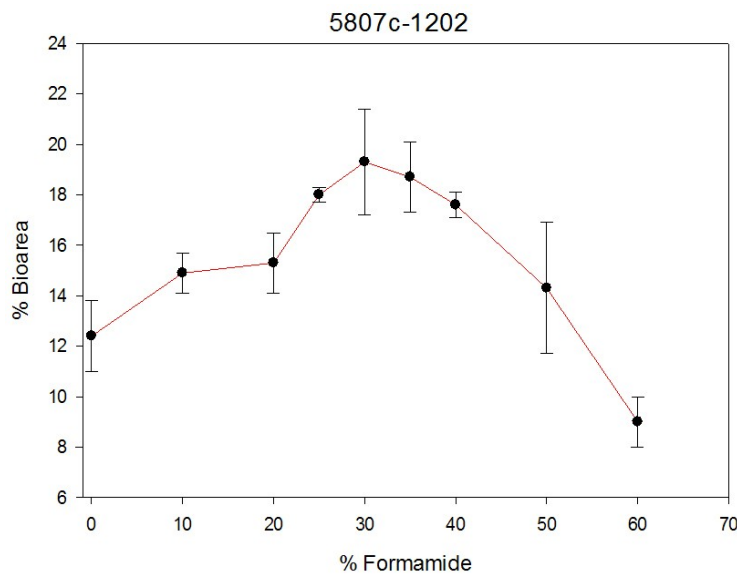


Figure C.23. Amount of cells targeted by probe 5807c-1202 in a DSS-treated wt mouse gut sample. The percentage of bioarea (y-axis) is plotted against concentration of formamide (x-axis). Black dots represent single data points and black bars show associated standard errors.

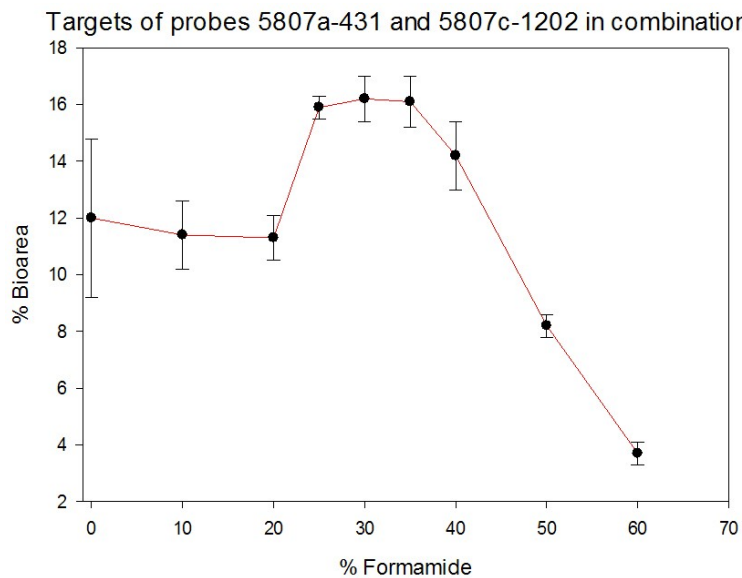


Figure C.24. Amount of overlapping targets detected by co-application of probe 5807a-431 and 5807c-1202 in a DSS-treated wt mouse gut sample. The percentage of bioarea (y-axis) is plotted against concentration of formamide (x-axis). Black dots represent single data points and black bars show associated standard errors.

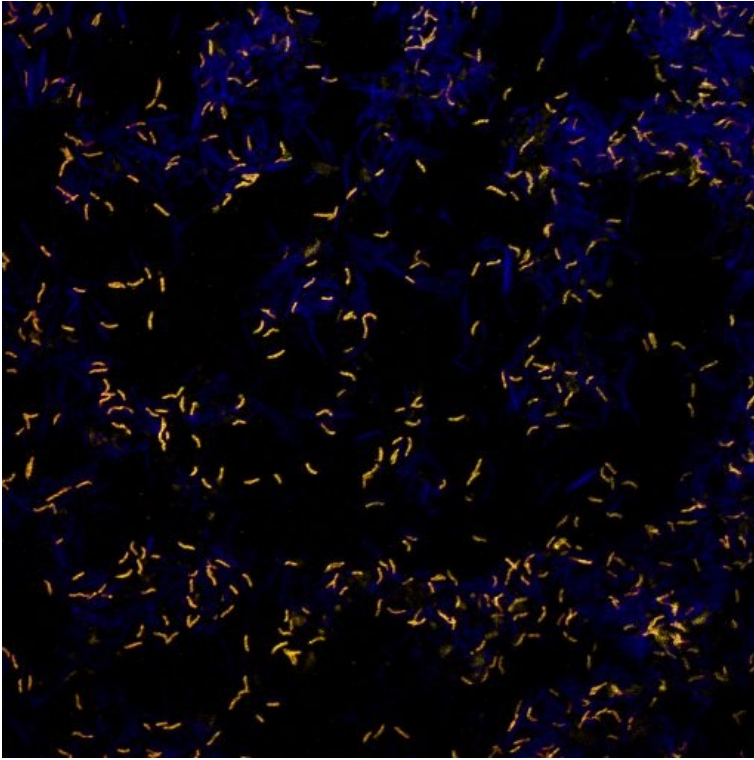


Figure C.25. Exemplary image showing overlapping targets of probes 5807a-431 and 5807c-1202 (shown in yellow) in FISH at a formamide concentration of 25% in a DSS-treated wt mouse gut sample. Blue signals highlight all bacteria targeted by EUBmix probe.

In addition to probe design and evaluation, a comprehensive list of already designed and evaluated probes targeting members of the gut microbiota was compiled. The detailed list of 64 probes is in Appendix A and includes probe names, its specificity and 5'-3' sequence.

C.2 Abundance of specific gut bacteria in healthy and DSS-treated mice

C.2.1 *Akkermansia muciniphila*

Quantification of *Akkermansia muciniphila* in samples taken from healthy and colitic mice showed, that it is only abundant in mice treated with DSS (Fig C.26) independent from their genotype. *Akkermansia muciniphila* was neither in wt controls nor in STAT1^{-/-} controls significantly abundant.

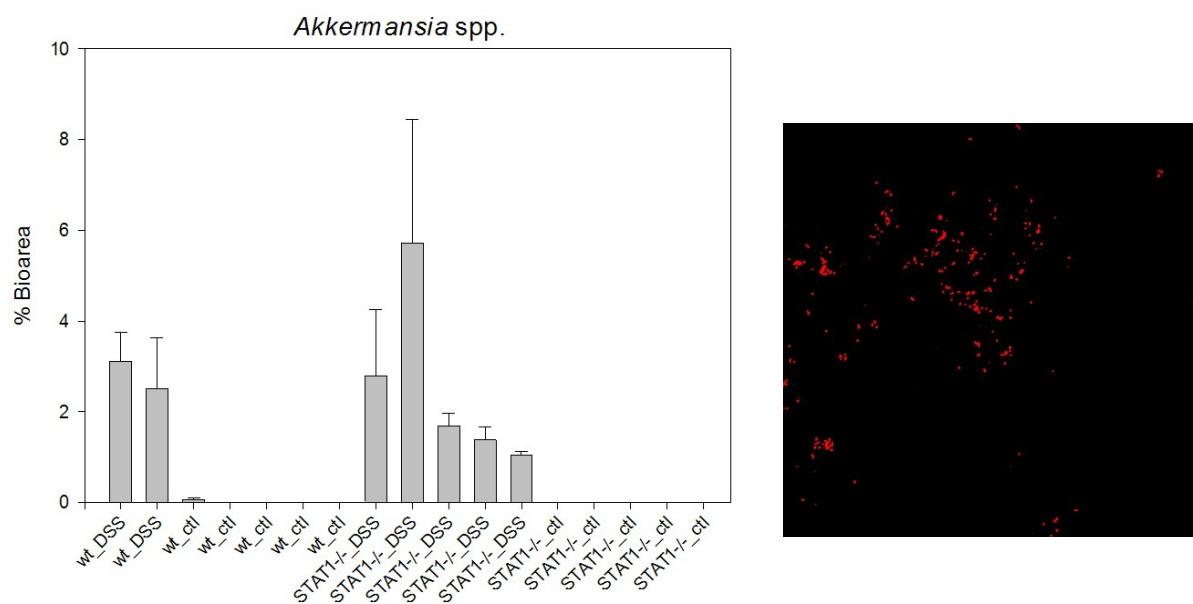


Figure C.26. Abundance of *Akkermansia muciniphila* in samples taken from untreated and DSS-treated wt and STAT1^{-/-} mice. The percentage of bioarea (y-axis) is plotted for each sample ID (x-axis) and shown in box plots with corresponding standard deviation shown as black bars.

C.2.2 *Mucispirillum schaedleri*

Bacteria from the genus *Mucispirillum* spp., targeted by probe Mcs487 and Mcs547, were highly enriched in samples taken from DSS-treated mice, but only in wt. This also accounts for the wt control samples (Fig. C.27), to a much lower percentage though.

The amount of targeted cells in samples from DSS-treated STAT1^{-/-} mice was lower than in samples from DSS-treated wt mice. However, *Mucispirillum schaedleri* was not detectable in healthy STAT1^{-/-} mice samples and two colitic STAT1^{-/-} samples (Fig. C.27).

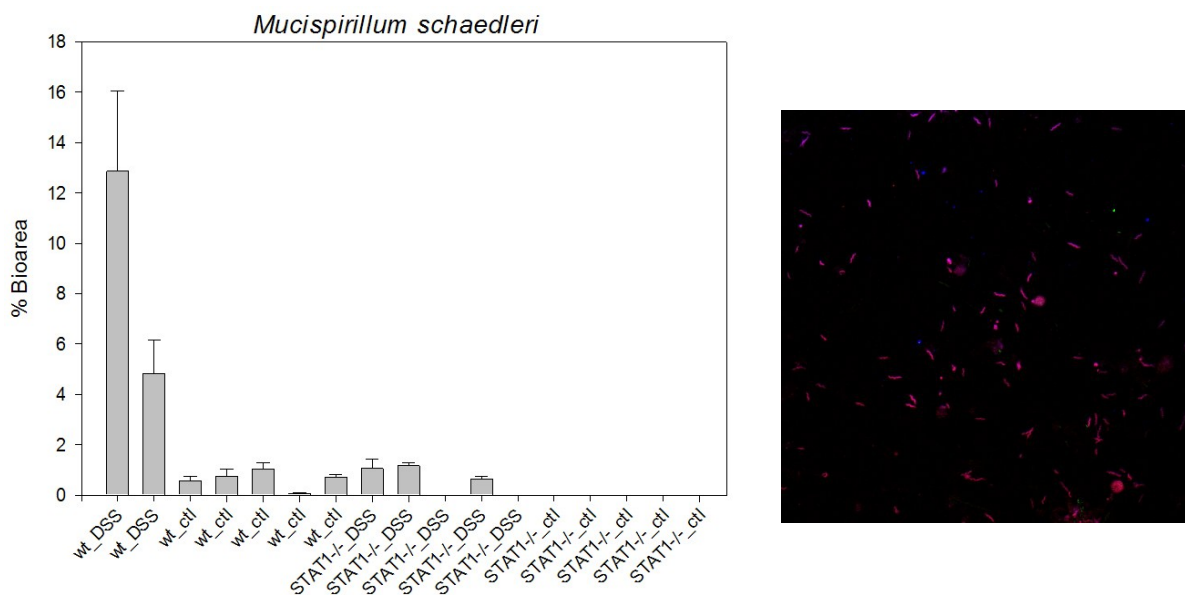


Figure C.27. Abundance of *Mucispirillum schaedleri* in samples taken from untreated and DSS-treated wt and STAT1^{-/-} mice. The percentage of bioarea (y-axis) is plotted for each sample ID (x-axis) and shown in box plots with corresponding standard deviation shown as black bars.

C.2.3 *Lachnospiraceae* OTU_11021

Quantification data of *Lachnospiraceae* OTU_11021 revealed, that this OTU is only abundant to a very high percentage in samples taken from healthy control mice, genotype-independent. No signal was obtained in any sample taken from DSS-treated mice (Fig. C.28).

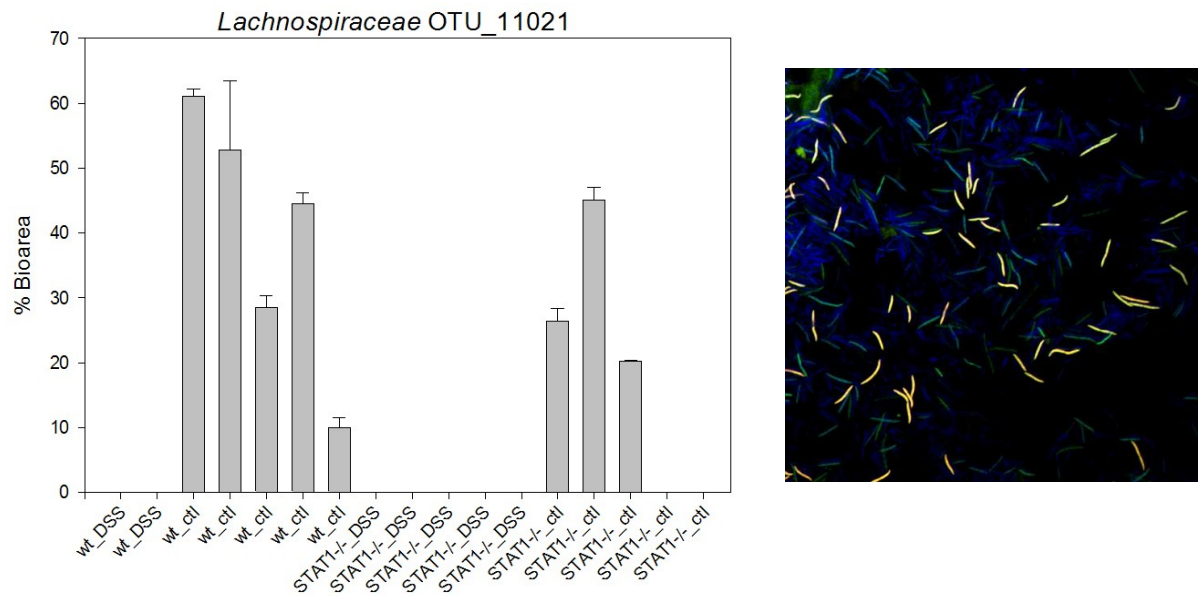


Figure C.28. Abundance of *Lachnospiraceae* OTU_11021 in samples taken from untreated and DSS-treated wt and STAT1^{-/-} mice. The percentage of bioarea (y-axis) is plotted for each sample ID (x-axis) and shown in box plots with corresponding standard deviation shown as black bars.

C.2.4 *Lachnospiraceae* OTU_9468

In contrast to OTU_11021, OTU_9468 – also from the group *Lachnospiraceae* – was only detectable in DSS-treated mice samples in STAT1^{-/-} (Fig. C.29). The combination of probe DSS9468a-999 and DSS9468b-1259 did not target any cell in untreated control samples.

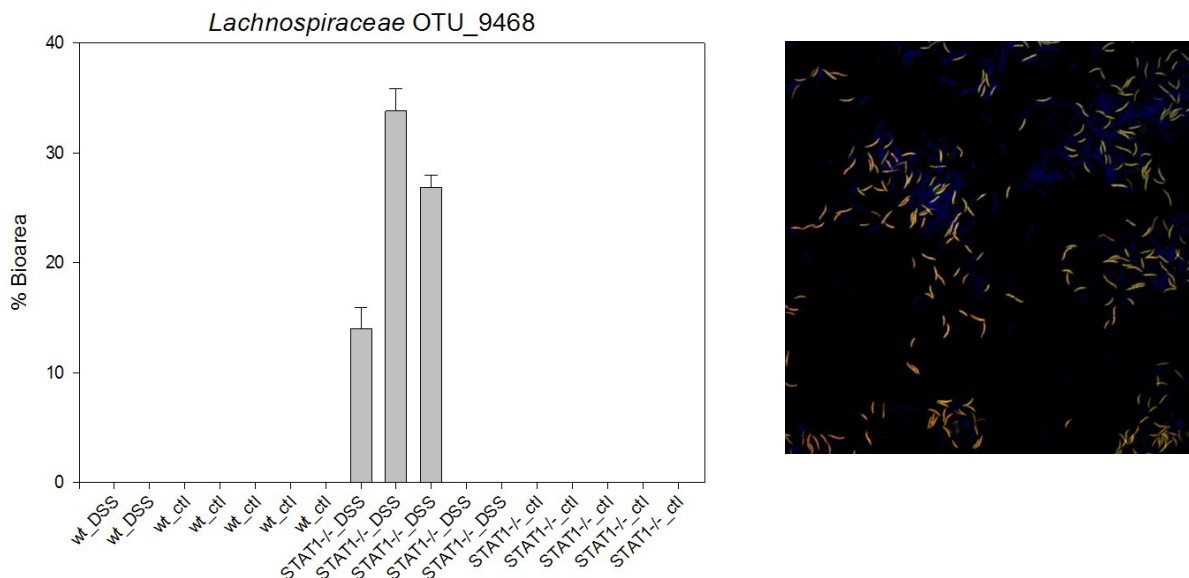


Figure C.29. Abundance of *Lachnospiraceae* OTU_9468 in samples taken from untreated and DSS-treated wt and STAT1^{-/-} mice. The percentage of bioarea (y-axis) is plotted for each sample ID (x-axis) and shown in box plots with corresponding standard deviation shown as black bars.

C.3 Comparison of bacterial shifts in colitis development

In samples taken over a period of one week, to analyze a shift in microbial community during colitis development, *Akkermansia muciniphila* was less abundant compared to first analysis and showed big individual variability. However, mean abundances of *Akkermansia muciniphila* in Tyk2^{-/-} mice increased over time. This holds also true for samples from wt mice, which were treated with DSS in three sequential challenges over a period of 58 days. Although there is high variability within the samples, *Akkermansia muciniphila* showed a much higher abundance than in control samples from day 0 but not control samples from day 58, which had the highest mean relative abundance of target cells.

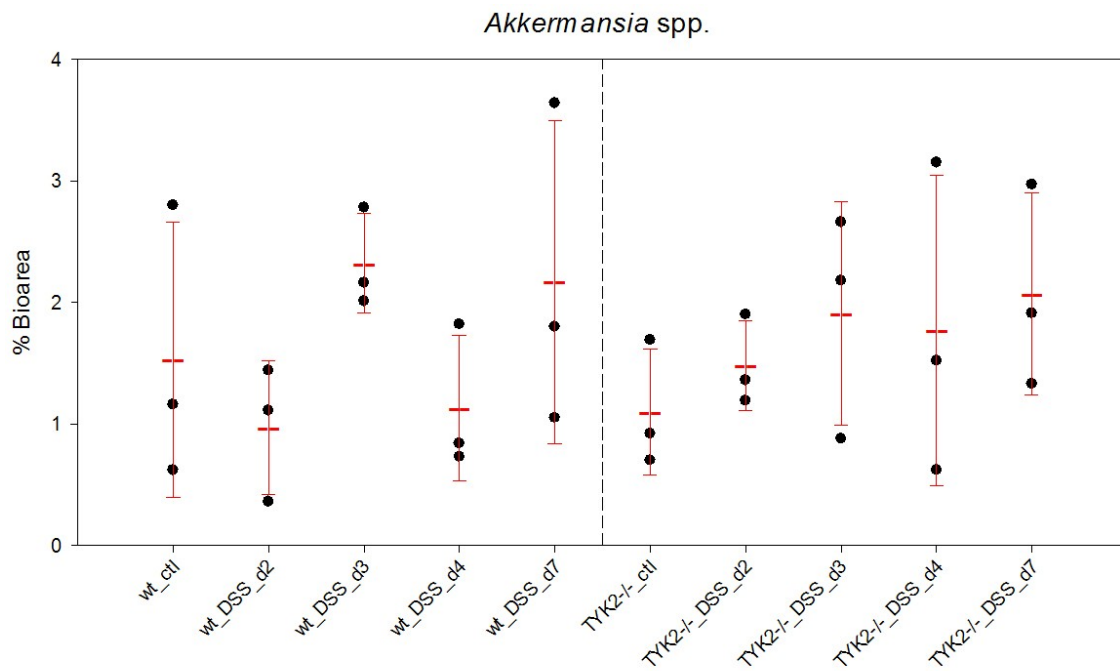


Figure C.30. Abundance of *Akkermansia muciniphila* in samples taken from DSS-treated wt and Tyk2^{-/-} mice at day 0, 2, 3, 4 and 7. The percentage of bioarea (y-axis) is plotted for each triplicate per sample as black dots (x-axis). Mean values with corresponding standard deviations are shown as red bars.

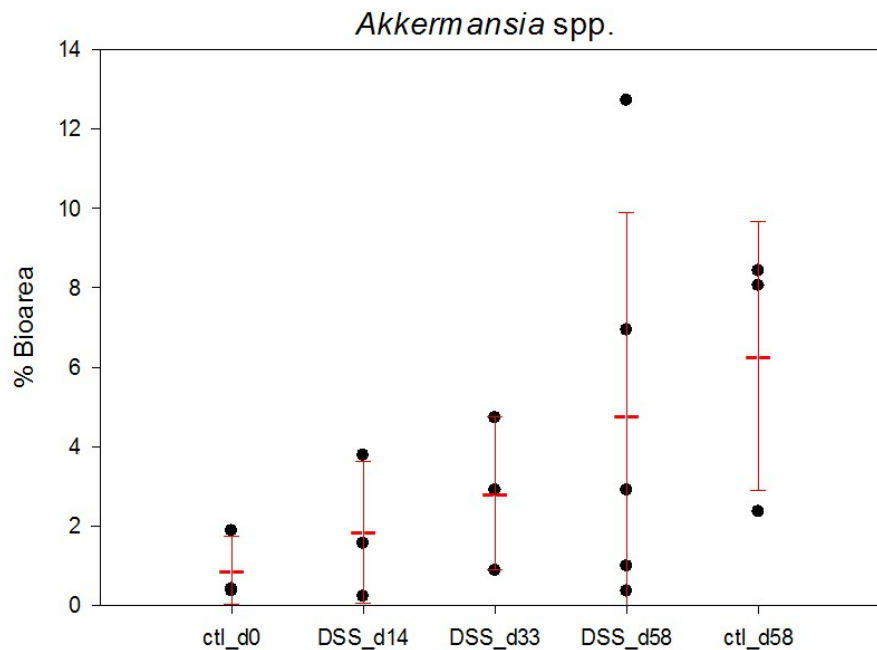


Figure C.31. Abundance of *Akkermansia muciniphila* in samples taken from DSS-treated wt mice at day 14, 33 and 58 including control samples at day 0 and 58. The percentage of bioarea (y-axis) is plotted for each triplicate per sample as black dots (x-axis). Mean values with corresponding standard deviations are shown as red bars.

FISH-analysis of the genus *Mucispirillum schaedleri* revealed that in wt and Tyk2^{-/-} mice this genus increases over time in colitis development. In Tyk2^{-/-} mice this genus was detected in the controls but almost doubled until day 7 from 0,7% to 1,5%. In multiple colitis development, an increased level of *Mucispirillum schaedleri* was obtained for samples in day 33 (5,5%) and day 58 (4%). Abundances in control samples from day 58 were higher than those from control samples from day 0.

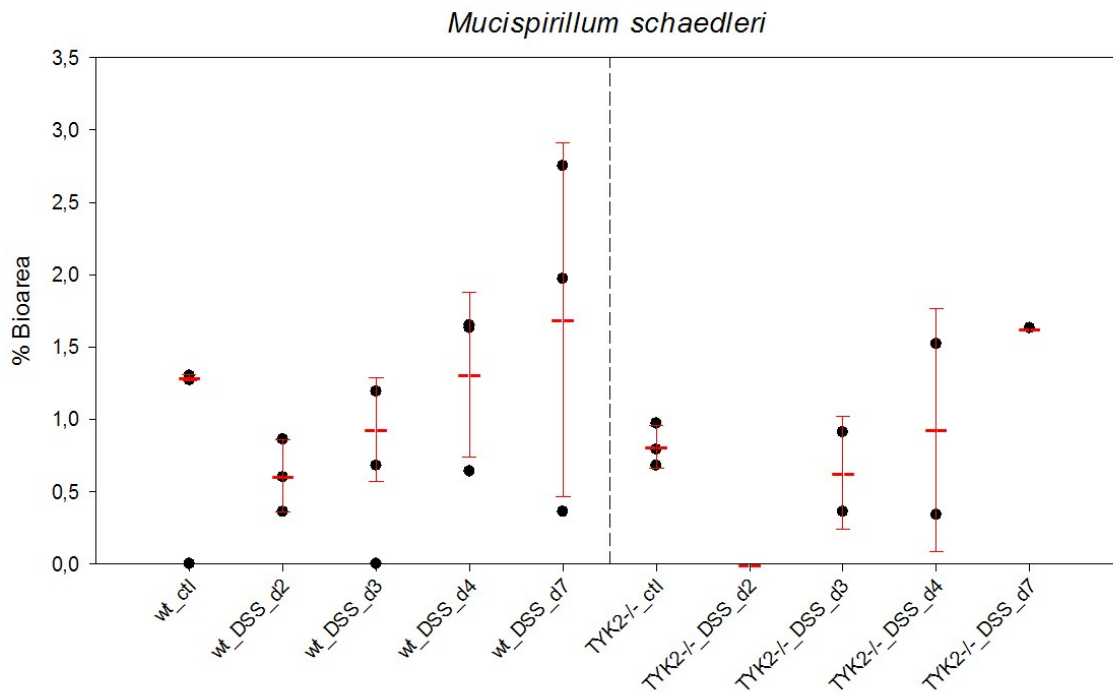


Figure C.32. Abundance of *Mucispirillum schaedleri* in samples taken from DSS-treated wt and Tyk2^{-/-} mice at day 0, 2, 3, 4 and 7. The percentage of bioarea (y-axis) is plotted for each triplicate per sample as black dots (x-axis). Mean values with corresponding standard deviations are shown as red bars.

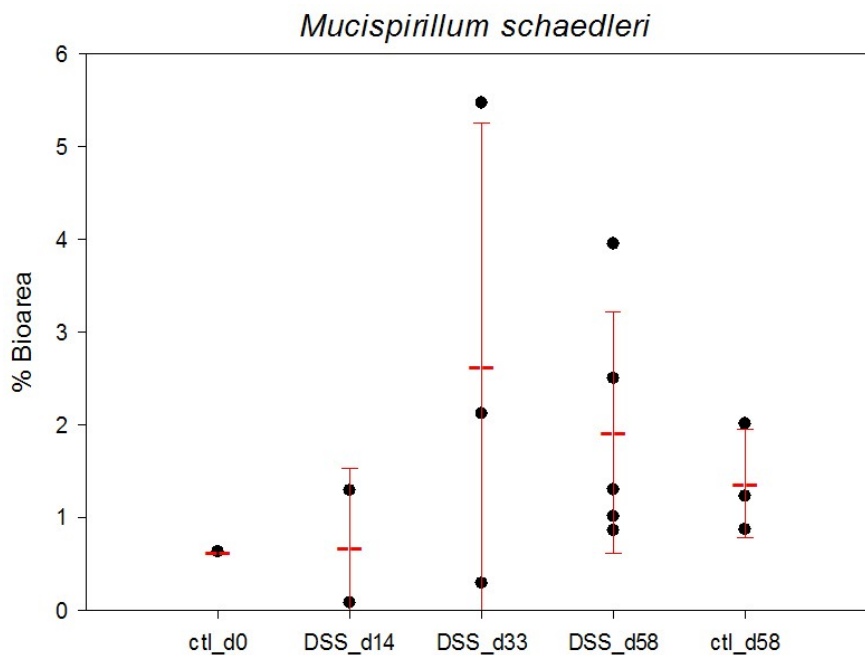


Figure C.33. Abundance of *Mucispirillum schaedleri* in samples taken from DSS-treated wt mice at day 14, 33 and 58 including control samples at day 0 and 58. The percentage of bioarea (y-axis) is plotted for each triplicate per sample as black dots (x-axis). Mean values with corresponding standard deviations are shown as red bars.

Lachnospiraceae OTU_11021 showed a distinct behavior in FISH-analysis as it was reduced to non-detectable levels during DSS-treatment. In *Tyk2^{-/-}* mice samples, OTU_11021 accounted for up to 22% in a single case in the microbial community and showed no detectable signal after three days of DSS-treatment. In the multiple DSS exposure study with wt mice, OTU_11021 made up to 33% in control samples from day 0 and reached only 2,7% in samples from DSS-treated mice. Control samples taken at day 58 showed again an increased level of OTU_11021 compared to samples from colitic mice.

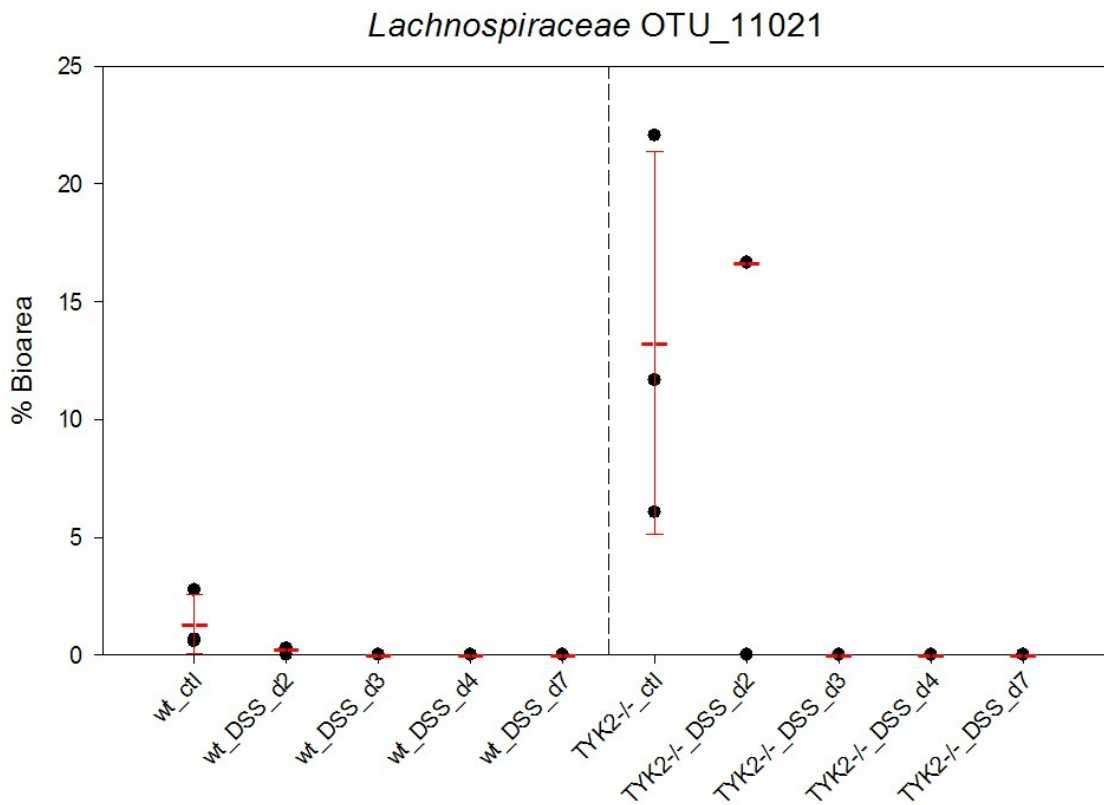


Figure C.34. Abundance of *Lachnospiraceae* OTU_11021 in samples taken from DSS-treated wt and Tyk2^{-/-} mice at day 0, 2, 3, 4 and 7. The percentage of bioarea (y-axis) is plotted for each triplicate per sample as black dots (x-axis). Mean values with corresponding standard deviations are shown as red bars.

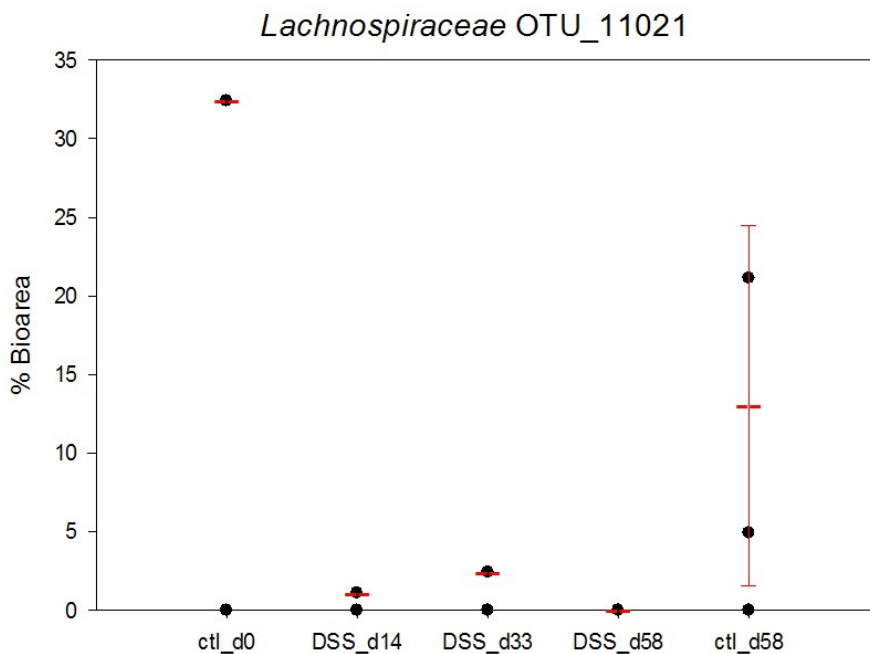


Figure C.35. Abundance of *Lachnospiraceae* OTU_11021 in samples taken from DSS-treated wt mice at day 14, 33 and 58 including control samples at day 0 and 58. The percentage of bioarea (y-axis) is plotted for each triplicate per sample as black dots (x-axis). Mean values with corresponding standard deviations are shown as red bars.

As in previous analyses, OTU_9468 was highly abundant in samples from DSS-treated mice. Wt samples showed no enrichment in OTU_9468. This is not the case for Tyk2^{-/-} mice. During seven days of colitis development, OTU_9468 was detectable only to a low amount in some samples until day 4. At day 7, this phylotype was abundant (22% relative abundance) in only one of three replicate mice. In wt samples during multiple colitis this OTU remained low and the highest percentage of bioarea was obtained in control sample at day 58.

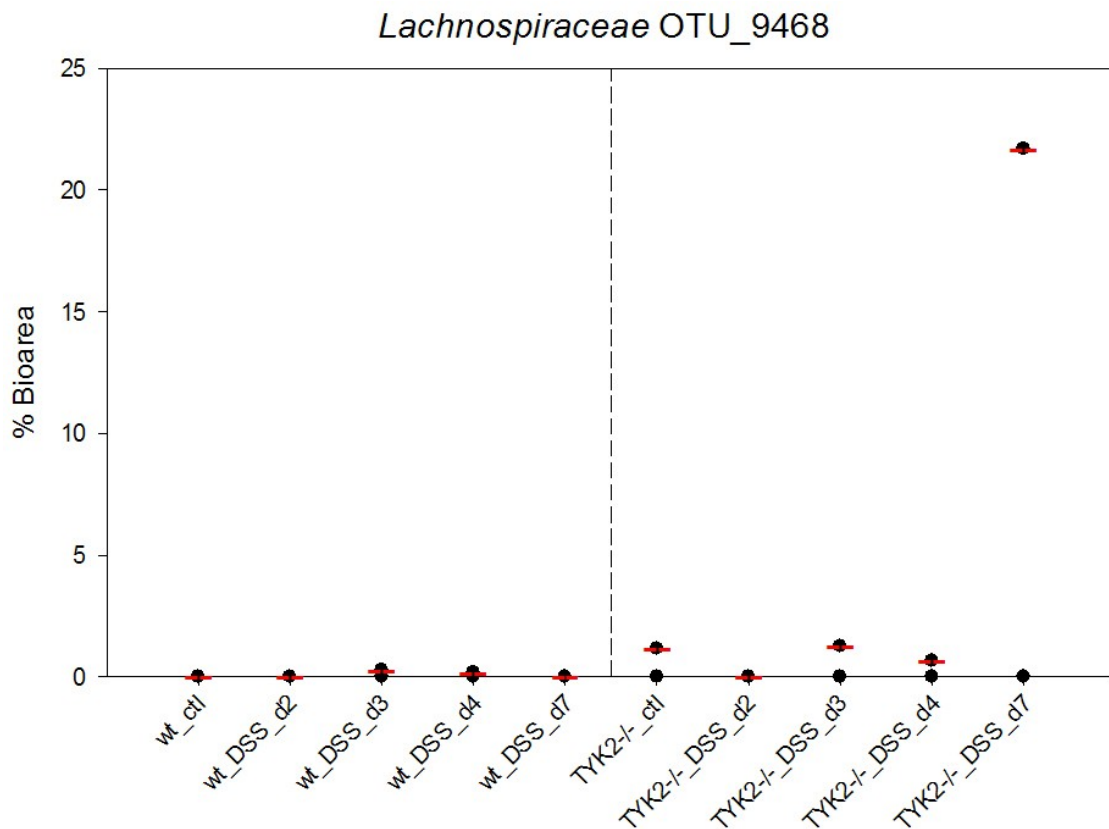


Figure C.36. Abundance of *Lachnospiraceae* OTU_9468 in samples taken from DSS-treated wt and Tyk2^{-/-} mice at day 0, 2, 3, 4 and 7. The percentage of bioarea (y-axis) is plotted for each triplicate per sample as black dots (x-axis). Mean values with corresponding standard deviations are shown as red bars.

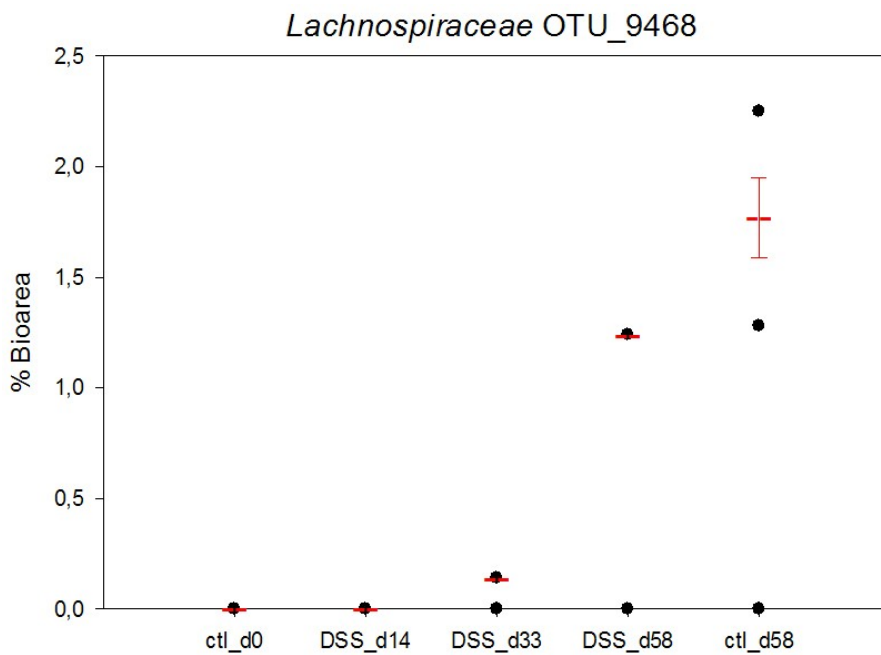


Figure C.37. Abundance of *Lachnospiraceae* OTU_9468 in samples taken from DSS-treated wt mice at day 14, 33 and 58 including control samples at day 0 and 58. The percentage of bioarea (y-axis) is plotted for each triplicate per sample as black dots (x-axis). Mean values with corresponding standard deviations are shown as red bars.

Bacteroides OTU_9164 showed an increase after three days in wt samples, followed by a decrease by day 7. After 58 days of multiple DSS-treatment, the percentage of bioarea of OTU_9164 rose from 0,5% at day 0 up to 4,8% at day 58. The control samples at day 58 were less enriched making up to 2%, but still higher than in control samples taken at day 0. OTU_9164 could not be detected in samples from *Tyk2^{-/-}* mice in the control day 0 and after seven days of DSS-treatment. At day 2, 3 and 4 relative abundance for this OTU steadily increased, but were lost at day 7.

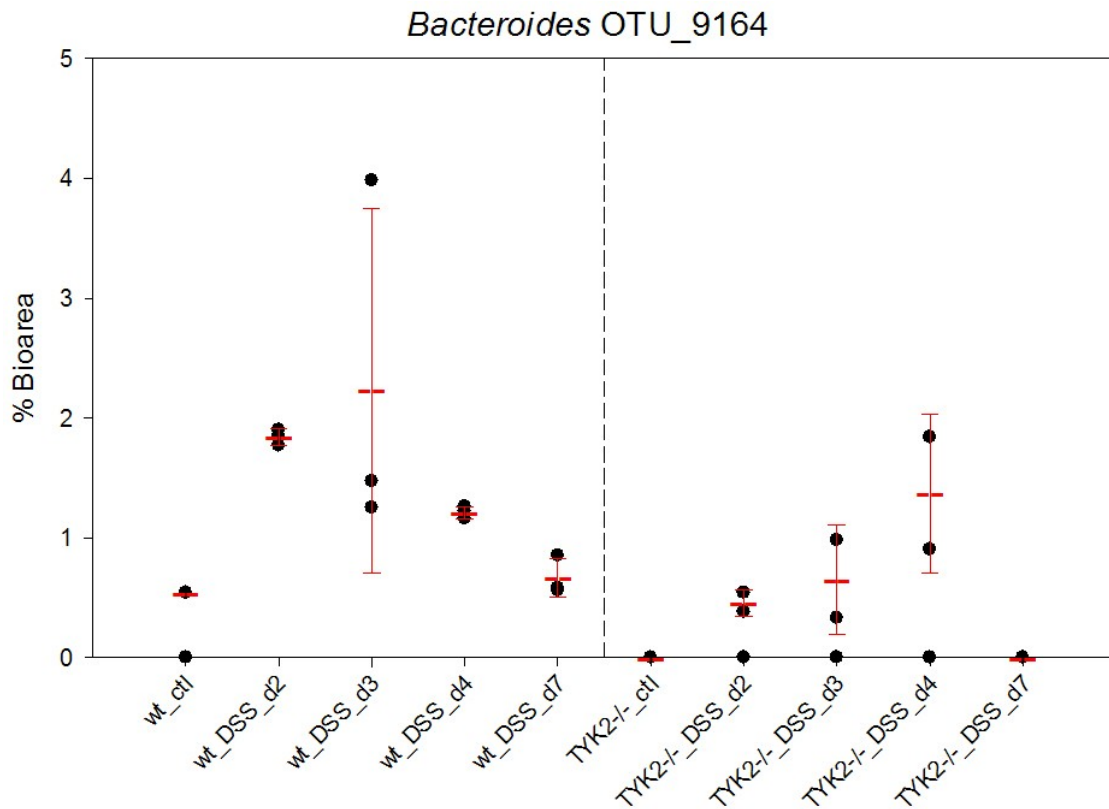


Figure C.38. Abundance of *Bacteroides* OTU_9164 in samples taken from DSS-treated wt and Tyk2^{-/-} mice at day 0, 2, 3, 4 and 7. The percentage of bioarea (y-axis) is plotted for each triplicate per sample as black dots (x-axis). Mean values with corresponding standard deviations are shown as red bars.

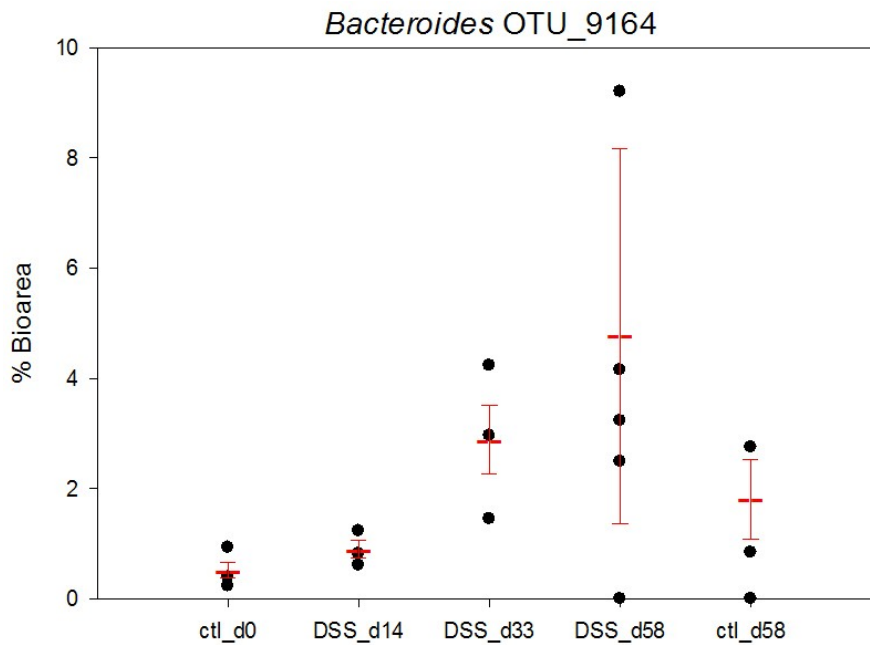


Figure C.39. Abundance of *Bacteroides* OTU_9164 in samples taken from DSS-treated wt mice at day 14, 33 and 58 including control samples at day 0 and 58. The percentage of bioarea (y-axis) is plotted for each triplicate per sample as black dots (x-axis). Mean values with corresponding standard deviations are shown as red bars.

Regarding *Ruminococcaceae* OTU_5807, quantification data showed a higher enrichment in samples taken from wt mice ($\bar{x}=4,5\%$) than from Tyk2^{-/-} mice ($\bar{x}=2,5\%$). In control samples from both genotypes, OTU_5807 was already abundant at day 0, but increased in wt mice during DSS-treatment in a single case up to 14,3%. In Tyk2^{-/-} mice the highest abundance was reached at day 3 with 3,8% bioarea. Progressing DSS-treatment in Tyk2^{-/-} mice resulted in lower enrichments of OTU_5807. In multiple colitis development in wt mice, signals were only detected at day 33 and day 58. At day 33 OTU_5807 was less abundant than at day 58, but again, the control samples at day 58 from untreated wt mice showed the highest enrichment in this OTU.

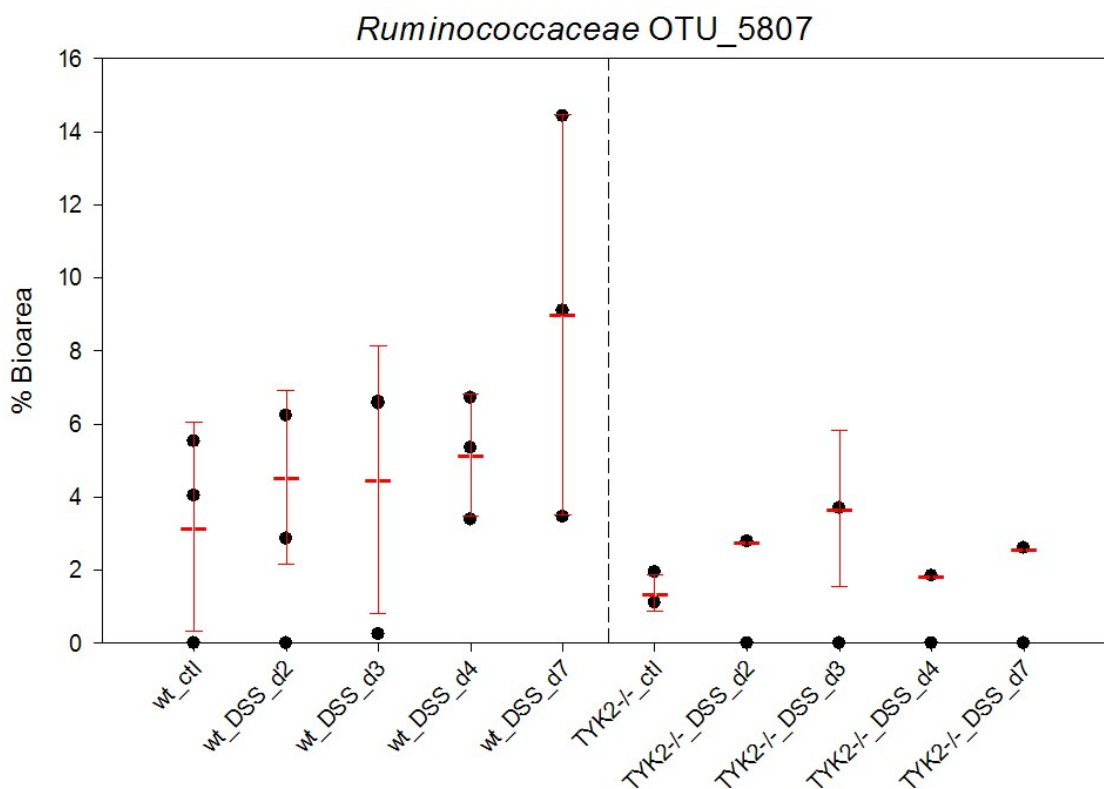


Figure C.40. Abundance of *Ruminococcaceae* OTU_5807 in samples taken from DSS-treated wt and Tyk2^{-/-} mice at day 0, 2, 3, 4 and 7. The percentage of bioarea (y-axis) is plotted for each triplicate per sample as black dots (x-axis). Mean values with corresponding standard deviations are shown as red bars.

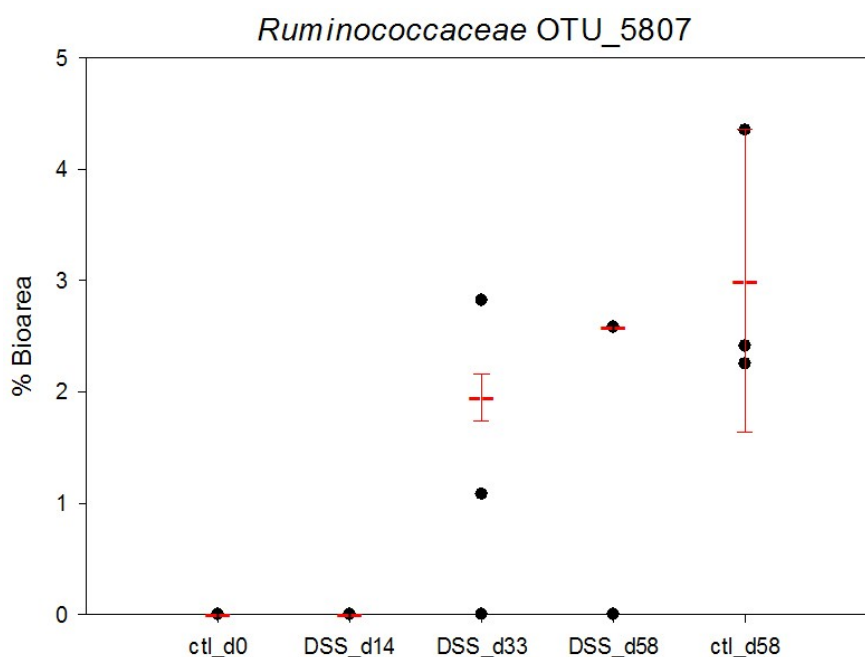


Figure C.41. Abundance of *Ruminococcaceae* OTU_5807 in samples taken from DSS-treated wt mice at day 14, 33 and 58 including control samples at day 0 and 58. The percentage of bioarea (y-axis) is plotted for each triplicate per sample as black dots (x-axis). Mean values with corresponding standard deviations are shown as red bars.

C.4 Preparation of LR-White embedded samples for NanoSIMS analysis

The following part describes the exact use of LR-White, its properties and its microscopic and spectrometric analysis.

C.4.1 Preparation and recording of sections from LR-White on CLSM and LMD

In first attempts, LR-White sections were cut to different thicknesses, thick enough to gain highest fluorescence by optimal probe uptake of the substrate and at the same time thin enough to enable imaging on NanoSIMS. Hybridizations with LR-White sections were performed on standard glass slides for FISH and handled with care because of the easy detachment of the section. Careful handling reduced the risk of losing the section, but did not help all the time, so PBS with 0,2% agarose was pipetted on-and-off on the section, which attached the section to the object slide and did not inhibit probe uptake during hybridization (Fig. C.42). Sizes of 0,3 / 0,5 / 0,7 μm showed good fluorescence intensity. A thickness of 0,3 μm troubled work on the microtome and ripped sections were common. Sections of 0,7 μm were much easier to handle, but the thick layer of LR-White interfered with measurements on

the NanoSIMS due to charging. 0,5 μm thick sections were straightforward to cut in the microtome, provided good FISH signals and were thin enough to avoid charge build-up in NanoSIMS. Therefore all further LR-White sections were cut to 0,5 μm .

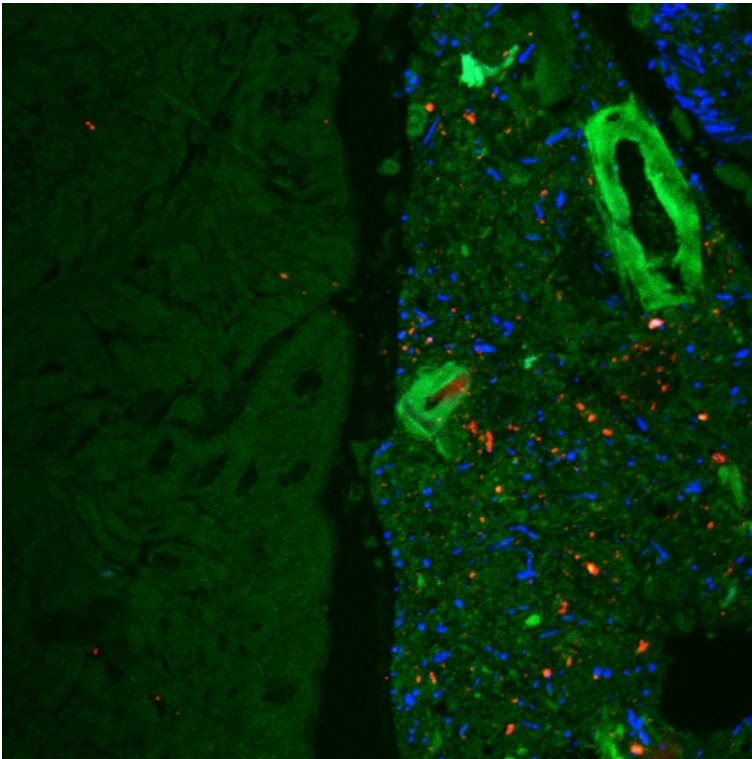


Figure C.42. Representative image of a 0,5 μm thick LR-White section attached to a slide with 0,2% agarose. In this case autofluorescent food-derived particles and tissues are shown in green. Blue signals highlight *Eubacterium rectales* targeted by probe Erec482 and red signals represent the group *Bacteroides* targeted by probe Bac303.

For NanoSIMS analysis, sections had to be mounted on the electrically conducting sample carriers. Carriers made of silicon were initially used. This wafer piece had a shiny surface, was impermeable to light and reflected excitation light from the CLSM (Fig. C.43).

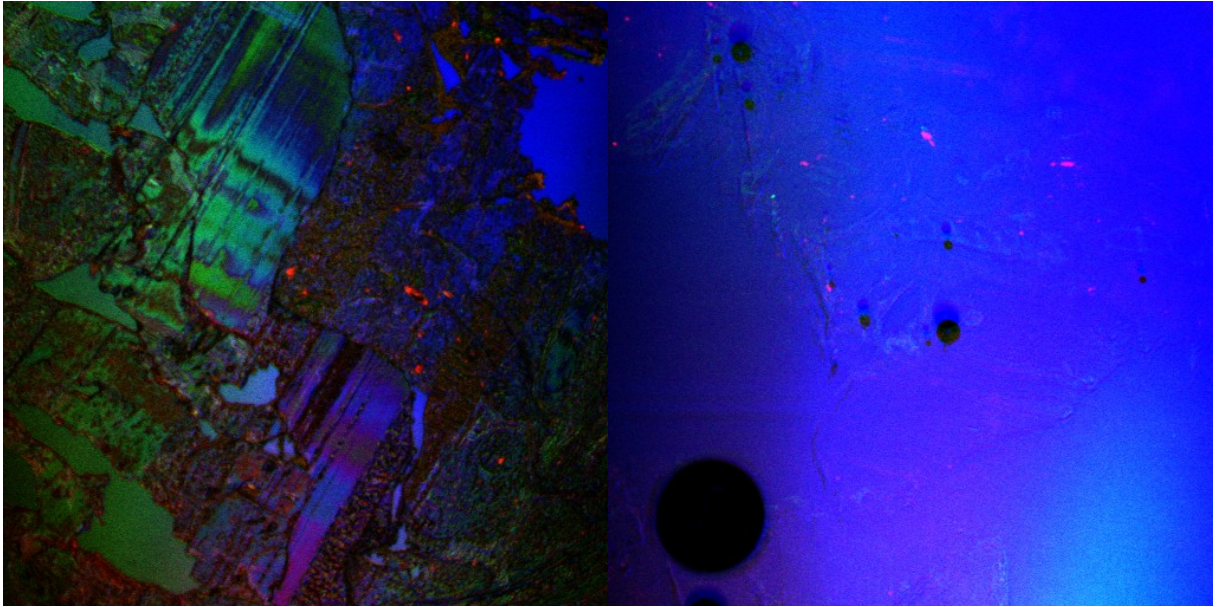


Figure C.43. Recorded images from CLSM showing reflection of incident laser light on a silicon sample carrier.

Images from LR-White sections on a silicon wafer piece were also recorded with an LMD microscope. It uses top-light illumination light and a much lower irradiation and enables microscopy of opaque specimen, therefore no interference of emitted light was detected (Fig. C.44). Each single channel was recorded and combined to get an image with all fluorescence channels (Fig. C.44). In case of using a single probe in one dye, only one greyscale channel was recorded and regarded as sufficient for analysis.

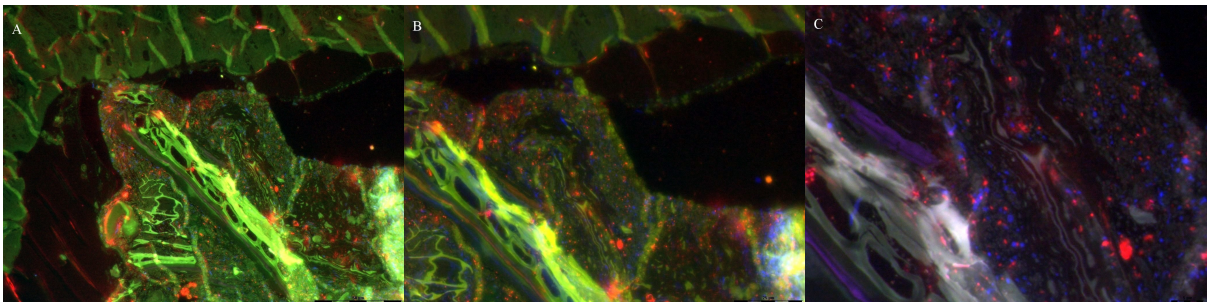


Figure C.44. LR-White section recorded with an LMD microscope with objective 40x (A), 63x (B) and 150x (C). Green signals indicate autofluorescent tissue and food particles. Red signals represent targets from probe Bac303 and blue signals from probe Erec482.

Further analysis of LR-white sections was performed on ITO coated glass slides, which are transparent and therefore be used with transmission microscopy. Hybridization parameters remained the same described previously. Imaging LR-White sections on CLSM was possible with the ITO coated glass slides (Fig. C.45 and C.46).

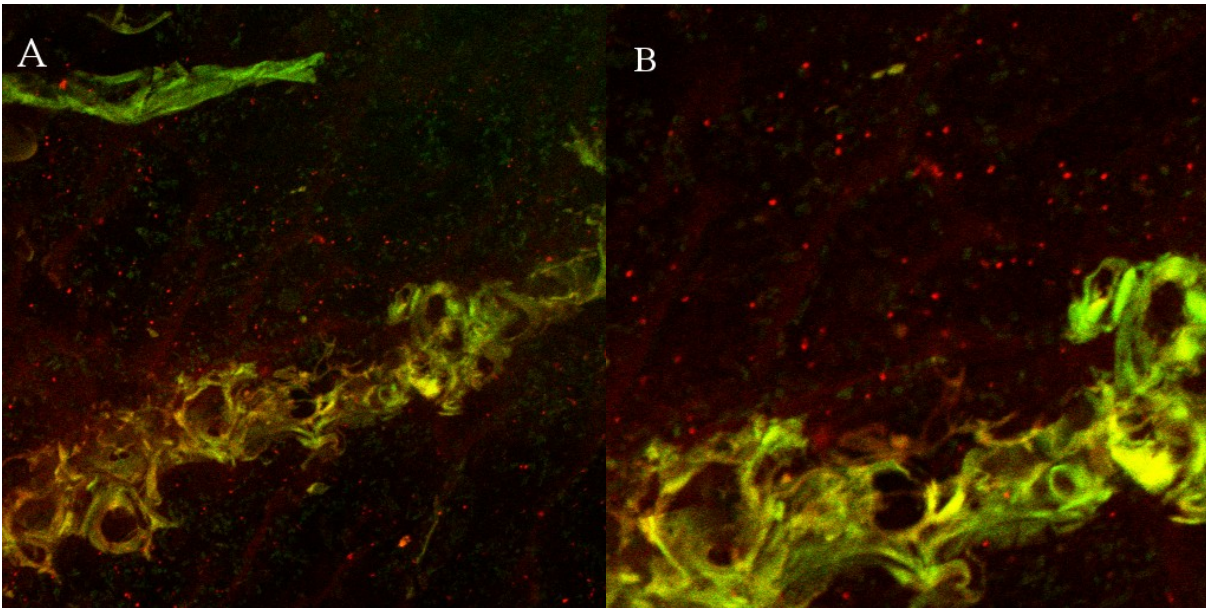


Figure C.45. LR-White section hybridized with probe Akk1437 (shown in red) on an ITO coated glass slide and recorded on CLSM. Green signals highlight autofluorescent tissue, red signals *Akkermansia muciniphila*. Figure A was recorded with 63x objective, Figure B is a close-up scene from the center of Figure A taken with 100x objective.

A general overview of the section was created with LEICA LMD software and images were recorded with increasing magnifications in greyscale (Fig. C.48). At magnifications using objective 10x, 20x and 40x additional images with digital interference contrast (DIC) were recorded and arranged with fluorescent images in greyscale.

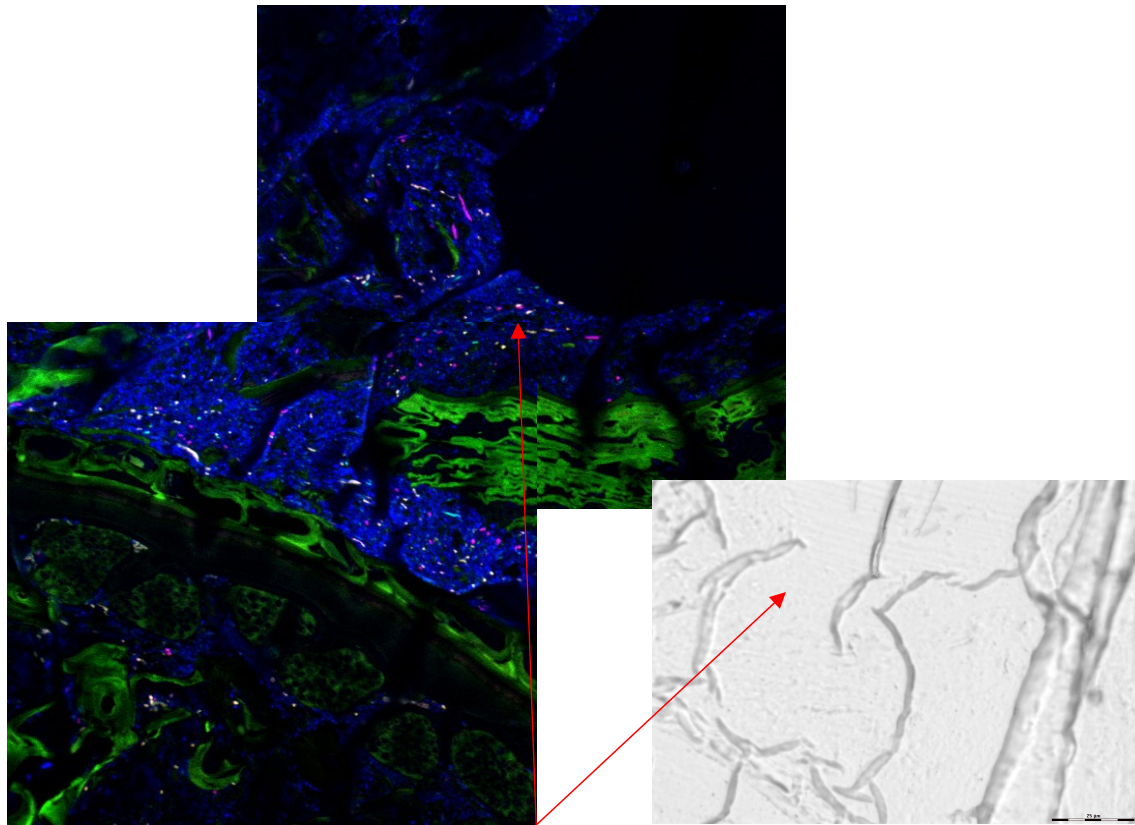


Figure C.46. Two images from LR-White section hybridized with probe Ctl11021a-1127, Ctl11021b-1448 and EUBmix on an ITO coated glass slide, recorded on CLSM with 63x objective and overlaid. Green signals highlight autofluorescent tissue, blue represent all bacteria targeted by EUBmix. Purple are non-target hits of probe Ctl11021a-1127 and yellow are targets OTU_11021 from the combination Ctl11021a-1127 and Ctl11021b-1448. Greyscale image shows DIC image recorded with LMD with 63x objective.

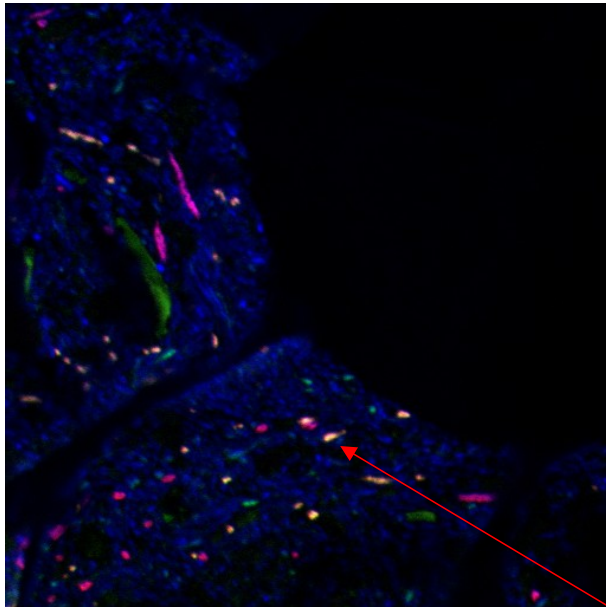


Figure C.47. Close-up image from Fig. C.46 recorded with 100x objective on CLSM shows non-target hits from probe Ctl11021a-1127 (shown in purple) and target hits from probes Ctl11021a-1127 and Ctl11021b-1448 (shown in yellow). Blue signals highlight all other bacteria targeted from probe EUBmix.

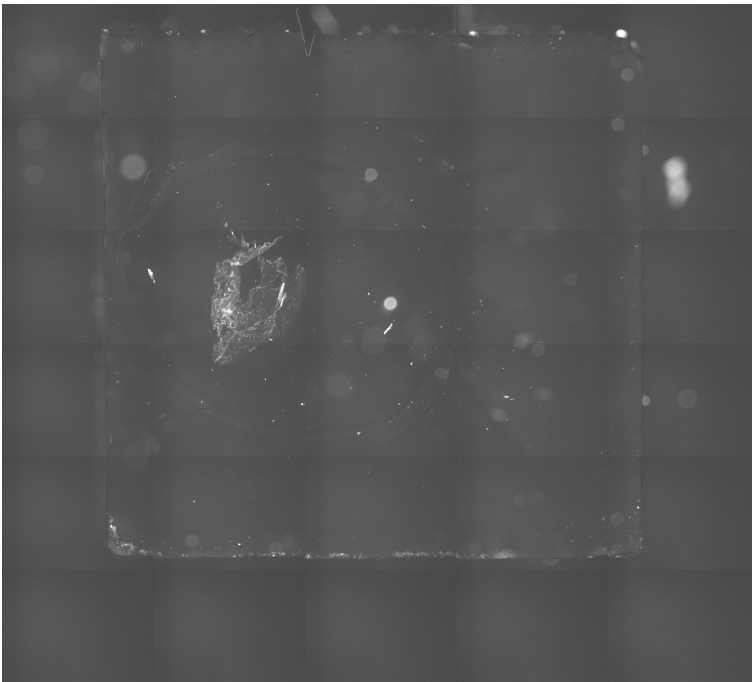
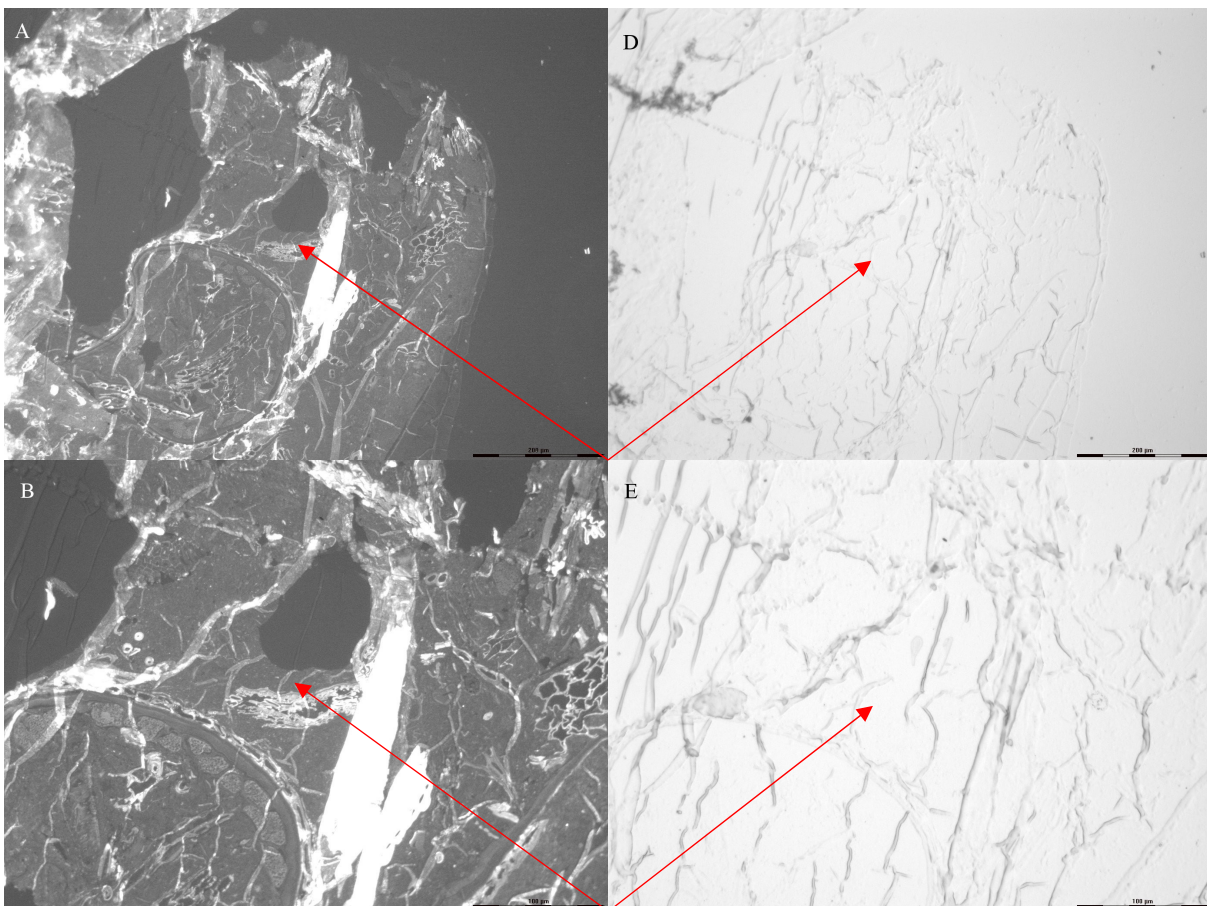


Figure C.48. 30 single images create an overview of LR-White section on an ITO coated glass slide recorded on the LMD microscope with a 6,3x objective.



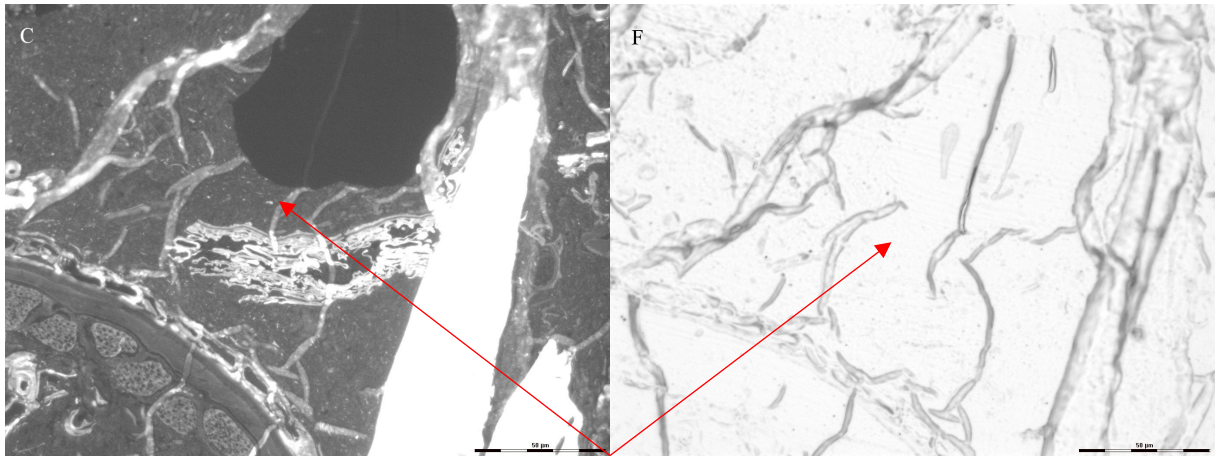


Figure C.49. LR-White sections recorded with the LMD microscope. Figure A-C were recorded with green fluorescence channel with objectives 10x, 20x and 40x. Figure D-F are images from DIC with 10x, 20x and 40x. Red arrows mark the spot of particularly interesting targets from FISH image (Fig. C.46 and C.47).

C.4.2 Preparation of whole cell samples on NanoSIMS wafers

It is desirable to analyze whole cells in addition to resin-embedded cells because the isotopic abundance level of the labeled cells is diminished by the infiltration with the natural abundant resin causing a dilution effect. The high carbon resin matrix also adds a background than can interfere with isotope analysis of ^{13}C . This is also true for ^{15}N , since the resin contains traces of nitrogen. Whole cell samples were prepared in the same manner as for standard FISH. The images were recorded and laser-marked on LMD as previously described. As seen in Fig. C.50 - C.52, whole cell samples were more dense and therefore more target cells could be detected.

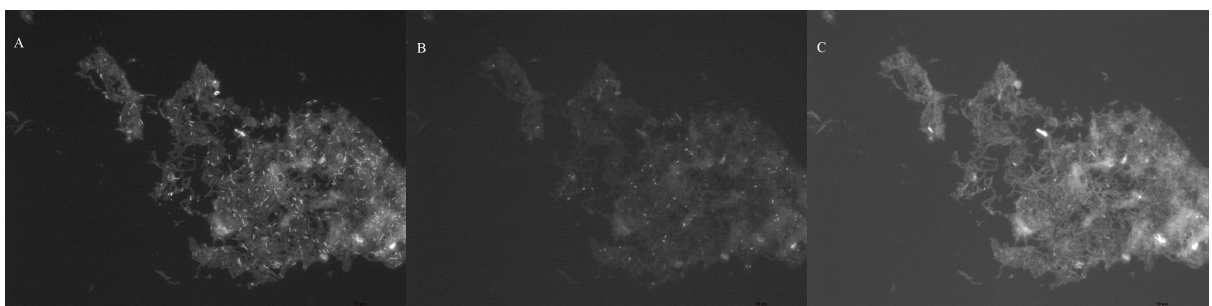


Figure C.50. Single-channel images taken with LMD 40x objective from a whole cell sample on a silicon sample carrier hybridized with probes targeting *Bacteroides* OTU_9164, *Ruminococcus* OTU_5807 and *Mucispirillum* spp. (Mcs487 and Mcs547). Figure A-C show signals of each channel (A: CY3, B: CY5, C: FLUOS).

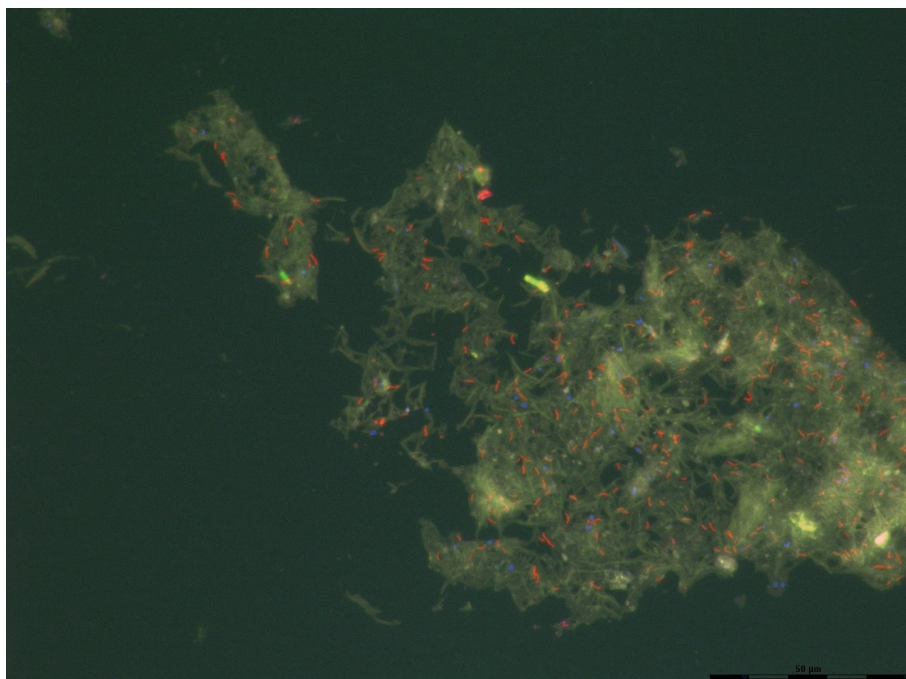


Figure C.51. Additional overlay of all three single-channel images (Fig. C.50). *Bacteroides* OTU_9164 are shown in blue, *Ruminococcus* OTU_5807 in red and signals from combination of probes Mcs487 and Mcs547 are shown in purple.

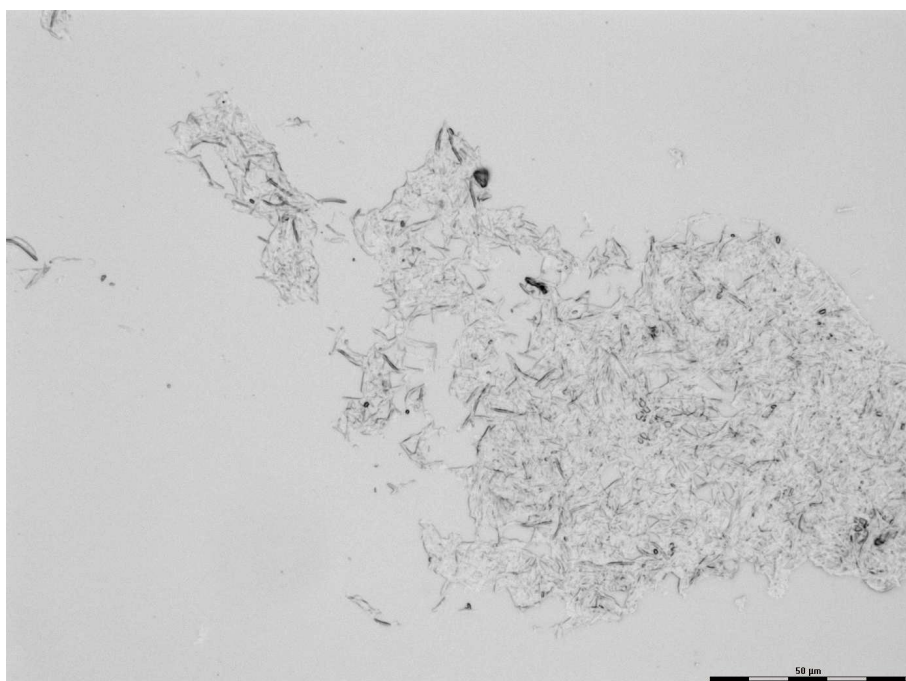


Figure C.52. DIC image of whole cell sample from Fig. C.51 showing bacterial cluster.

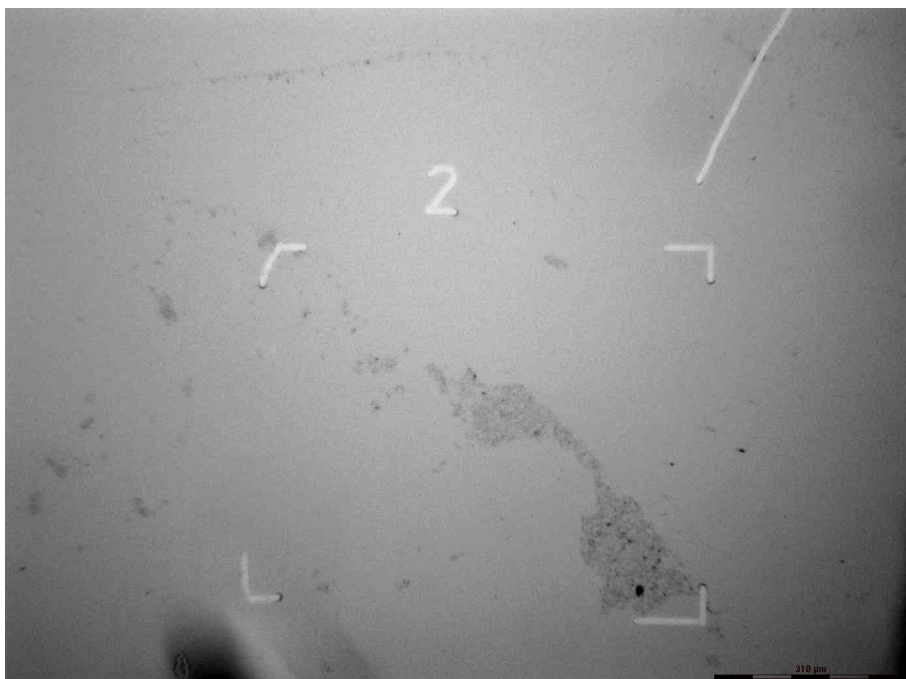


Figure C.53. DIC image of bacterial cluster after laser-marking with an LMD microscope recorded with a 6,3x objective.

C.4.3 Performance of LR-White: FISH signal intensity and re-use of sections

LR-White sections and whole cell samples were hybridized with EUBmix in FLUOS, CY3 and CY5 and signal intensities were compared. For LR-White resin, sections were re-used for a total of three hybridizations and intensities were measured.

Signal intensities of LR-White sections showed less intensity in sections hybridized with EUBmix-FLUOS (Fig. C.54), whereas intensities of CY3- and CY5-labeled probes were higher and at same level (Fig. C.55 and C.56). In comparison to whole cell samples, probes in LR-White sections were less intense, especially CY5-labeled ones (Fig C.56). In multiple usage of one section, mean fluorescence intensity decreased after each hybridization for all labeled dyes tested (Fig. C.57 and C.58).

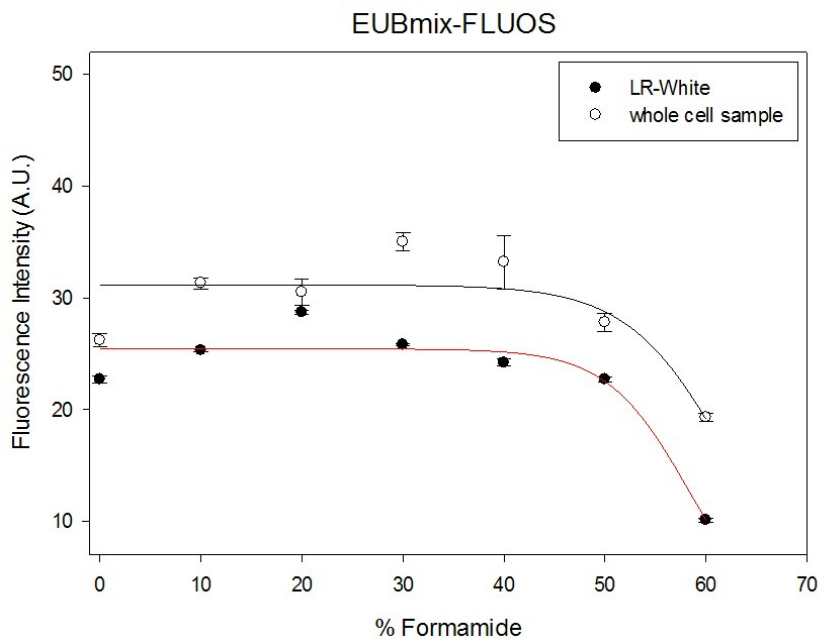


Figure C.54. Formamide curve of probe EUBmix with FLUOS-label. Mean fluorescence intensity (y-axis) is plotted against concentration of formamide (x-axis). Black dots represent single data points and black bars show associated standard errors. The red line highlights the sigmoid curve fit for intensities in LR-White sections and black line for intensities in whole cell samples.

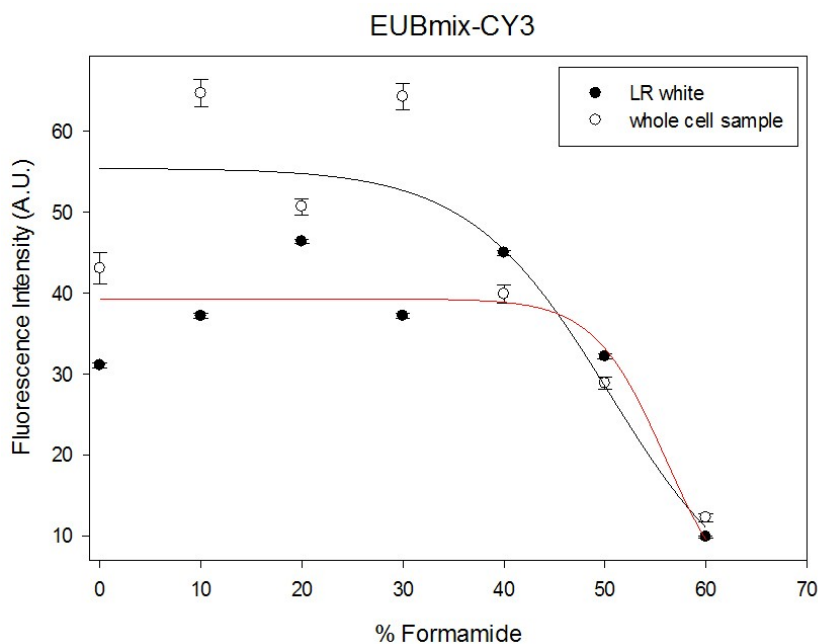


Figure C.55. Formamide curve of probe EUBmix with CY3-label. Mean fluorescence intensity (y-axis) is plotted against concentration of formamide (x-axis). Black dots represent single data points and black bars show associated standard errors. The red line highlights the sigmoid curve fit for intensities in LR-White sections and black line for intensities in whole cell samples.

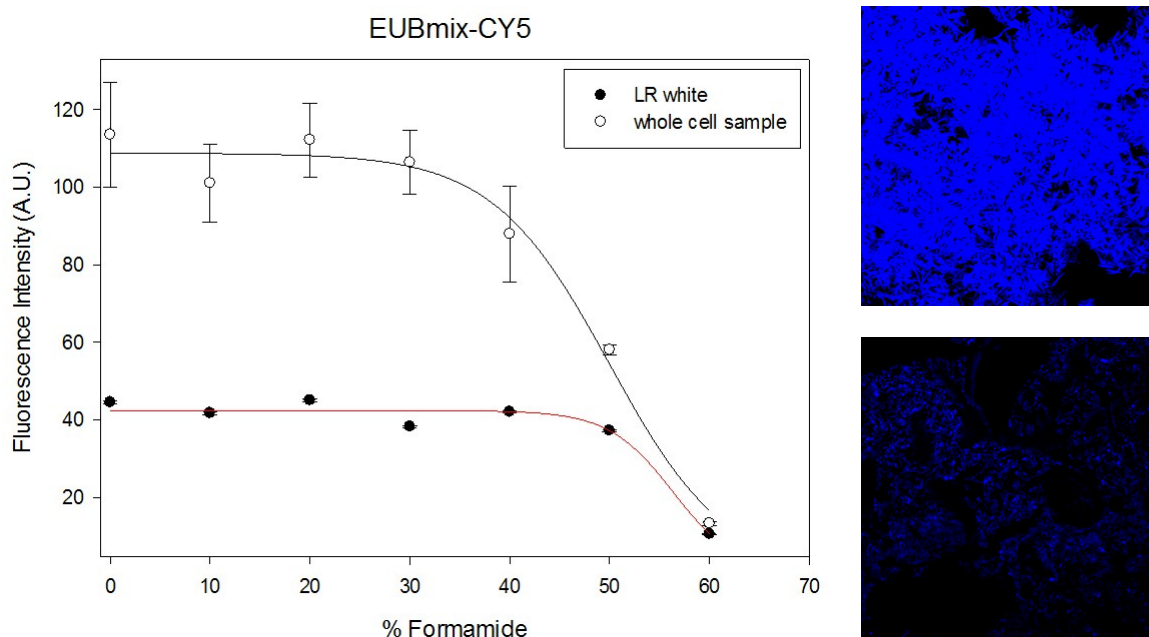


Figure C.56. Formamide curve of probe EUBmix with CY5-label. Mean fluorescence intensity (y-axis) is plotted against concentration of formamide (x-axis). Black dots represent single data points and black bars show associated standard errors. The red line highlights the sigmoid curve fit for intensities in LR-White sections and black line for intensities in whole cell samples.

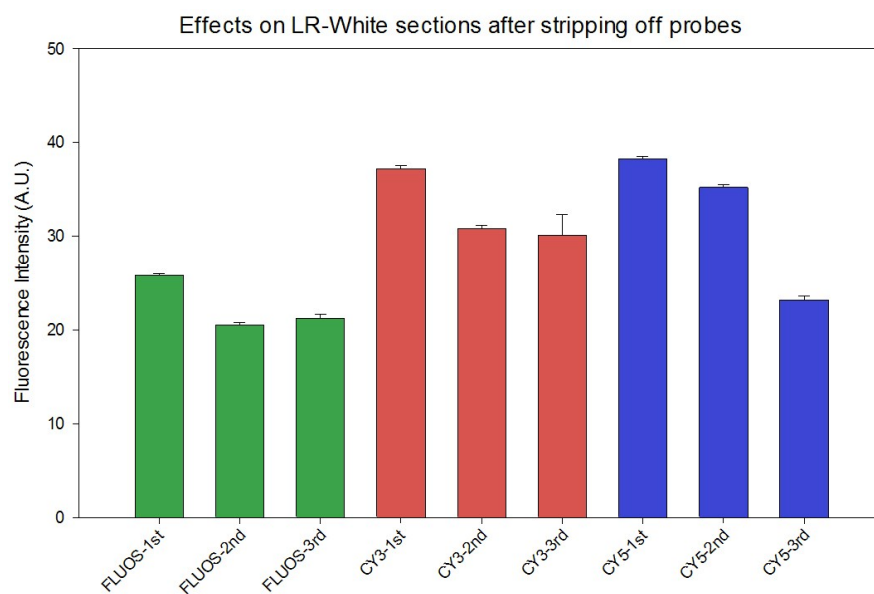


Figure C.57. Series of hybridizations on one LR-White section per dye at a formamide concentration of 30%. After each hybridization probes were stripped off. Each box plot shows the mean fluorescence intensity (y-axis) per hybridization. Green bars represent FLUOS-labeled probes, red bars CY3- and blue bars CY5-labeled probes. Associated standard errors are shown as black bars.

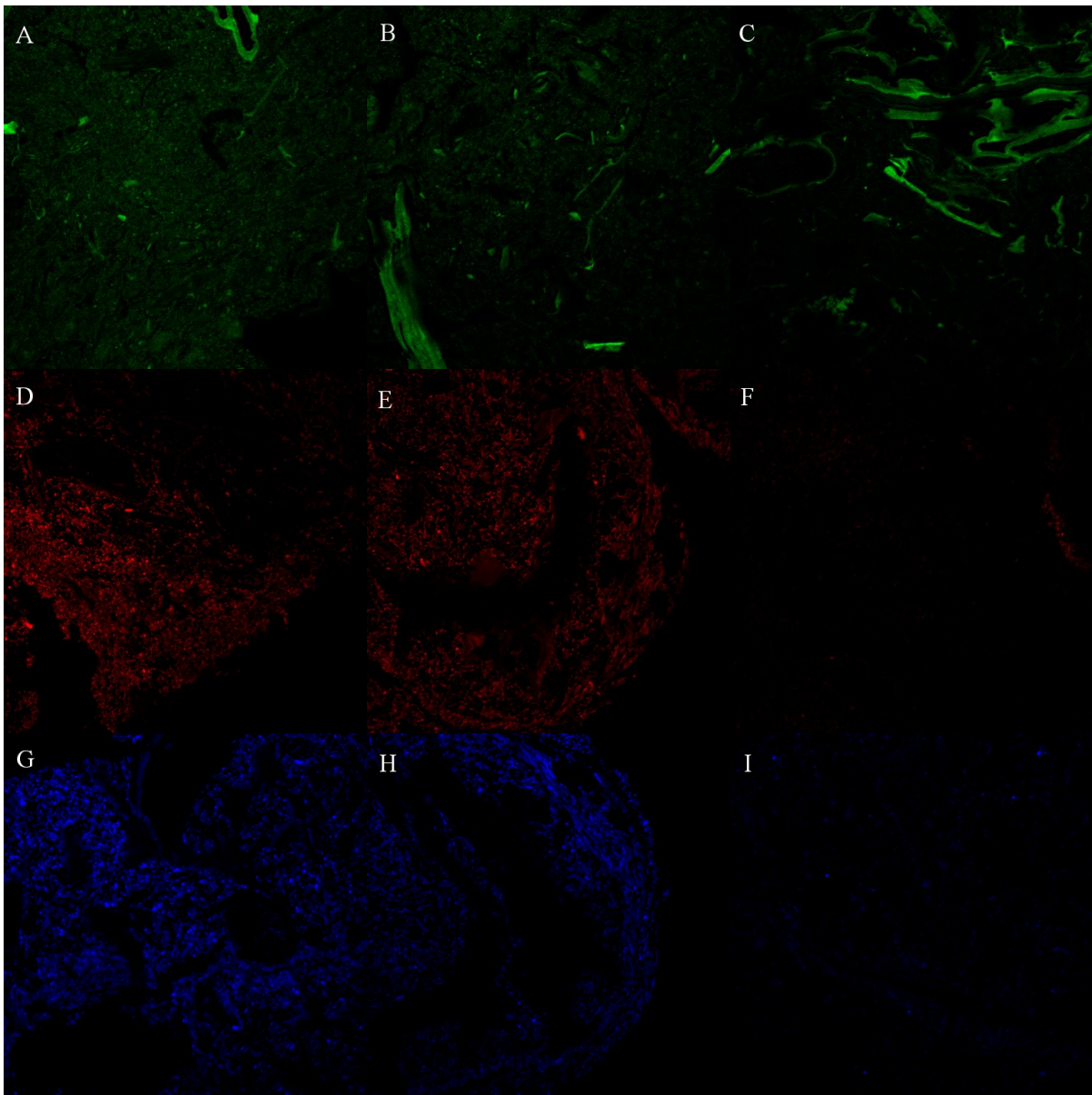


Figure C.58. LR-White sections hybridized with probe EUBmix at 30% formamide labeled with FLUOS (A-C), CY3 (D-F) and CY5 (G-I) after first (left), second (center) and third (right) hybridization.

D Discussion

D.1 Design and optimization of probes

D.1.1 *Akkermansia* spp. (Probe AKK1437)

The aim of this experiment was to find out, whether the suggested FA-concentration of 20% (Derrien et al., 2008) performs best. The evaluation of this probe (Fig C.1) indicated that the highest signal intensity was not at a formamide concentration of 20% which was probably caused by a lower accessibility of the probe and a less stable RNA-probe duplex. For use of this probe in FISH, a formamide concentration of 30-35% resulted in highest signal intensity, whereas less intense signals were observed at formamide concentrations below 30%. In fact, at 40% formamide the intensity decreased. At this point the formamide destabilized the binding of the probe to the rRNA. Representative images of signal intensities (Fig. C.1) at 20% and 30% formamide have underlined the fact, that use of 30% formamide resulted in brighter signals. Nevertheless, this probe suited very well to detect *Akkermansia muciniphila* in environmental samples at a formamide concentration of 30-35%.

D.1.2 16S rRNA-targeted FISH probes for *Mucispirillum schaedleri*

Two probes were designed to target *M. schaedleri* and the signal intensity formamide curves of the probes showed the same trend, which allowed co-application in a single hybridization. For high signal intensities and optimal stringency, a formamide concentration of 25-35% is appropriate for hybridization (Fig. C.2 and C.3). The perfect overlap of these probes also allowed a co-application of other probes in CY3- and CY5-label as Mcs487-CY3 and Mcs547-CY5 resulted in purple signals, which could be easily differentiated from any other signal. Another feature was the distinct spiral-shape of *Mucispirillum schaedleri* (Fig. D.1), allowing for an uncomplicated and fast detection even in highly autofluorescent environmental samples.

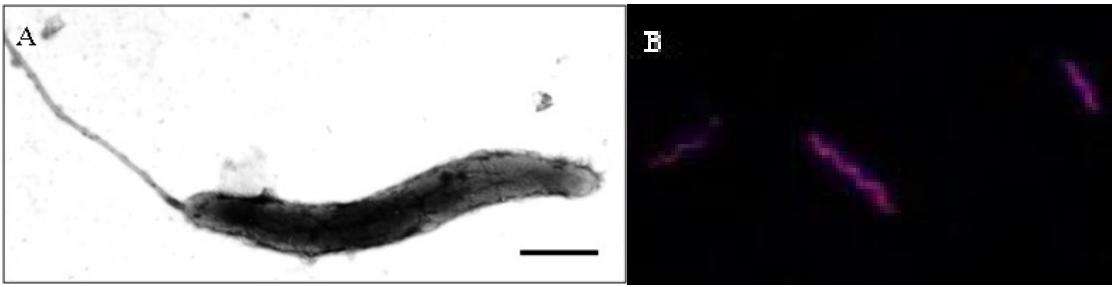


Figure D.1. Transmission electron micrography of *Mucispirillum schaedleri* sp. nov., a spiral-shaped bacterium with bipolar flagella measuring $4 \times 0,4 \mu\text{m}$ in size. Negative stain. Bar, $0,66 \mu\text{m}$. Image from Robertson et al., 2005. **B.** FISH-image of *Mucispirillum schaedleri* hybridized with probe Mcs487 and Mcs547 recorded on CLSM with 100x objective.

D.1.3 *Desulfovibrio piger* (Probe Dsp158)

Desulfovibrio piger is non-motile, gram-negative and forms straight rods (Postgate, 1984a). As it is a sulfur reducing bacteria metabolic hydrogen sulfide has a cytotoxic effect and is proposed to play a role in IBD (Gibson et al., 1991, Pitcher & Cummings, 1996). In evaluation of the probe Dsp158 a pure culture of *Desulfovibrio piger* was used. High signal intensities were obtained and further hybridizations, including this probe at a concentration of 30% formamide, gave bright and distinct signals. Its relative abundance in mouse gut samples was low or below detection limit. However, this newly designed probe allows very good detection of the target *Desulfovibrio piger* (Fig. C.5).

D.1.4 *Lachnospiraceae* OTU_11021 (Probes Ctl11021a-1127 and Ctl11021b-1448)

Probe design for OTU_11021 was very challenging, as this OTU showed very high sequence similarity to non-targets and detection by a single probe was not possible. Two probes with overlapping targets were necessary to detect this OTU. The evaluation of each single probe showed different maxima of intensities, so additionally FISH-images were compared to determine the best concentration of formamide in order to achieve optimal signal intensities for both probes and to obtain the highest contrast of target hits to non-target hits.

A formamide concentration of 30-35% gave most optimal results and allowed proper differentiation of targets and non-targets (Fig. C.6 - C.8). Theoretically, probes Ctl11021a-1127 and Ctl11021b-1448 can be co-applied with other probes in the same fluorescent label due to the target OTU_11021 being a very large rod compared to other bacteria and

differentiation on microscopic images can be achieved through color of fluorescence dyes and size.

D.1.5 *Lachnospiraceae* OTU_9468 (Probe DSS9468a-999 and DSS9468b-1259)

For the design of probes targeting OTU_9468, the same procedure was applied as for probes targeting OTU_11021. In contrast to OTU_11021, however, OTU_9468 is much smaller (Fig. C.11). Signal intensities in images were also compared. The best signal intensities and contrast between target- and non-target hits were obtained at a formamide concentration of 10%. A big advantage of co-application of two probes targeting one OTU is the fact that through the use of multiple probes, not only the detection of one OTU is possible, as the target appears in another color in fluorescence images than the single dye. The use of multiple probes requires a high probe specificity and no overlapping non-targets (false positive signals). This can be achieved by using actual sequencing data in probe design and re-evaluation of already existing probes.

D.1.6 *Bacteroides* OTU_9164 (Probe 9164a-1000 and 9164b-177)

To show the stringency and specificity of each probe, the quantification of targets was performed in environmental samples. Detection of probe 9164a-1000 was possible up to 30% formamide (Fig. C.12 and C.13). By adding more than 30% formamide, signal intensities were too low to make out single cells in bacterial clusters. Regarding quantification data, the amount of target cells decreased at 25%. At 35%, almost no targets were observed due to low intensities. Single cells could not be differentiated from autofluorescent background or bacterial clusters. When it came to the amount of target cells, similar results for probe 9164b-177 were obtained but signal intensities of probe 9164b-177 were much higher. A comparison of FISH images was necessary to evaluate hybridization parameters in order to obtain best signal intensities and contrast of target cells, which in this case was 25% (Fig. C.17).

D.1.7 *Ruminococcaceae* OTU_5807 (Probe 5807a-431, 5807b-986 and 5807c-1202)

For detection of OTU_5807 all three probes suit well, as FISH images show high signal

intensities. 5807a-431 was FLUOS-labeled and 5807c-1202 CY3-labeled. This combination of FLUOS- and CY3-dye in overlapping targets resulted in yellow to orange signals that could be easily discriminated against EUBmix in CY5 (Fig. C.25). As 5807b-986 was CY5-labeled, combination with FLUOS- or CY3-labeled probe showed less contrast against EUBmix in FLUOS or CY3, leading to best combination of 5807a-431 and 5807c-1202. Comparing signal intensities and stringency of this probe in single and in combination, a formamide concentration of 25-35% can be applied for hybridizations.

D.2 Abundance of specific gut bacteria in healthy and DSS-treated mice

Examining the the abundance of *Akkermansia* spp. in DSS-treated and untreated mice, irrespective of their genotype, this bacteria seems to be a promising candidate for indicating induced colitis. However, in the long-term study over a period of 58 days, this trend was not observed as abundances even within one sampling day showed high variability. An explanation for this variability could be a maternal effect of the mice. Although the relative abundance of targeted cells increased over time and after each treatment, control samples taken from day 58 also showed high abundance of *Akkermansia* spp.. Possible reasons could be a bacterial transfer caused by co-housing.

Mucispirillum spp. played a similar role as *Akkermansia* spp., as the relative abundance of cells increased during colitis development. In contrast to *Akkermansia* spp. it could not be detected in any healthy STAT1^{-/-} mice but was abundant in three out of five samples taken from DSS-treated STAT1^{-/-} mice. FISH signals for *Mucispirillum* spp. were obtained in all wt mice, but to a much higher percentage in DSS-treated ones. During colitis development from day 0 to day 7 a steady increase in wt and Tyk2^{-/-} was detected, which also occurred in induced multiple colitis treatment. However, samples taken from day 33 were generally more enriched in *Mucispirillum* spp. than samples taken from day 58. The latter contained *Mucispirillum* spp., which could also support the theory of a bacterial transfer during co-housing.

According to quantification data group *Lachnospiraceae* OTU_11021 suits very well as an early indicator for induced colitis in mice. In any control sample, whether wt, STAT1^{-/-} or Tyk2^{-/-}, this OTU was sometimes, though not always, highly abundant and was not detected

after three three days of DSS treatment. In multiple colitis treatments at day 14 and day 33 minor amounts – compared to previous data – were detected, which supports the role of OTU_11021 as an early indicator for colitis development. Another explanation for rapid loss of such an abundant bacterial OTU could be an interference with DSS, which might inhibit bacterial growth. A later detection of OTU_11021 at day 14 and day 33 could be the consequence from a possible growth phase during time of recovery, when no DSS was administered.

In Tyk2^{-/-} mice group *Lachnospiraceae* OTU_9468 was detected in significant amounts after 7 days of DSS treatment, where else in wt samples, this OTU could not be detected. A possible reason for this delayed and less rapid growth lies with the knockout of Tyk2^{-/-} in the JAK/STAT signaling pathway, which led to a declined immune response and enabled growth for OTU_9468. The highest abundance of OTU_9468 in multiple colitis development was obtained in control samples from day 58, which could be consequence from co-housing or maternal effects of the mice. As OTU_9468 was only highly abundant in Tyk2^{-/-} mice after 7 days of DSS-treatment, this OTU is no indicator for induced colitis, but highlights the tremendous bacterial shift during DSS-treatment.

Bacteroides OTU_9164 also increased in relative abundance with DSS treatment in late response. In all samples from colitis development, the occurrence of OTU_9164 in the first seven days was much lower than compared to samples taken from later time points during multiple colitis development. At day 14 to day 58, gut environment obviously offered better growth conditions for OTU_9164 and led to a steady increase over time, making *Bacteroides* OTU_9164, as *Lachnospiraceae* OTU_9468, a late DSS-induced colitis indicator.

Focusing on *Ruminococcaceae* OTU_5807, highest abundance was observed after seven days of DSS-treatment and occurred only at day 33 and day 58 in single cases, which may be caused by a change in microbial community towards other bacteria, as for example previously described late indicators – OTU_9468 and OTU_9164 – outcompeting early indicator OTU_5807. This theory is underlined by the fact that this OTU established better in control samples at day 58 than in any other sample taken after one week of DSS-treatment, therefore making OTU_5807 a good early indicator for induced colitis.

D.3 LR-White sections for NanoSIMS analysis

LR-White sections for FISH preserve the structure of the sample and allow the location of bacteria in the gut. For this procedure, specific material and methods had to be adapted. Cutting sections requires glass knives with a sharp edge, which must be exchanged after some cuts depending on the size of embedded samples. Dull edges resulted in small superficial scratches and blurred images (Fig. C.45). The problem of losing the section while changing buffers during hybridization is due to the easy detachment of the sections from the slide. To avoid such circumstances, PBS containing 0,2% agarose increased sample adhesion and no decrease in signal intensities or probe uptake was observed on standard glass slides. Silicon sample carriers are opaque, but highly reflective and cause intense and unspecific background in CLSM most likely originating from the reflection of the incident laser light at the Si surface (Fig. C.43). In contrast, the Leica LMD is a microscope with an air objective, therefore no oil and no cover slip that could affect or destroy the sample is required. Images could still be recorded with the LMD but images were less detailed as ones from the CLSM, though regardless allowed analysis of single cells (Fig. C.44). The limited quality of the images taken with the LMD could not be improved, so ITO coated glass slides were used, which enabled image recording on the CLSM. ITO coated glass slides are transparent but also electrically conductive, which make them perfect to use with both the CLSM and NanoSIMS. In addition to FISH images on the CLSM, sections were laser-marked on the LMD microscope (Fig. C.53) and DIC images were recorded to find the right spot (Fig. C.46, C.49 and C.52). To ease the work of finding the correct location on the NanoSIMS it was necessary to arrange all images and mark position of targets to be measured (Fig. C.49).

As desired FISH targets in LR-white sections are sometimes quite rare, whole cell samples, which have a much higher cell count were used. Whole cell samples, which were spun down at low speed with a bench centrifuge to reduce the amount of autofluorescent particles. Another advantage of spinning down was to out dilute single cells and minimize bacterial clusters, as they hamper analysis with the NanoSIMS. Environmental whole cell samples could not be analyzed on the CLSM due to the use of an oil-objective, which made it necessary to mount the wafer. Unmounting the sample caused damage or loss and the same spot could not be found on the LMD microscope because of significant cell erosion.

Both sample types – LR-White and whole cell samples – have their special features and also disadvantages. A big disadvantage of LR-White is in particular the high carbon content of the

resin, which leads to a dilution of the ^{13}C label abundance and creates unspecific background during NanoSIMS measurements. Nevertheless LR-White suits very well for recording clear and sharp images on CLSM (Fig. C.46) and allows localization of distinct bacteria, but target cells are rare compared to whole cell samples, which on the other hand can only be recorded with LMD. The disadvantage of the LMD recording images in lower quality than the CLSM is a matter of physics but can be minimized by the use of a 63x, instead of a 40x objective.

D.3.1 FISH signal intensity and re-hybridization capacity of LR-White sections

Signal intensities in LR-White are in fact lower compared to intensities in whole cell samples (Fig. C.54 – C.56). However, the identification of target cells is possible, also with CY5-label, which is much less intense compared to use with whole cell samples. For CY3-label, signal intensities in LR-White resin were sufficient to allow proper analysis. Probes with FLUOS-label troubled work with LR-White sections, as they contain lots of autofluorescent food particles and tissue, which are also detected in FLUOS-channel. The use of FLUOS-labeled probes in LR-White sections is not recommended, as target cells appear in same color as autofluorescent objects and signal intensities after multiple use decrease below detection limit and are even less intense than autofluorescent particles. For CY3- and CY5-label multiple use of one section is possible but signal intensities decrease too. However, autofluorescence is not detected within these channels and enables a detection of target cells much better than with FLUOS-label.

E Summary

This study aimed for the application of FISH for identification and quantification of bacteria in the gut. To ensure a more detailed analysis of the bacterial composition, probes need to be designed based on new phylogenetic data regarding 16S rRNA. This implements that re-evaluation of existing probes is crucial. In this specific case, probe Akk1437 detecting *Akkermansia* spp. was re-evaluated and the hybridization condition was optimized by adjusting the formamide concentration. To gain more insight in microbial diversity – especially during induction of colitis – probes specific for *Mucispirillum schaedleri*, *Lachnospiraceae* OTU_11021 and OTU_9468, *Bacteroides* OTU_9164 and *Ruminococcaceae* OTU_5807 were designed and evaluated. All probes showed very good signal intensities and suit well for detection in environmental samples. LR-White resin was combined with FISH to localize bacteria in the gut. Probes were tested concerning uptake and signal intensities in the LR-White resin.

Quantification data revealed a big impact of DSS treatment and inflammation on the gut microbiota during DSS-induced colitis in wt as well as STAT1^{-/-} and Tyk2^{-/-}. Such shifts in abundances also occurred to phylotypes within the same family, pointing out the importance of a high phylogenetic resolution within family-level. In both DSS-treated and untreated mice, possible indicators emerged, including mucus degrading bacteria such as *Akkermansia muciniphila* and *Mucispirillum schaedleri* with its distinct spiral shape (Fig. D.1). In case of *Lachnospiraceae*, abundance shifts of two OTUs were contrary, as one indicated health status and the other increased during DSS treatment.

For analysis of possible mucin degradation, ¹⁵N- and ¹³C-labeled samples were analyzed with NanoSIMS. Measurements were performed on LR-White sections and whole cell samples, attached with agarose to an ITO coated glass slides. Compared to silicon sample carriers, ITO coated glass slides allowed imaging on the CLSM, which resulted in higher resolution and are the best option for fluorescence imaging and secondary ion mass spectrometry.

In summary, this study enlarges the already powerful methodological armament when it comes to analysis of the bacterial composition in gut microbiota and its structure and function. It also highlights the significance of a 16S rRNA analysis with FISH based on phylotype-, or species-level.

E.1 Zusammenfassung

Diese Studie behandelt die Anwendung von FISH zur Identifikation und Quantifizierung von Bakterien im Darm. Um eine detaillierte Analyse der bakteriellen Zusammensetzung gewährleisten zu können, müssen Sonden anhand von aktuellen phylogenetischen Datensätzen bezüglich 16S rRNA erstellt werden. Das setzt eine Neuevaluierung bereits bestehender Sonden voraus. Im Speziellen wurde die bereits bestehende Sonde zur Detektion von *Akkermansia* spp. Akk1437 re-evaluiert und die Formamidkonzentration während der Hybridisierung optimiert. Um mehr Einsicht in die mikrobielle Diversität, vor allem während einer fortschreitenden Darmentzündung, zu erlangen, wurden Sonden für *Mucispirillum schaedleri*, *Lachnospiraceae* OTU_11021 und OTU_9468, *Bacteroides* OTU_9164 und *Ruminococcaceae* OTU_5807 entwickelt und evaluiert. Alle Sonden zeigten sehr gute Signalintensitäten und eignen sich für die Verwendung in Umweltproben. Für die Lokalisierung von Bakterien im Darm wurde das Einbettungsmedium LR-WHITE mit FISH kombiniert und bezüglich Aufnahme und Signalintensitäten von Sonden getestet.

Quantifizierungsdaten zeigten in wt-, als auch in STAT1^{-/-}- und Tyk2^{-/-}-Mäusen, dass eine Behandlung mit DSS einen großen Einfluss auf Entzündungsreaktionen und die bakterielle Ökologie hat. Veränderungen in der Häufigkeit bestimmter Mikroorganismen wurden auch auf Familien-Ebene festgestellt, was die Bedeutung von einer hohen phylogenetischen Auflösung auf Familien-Ebene unterstreicht. Sowohl in Mäusen, welche mit DSS behandelt wurden, als auch in unbehandelten Mäusen, wurden mögliche Indikatoren erfasst. Hierzu zählen mucusabbauende Bakterien wie *Akkermansia muciniphila* und das spiralförmige *Mucispirillum schaedleri* (Fig. D.1). Im Falle von *Lachnospiraceae* wurden zwei Indikator-OTUs detektiert, die während einer Behandlung mit DSS und einer fortschreitenden immunologischen Reaktion in ihrer Häufigkeit zunehmen beziehungsweise abnehmen.

Um den Abbau von Mucus zu analysieren wurden ¹⁵N- und ¹³C-markierte Proben mit dem NanoSIMS gemessen. Sowohl dehydrierte Umweltproben als auch LR-WHITE-Schnitte wurden vor der Messung mit Agarose auf einem ITO beschichteten Objektträger aus Glas fixiert. ITO beschichtete Objektträger aus Glas ermöglichen, im Vergleich zu Objektträgern aus Silizium, eine Auswertung am CLSM, was eine höhere Auflösung ermöglicht, und sind die beste Wahl für Fluoreszenzmikroskopie und SIMS.

Diese Studie erweitert das umfassende methodologische Spektrum in der Analyse der

bakteriellen Zusammensetzung im Darm und ihre Struktur und Funktion. Sie zeigt auch die Bedeutung von 16S rRNA Analysen via FISH auf Phylotyp- und Spezies-Ebene.

F Appendix

The appendix includes a comprehensive probe list of 64 already designed and evaluated probes targeting members of the gut microbiota and describes additional methods performed during this study.

Table F.1. List of published probes specific for gut microbiota. According to reference articles no formamide was used for oligonucleotides with a given temperature of dissociation T_d . If formamide was added to buffer, hybridization temperature was 46 °C.

Probe name	Specificity	Probe sequence (5' – 3') ¹	T_d ²	Formamide [%] ³	Lysozyme treatment	Reference
ASF519	<i>Bacteroides</i> sp. ASF519	GACTCTGTTTCCAGAGCTGTCAATA	50			Momose et al., 2011
Ato291	<i>Atopobium</i> cluster	GGTCGGTCTCTCAACCC	50			Harmsen et al., 2000
Bac303	<i>Bacteroides</i> , <i>Prevotella</i>	CCAATGTGGGGGACCTT	49			Manz et al., 1996
Bacid 1	<i>Bacteroides</i> <i>acidifaciens</i> group 1	AACATGTYTCCACGTTATTCAGG	50			Momose et al., 2011
Bacid 2	<i>Bacteroides</i> <i>acidifaciens</i> group 2	AACATGTTTCCACATTATTCAGG	50			Momose et al., 2011
Bacid3	<i>Bacteroides</i> <i>acidifaciens</i> group 3	GGCATGTCTCCACGCCGTTTCATT	50			Momose et al., 2011
Bcac	<i>Bacteroides caccae</i>	TAAAACCCATGCGGGAAATATATGC	50			Momose et al., 2011
Bdis 656	<i>Bacteroides distasonis</i>	CCGCCTGCCTCAAACATA	50			Franks et al., 1998
Bfra602	<i>Bacteroides fragilis</i>	GAGCCGCAAACCTTTCACAA		30		Franks et al., 1998
Bfra998	<i>Bacteroides fragilis</i>	GTTTCCACATCATTCCACTG	50			Rigottier-Gois et al., 2003
Bifl64	<i>Bifidobacterium</i>	CATCCGGCATTACCACCC		20		Langendijk et al., 1995
Bot	<i>Bacteroides ovatus</i> , <i>Bacteroides</i> <i>thetaiotaomicron</i>	GCCTTACGGCTATACTGTT	50			Momose et al., 2011

Probe name	Specificity	Probe sequence (5' – 3') ¹	T _d ²	Formamide [%] ³	Lysozyme treatment	Reference
Bova	<i>Bacteroides ovatus</i>	CAACAGCCTTACGGCTA	50			Momose et al., 2011
Bthe	<i>Bacteroides thetaiotaomicron</i>	CATTGCGCTTGCGGCTA	50			Momose et al., 2011
Buni	<i>Bacteroides uniformis</i>	GACATGTCTCCACATCATTCACT	50			Momose et al., 2011
Bvulg1017	<i>Bacteroides vulgatus</i>	ATTAATCTTCCTTTCAGAAGGCTGT	50			Rigottier-Gois et al., 2003
Chis150	<i>Clostridium</i> cluster I and II	TTATGCGGTATTAATCTYCCTTT		30		Franks et al., 1998
Clep866	<i>Ruminococcus albus</i> , <i>Ruminococcus flavefaciens</i> , <i>Ruminococcus bromii</i> , <i>Ruminococcus callidus</i> , <i>Faecalibacterium prausnitzii</i> , <i>Clostridium leptum</i> , <i>Clostridium sphaerophagum</i> , <i>Eubacterium siraeum</i>	GGTGGATWACTTATTGTG		30		Lay, 2005
Clep886 Competitor 1		GGTGGAAWACTTATTGTG		30		Lay, 2005
Clep886 Competitor 2		GGTGGATWACTTATTGCG		30		Lay, 2005

Probe name	Specificity	Probe sequence (5' – 3') ¹	T _d ²	Formamide [%] ³	Lysozyme treatment	Reference
Clit135	<i>Clostridium</i> cluster XI	GTTATCCGTGTGTACAGGG	51			Franks et al., 1998
Cor653	<i>Coriobacterium</i> and <i>Collinsella</i>	CCCTCCCMTACCGGACCC	50			Harmsen et al., 2000b
Cvir1414	<i>Clostridium viride</i> , <i>Eubacterium plautii</i>	GGGTGTTCCCGRCTCTCA		30		Lay, 2005
Cvir1414 Competitor 1	<i>Clostridium colgenvo</i> , AB009186	GGGTGTTDCCGRCTCTCA		30		Lay, 2005
Cvir1414 Competitor 2	AB009232	GGGTGTTCCCGRCTTTCA		30		Lay, 2005
Cvir1414 Competitor 3	<i>Fusobacterium praus</i>	GGGTCCCCCGRCTCTCA		30		Lay, 2005
Ebar1237	<i>Eubacterium barkeri</i>	AAUGGGUUGGGACAAAGG	51			Schwartz, 2000
Ebif462	<i>Eubacterium biforme</i>	GGGAAUGAUGAGUGAGUG	51			Schwartz, 2000
Econ1122	<i>Eubacterium</i> <i>contortum</i>	AGUAGCCAGCGGUUUAGGCC	51			Schwartz, 2000
Ecyl387	<i>Eubacterium</i> <i>cylindroides</i> , <i>Clostridium innocuum</i> , <i>Eubacterium biforme</i> , <i>Eubacterium</i> <i>tortuosum</i> , <i>Eubacterium dolichum</i> , <i>Streptococcus</i>	CGCGGCATTGCTCGTTCA		20		Harmsen, 2002

Probe name	Specificity	Probe sequence (5' – 3') ¹	T _d ²	Formamide [%] ³	Lysozyme treatment	Reference
Ecyl461	<i>pleomorphus</i> <i>Eubacterium</i>	AGGGAAUGAUCCGUGGGU	51			Schwartz, 2000
Edes635	<i>cylindroides</i> <i>Eubacterium</i>	AGACCARCAGTTTTGAAA		30	10 min	Lay, 2005
Edol183	<i>desmolans</i> <i>Eubacterium dolichum</i>	CGAGGCAUCUCGGAGACA	51			Schwartz, 2000
Ehad579	<i>Eubacterium hadrum</i>	CGUAGGUGGUAUGGCAAGUC	54			Schwartz, 2000
Ehal1469	<i>Eubacterium hallii</i> , <i>Clostridium</i> <i>herbivorans</i> , <i>Clostridium</i> <i>polysaccharolyticum</i>	CCAGTTACCGGCTCCACC		20		Harmsen, 2002
Elen194	<i>Eubacterium lentum</i>	AAAGCCCAGACGGCAAGG	51			Schwartz, 2000
Elim1433	<i>Eubacterium limosum</i>	AGCCUGUGAGAGAACCGC	51			Schwartz, 2000
Emon84	<i>Eubacterium</i> <i>moniliforme</i>	CGGGAAAUGGAUUAGCGG	51			Schwartz, 2000
Enter1432	<i>Enterobacter</i>	CTTTTGCAACCCACT				Sghir et al., 2000
Erec482	<i>Clostridium coccoides</i> , <i>Eubacterium rectale</i>	GCTTCTTAGTCARGTACCG	52			Franks, 1998
Even66	<i>Eubacterium</i> <i>ventriosum</i>	CGAAGCACCUUGGACAGA	55			Schwartz, 2000

Probe name	Specificity	Probe sequence (5' – 3') ¹	T _d ²	Formamide [%] ³	Lysozyme treatment	Reference
Fprau645	<i>Faecalibacterium prausnitzii</i>	CCTCTGCACTACTCAAGAAAAAC	50			Suau, 2001
Lab158	<i>Lactobacillus</i> , <i>Enterococcus</i>	GGTATTAGCAYCTGTTTCCA		10		Harmsen, 1999
Lach571	<i>Lachnospiraceae</i> cluster XIVa: <i>Lachnospiraceae</i> <i>multipara</i> , <i>Eubacterium eligens</i> , <i>Lachnospiraceae</i> <i>pectinoschiza</i>	GCCACCTACACTCCCTTT		40		Harmsen, 2002
Pdis	<i>Parabacteroides distasonis</i>	CCGCCTGCCTCAAACATA	50			Franks et al., 1998
Phasco741	<i>Phascolarctobacterium faecium</i> , <i>Acidaminococcus fermentans</i> , <i>Succiniclasticum ruminis</i>	TCAGCGTCAGACACAGTC		0		Harmsen, 2002
Prop853	<i>Clostridial</i> cluster IX	ATTGCGTTAACTCCGGCAC	50			Walker et al., 2005
Rbro730	Cluster IV: <i>Clostridium</i>	TAAAGCCCAGYAGGCCGC		20	15 min	Harmsen, 2002

Probe name	Specificity	Probe sequence (5' – 3') ¹	T _d ²	Formamide [%] ³	Lysozyme treatment	Reference
	<i>sporosphaeroides</i> , <i>Clostridium leptum</i> , <i>Clostridium</i> <i>methylopentosum</i> , <i>Ruminococcus bromii</i>					
Rbro730 Competitor 1	<i>Ruminococcus albus</i>	TAAAGCCCAGYAAGCCGC		30		Lay, 2005
Rbro730 Competitor 2	<i>Fusobacterium praus</i>	GGTGCCCAGYAGGCCGC		30		Lay, 2005
Rcal733	<i>Ruminococcus callidus</i>	CAGTAAAGGCCCAGTAAGCC		30		Lay, 2005
Rcal733 Competitor	<i>Ruminococcus</i> <i>flavefaciens</i>	CAGTAAAAGCCCAGTAAGCC		30		Lay, 2005
Rfla729	Cluster IV: <i>Ruminococcus albus</i> , <i>Ruminococcus</i> <i>flavefaciens</i>	AAAGCCCAGTAAGCCGCC		20	15 min	Harmsen, 2002
Rfla729	<i>Ruminococcus albus</i> , <i>Ruminococcus</i> <i>flavefaciens</i>	AAAGCCCAGTAAGCCGCC		30		Lay, 2005
Rfla729 Competitor 1	<i>Clostridium sporosph</i>	AAAGCCCAGTAGGCCGCC		30		Lay, 2005
Rfla729 Competitor 2	<i>Clostridium leptum</i>	AAGGCCCAGTAAGCCGCC		30		Lay, 2005
Rfla729 Competitor 3	<i>Eubacterium siraeum</i>	AAAGCCCAGCAAGCCGCC		30		Lay, 2005
Rfla729 Competitor 4	<i>Clostridium colinum</i>	TCAGTCCAGTAAGCCGCC		30		Lay, 2005

Probe name	Specificity	Probe sequence (5' – 3') ¹	T _d ²	Formamide [%] ³	Lysozyme treatment	Reference
Rint623	<i>Roseburia</i> cluster	TTCCAATGCAGTACCGGG	54			Hold et al., 2003
Rint623 helper probe		GTTGAGCCCCGGGCTTT	54			Aminov et al., 2006
Rrec584	<i>Roseburia</i> subcluster	TCAGACTTGCCGYACCGC	54			Walker et al., 2005
Strc493	<i>Streptococcus/Lactoco</i> <i>ccus</i>	GTTAGCCGTCCCTTTCTGG	50		10 min	Franks et al., 1998
Strc493 Competitor	<i>Lactobacillus lactis</i> , <i>Lactobacillus mesente</i>	TTTAGCCGTCCCTTTCTGG		30		Lay, 2005
Veil223	<i>Veillonella dispar</i> , <i>Veillonella parvula</i> , and <i>Veillonella atypica</i>	AGACGCAATCCCCTCCTT		0		Harmsen, 2002

¹ Abbreviations according to IUPAC:

M = A/C; R = A/G; W = A/T; Y = C/T

² Temperature of disassociation

³ Formamide concentration with high stringency. Values in brackets show the formamide concentration used for FISH analysis in this study.

F.1 IRMS sample preparation

F.1.1 Chemicals used

Table F.2. Chemicals used

Chemicals	Manufacturer
Acetic acid	Carl Roth GmbH & Co., Karlsruhe, Germany
Acetonitrile	Carl Roth GmbH & Co., Karlsruhe, Germany
Ammoniumbicarbonat	Fluka Chemie AG, Buchs, Switzerland
Ammonium persulfat (APS)	GE Healthcare Bio-Sciences AB, Uppsala, Sweden
Ammonium sulfate (NH ₄) ₂ SO ₄	Carl Roth GmbH & Co., Karlsruhe, Germany
Coomassie Brilliant Blue G-250	Carl Roth GmbH & Co., Karlsruhe, Germany
Dithiothreitol (DTT)	Fluka Chemie AG, Buchs, Switzerland
Guanidinium chloride reduction buffer	Carl Roth GmbH & Co., Karlsruhe, Germany
Iodoacetamide	Sigma-Aldrich Chemie GmbH, Steinheim, Germany
Methanol	Carl Roth GmbH & Co., Karlsruhe, Germany
Orthophosphoric acid	Carl Roth GmbH & Co., Karlsruhe, Germany
Polyacrylamide	Carl Roth GmbH & Co., Karlsruhe, Germany
Tetramethylethylenediamin (TEMED)	Carl Roth GmbH & Co., Karlsruhe, Germany
Trifluoroacetic acid	Sigma-Aldrich Chemie GmbH, Steinheim, Germany
Trypsin Gold MS-Grade	Promega, Madison, WI, USA

F.1.2 Disposable items

Table F.3. Disposable items used

Disposable item	Manufacturer
Amicon Ultra centrifugal filters – 0,5 ml 10K	Millipore GmbH, Vienna, Austria
Protein LoBind Tubes	Eppendorf AG, Hamburg, Germany
MultiScreen 96-well plates	Millipore Corporation, Billerica, MA, USA

F.1.3 Technical Equipment

Table F.4. Technical equipment used

Instrument	Manufacturer
Concentrator 5301	Eppendorf AG, Hamburg, Germany
Heatblock VWR Digital Heatblock	VWR international, West Chester, PA, USA
Mini-PROTEAN Casting Stand Mini-PROTEAN Tetra Cell	Bio-Rad Laboratories GmbH, Munich, Germany
OHAUS® Analytical Plus balance	Ohaus Corporation, Pine Brook, NJ, USA
Platform Shaker 2300	New Brunswick Co., Inc., Madison NJ, USA
PocketBloc® Thermomixer	Biozym Scientific GmbH, Hessisch Oldendorf, Germany
Sartorius BL 3100	Sartorius AG, Göttingen, Germany
SpeedVac	Bachhofer, Reutlingen, Germany

F.1.4 Buffers and solutions

Table F.5. Components of upper buffer

Ingredient	Quantity
Tris HCl	30,3 g
10% SDS	20 ml
MQ	ad 500 ml

Table F.6. Components of lower buffer

Ingredient	Quantity
Tris HCl	90,8 g
10% SDS	20 ml
MQ	ad 500 ml

Table F.7. Components of upper gel

Ingredient	Quantity
Upper buffer	0,63 ml
MQ	1,63 ml
30% Polyacrylamide	0,38 ml
APS	17,5 µl
TEMED	10 µl

Table F.8. Components of lower gel

Ingredient	Quantity
Lower buffer	2 ml
MQ	3,33 ml
30% Polyacrylamide	2,66 ml
APS	40 µl
TEMED	8 µl

Table F.9. Coomassie (colloidal) solution

Ingredient	Quantity
(NH ₄) ₂ SO ₄	100 g
Orthophosphoric acid	20 g
Methanol	25%
Coomassie Brilliant Blue G-250	0,625 g
MQ	ad 1000 ml

Table F.10. Fixing solution

Ingredient	Quantity
Ethanol	40%
Acetic acid	10%
MQ	ad 1000 ml

Table F.11. ABC-Buffer

Ingredient	Quantity
Ammoniumbicarbonat	198 mg
MQ	ad 50 ml

ABC-Buffer + DTT

15 mg/ml DTT were added to ABC-Buffer

Iodoacetamide solution

10 mg/ml Iodoacetamide were added to ABC-Buffer

F.1.5 Isopycnic fractionation of secreted mucosa (Davies and Carlstedt, 2000)

0,5 ml 6M guanidinium chloride reduction buffer containing 10 mM DTT was added to samples and incubated for approximately 5 h at 37 °C. Iodoacetamide was added to give a 25 mM solution and incubated O/N in dark at RT. Samples were transferred to Amicon Ultra-0,5 MILLIPORE filter tubes and centrifuged at 4 °C at a speed of 14000 g for 20 minutes. Supernatant was collected and used for SDS-PAGE.

F.1.6 SDS-PAGE

SDS-PAGE gels with a concentration of 10% were produced by pouring lower gel and covered with Isopropanol for at least 20 min to solidify. Isopropanol was decanted, upper gel poured and combs including 10 slots applied. The samples were mixed with Laemmli-buffer (1x) in ratio 1:1 and 6 µl used per slot. A voltage of 110 V was applied for 90 minutes. For each sample, a whole 10-lane-gel was used (2x 170 kD marker; 8 lanes with 6 µl sample mix each).

Gels were washed for 5 minutes with MQ and fixed for 20 minutes in fixing solution. After washing 2 x 10 minutes with MQ, gel was transferred to Coomassie (colloidal) solution O/N and washed 2 x 30 minutes with MQ. Gel bands were excised on a glass petri dish with a standard scalpel and transferred to 1,5 ml tubes to be prepared for MS.

F.1.7 Trypsin digest

F.1.7.1 Destaining of gel

Each excised gel band was covered with 300 µl ABC-buffer and 240 µl acetonitrile and shook for 15 min at 900 rpm at 20 °C several times until gel was destained. Gel pieces were covered in acetonitrile and placed on a shaker for 5 minutes, after which they were spin-dried.

F.1.7.2 Reduction and Alcylation

200 µl ABC+DTT were applied to sample and mixed for 30 minutes (56 °C, 900 rpm). ABC-

buffer was removed and after acetonitrile was added for 5 minutes (20 °C, 900 rpm), 200 µl Iodoacetamide solution was applied and removed again.

F.1.7.3 Trypsin Gold digest

Gel bands were washed 3x in ABC-Buffer, incubated with acetonitrile for 5 minutes on a shaker and spin-dried. Samples were rehydrated on ice with 15 µl of Trypsin-solution (12,5 ng/µl) and covered with 300 µl ABC-buffer O/N at 37 °C. Digest was stopped by adding 34,65 µl 10% trifluoroacetic acid (end concentration 1%) and samples were sonicated with Ultrasonic cleaner (VWR International, Leuven, Belgium) in a water bath for 10 minutes. Supernatant was transferred to low binding protein tubes. In an additional extraction step 30 µl 0,1% trifluoroacetic acid were added to gel pieces and sonicated for 10 minutes. Supernatant of both extraction procedures was merged and stored at -80 °C.

F.1.8 Preparation for IRMS

Samples were dried up in the Speedvac and about 1 mg was weighed in tin cups and transferred to 96-well plates. Beforehand, tin cups were closed at the top and folded to small packages. In case of liquid samples, tin cups were placed upright into 1,5 ml tubes and filled with 40 µl of sample. After drying, samples were weighed.

Table F.12. Samples of plate 1 prepared for IRMS.

Sample ID	Sample type	Well	Empty tin cup (mg)	Tin cup with dried sample (mg)	Sample weight (mg)
F1_BS	Blood serum	A1	89,010	89,700	0,690
F2_BS	Blood serum	A2	88,640	89,320	0,680
F3_BS	Blood serum	A3	89,320	90,100	0,780
F4_BS	Blood serum	A4	88,990	89,630	0,640
F5_BS	Blood serum	A5	88,870	89,490	0,620
F6_BS	Blood serum	A6	88,540	88,960	0,420
F7_BS	Blood serum	A7	88,550	89,250	0,700
F8_BS	Blood serum	A8	88,540	89,180	0,640
F9_BS	Blood serum	A9	88,330	88,990	0,660
F10_BS	Blood serum	A10	88,620	89,180	0,560

Sample ID	Sample type	Well	Empty tin cup (mg)	Tin cup with dried sample (mg)	Sample weight (mg)
F11_BS	Blood serum	A11	89,020	89,710	0,690
F12_BS	Blood serum	A12	88,550	89,210	0,660
F13_BS	Blood serum	B1	88,260	88,910	0,650
F14_BS	Blood serum	B2	88,050	88,600	0,550
F15_BS	Blood serum	B3	89,500	90,380	0,880
F16_BS	Blood serum	B4	89,400	90,260	0,860
F17_BS	Blood serum	B5	88,820	89,560	0,740
F1_EF	Epithelial tissue	B7	88,450	88,830	0,380
F2_EF	Epithelial tissue	B8	89,600	89,850	0,250
F3_EF	Epithelial tissue	B9	89,040	89,180	0,140
F4_EF	Epithelial tissue	B10	89,040	89,150	0,110
F5_EF	Epithelial tissue	B11	88,650	89,270	0,620
F6_EF	Epithelial tissue	B12	88,930	89,540	0,610
F7_EF	Epithelial tissue	C1	87,800	88,830	1,030
F8_EF	Epithelial tissue	C2	88,690	89,880	1,190
F9_EF	Epithelial tissue	C3	88,620	88,960	0,340
F10_EF	Epithelial tissue	C4	88,300	89,500	1,200
F11_EF	Epithelial tissue	C5	88,750	89,710	0,960
F12_EF	Epithelial tissue	C6	88,330	88,650	0,320
F13_EF	Epithelial tissue	C7	89,310	90,410	1,100
F14_EF	Epithelial tissue	C8	89,430	90,590	1,160
F15_EF	Epithelial tissue	C9	88,450	89,630	1,180
F16_EF	Epithelial tissue	C10	88,810	89,700	0,890
F17_EF	Epithelial tissue	C11	88,420	89,300	0,880
F1_L	Lumen contents	D7	TARE		1,020
F2_L	Lumen contents	D8	TARE		0,730
F3_L	Lumen contents	D9	TARE		1,110
F4_L	Lumen contents	D10	TARE		1,100
F5_L	Lumen contents	D11	TARE		0,890
F6_L	Lumen contents	D12	TARE		1,150
F7_L	Lumen contents	E1	TARE		1,020
F8_L	Lumen contents	E2	TARE		0,890
F9_L	Lumen contents	E3	TARE		0,710

Sample ID	Sample type	Well	Empty tin cup (mg)	Tin cup with dried sample (mg)	Sample weight (mg)
F10_L	Lumen contents	E4	TARE		0,740
F11_L	Lumen contents	E5	TARE		1,200
F12_L	Lumen contents	E6	TARE		1,150
F13_L	Lumen contents	E7	TARE		0,890
F14_L	Lumen contents	E8	TARE		1,080
F15_L	Lumen contents	E9	TARE		1,190
F16_L	Lumen contents	E10	TARE		1,150
F17_L	Lumen contents	E11	TARE		1,140
AKK_L_G213	Lumen contents	F1	TARE		0,990
AKK_L_G214	Lumen contents	F2	TARE		1,110
AKK_L_G215	Lumen contents	F3	TARE		0,880
AKK_L_G216	Lumen contents	F4	TARE		0,680
AKK_L_G217	Lumen contents	F5	TARE		0,610
AKK_L_G218	Lumen contents	F6	TARE		1,000
AKK_L_G219	Lumen contents	F7	TARE		0,860
AKK_L_G220	Lumen contents	F8	TARE		0,830

Table F.13. Samples of plate 2 prepared for IRMS.

Sample ID	Sample type	Well	Empty tin cup (mg)	Tin cup with dried sample (mg)	Sample weight (mg)
F20_BS	Blood serum	A1	88,820	89,720	0,900
F21_BS	Blood serum	A2	88,840	89,730	0,890
F22_BS	Blood serum	A3	88,730	89,570	0,840
F23_BS	Blood serum	A4	89,630	90,570	0,940
F24_BS	Blood serum	A5	88,460	89,405	0,945
F25_BS	Blood serum	A6	89,290	90,120	0,830
F26_BS	Blood serum	A7	88,820	89,680	0,860
F27_BS	Blood serum	A8	88,250	89,090	0,840
F28_BS	Blood serum	A9	88,450	89,350	0,900
F29_BS	Blood serum	A10	88,430	89,300	0,870
F30_BS	Blood serum	A11	88,200	89,080	0,880
F31_BS	Blood serum	A12	87,910	88,730	0,820
F20_LS	Lumen contents	B1	TARE		0,980
F21_LS	Lumen contents	B2	TARE		1,010
F22_LS	Lumen contents	B3	TARE		1,260
F23_LS	Lumen contents	B4	TARE		0,946
F24_LS	Lumen contents	B5	TARE		1,210
F25_LS	Lumen contents	B6	TARE		1,183
F26_LS	Lumen contents	B7	TARE		1,100
F27_LS	Lumen contents	B8	TARE		1,050
F28_LS	Lumen contents	B9	TARE		1,100
F29_LS	Lumen contents	B10	TARE		0,960
F30_LS	Lumen contents	B11	TARE		1,110
F31_LS	Lumen contents	B12	TARE		0,990
Control 1	Mucosal proteins	C1	88,497	88,812	0,315
Control 2	Mucosal proteins	C2	88,251	88,563	0,312
Control 3	Mucosal proteins	C3	88,361	88,669	0,308
Control 4	Mucosal proteins	C4	88,617	88,918	0,301
Control 5	Mucosal proteins	C5	88,958	89,145	0,187
F3-1	Mucosal proteins	D1	88,635	88,855	0,220
F3-2	Mucosal proteins	D2	88,646	88,827	0,181
F3-3	Mucosal proteins	D3	88,492	88,664	0,172

Sample ID	Sample type	Well	Empty tin cup (mg)	Tin cup with dried sample (mg)	Sample weight (mg)
F3-4	Mucosal proteins	D4	89,229	89,440	0,211
F3-5	Mucosal proteins	D5	88,488	88,824	0,336
F5-1	Mucosal proteins	E1	89,281	89,334	0,053
F5-2	Mucosal proteins	E2	88,335	88,439	0,104
F5-3	Mucosal proteins	E3	88,299	88,439	0,140
F5-4	Mucosal proteins	E4	88,610	88,783	0,173
F5-5	Mucosal proteins	E5	88,615	88,710	0,095
F11-1	Mucosal proteins	F1	88,797	88,883	0,086
F11-2	Mucosal proteins	F2	88,639	88,712	0,073
F11-3	Mucosal proteins	F3	89,000	89,092	0,092
F11-4	Mucosal proteins	F4	87,961	88,071	0,110
F11-5	Mucosal proteins	F5	88,523	88,614	0,091

F.2 Creating a 16S-rRNA amplicon library for 454-pyrosequencing

F.2.1 Chemicals and disposable items

Table F.14. Chemicals and disposable items used

Chemicals	Manufacturer
1x Lysis Matrix A, 2 ml tubes	Qbiogene, Inc., CA, USA
10x ExTaq buffer	Fermentas Inc., Hanover, MD, USA
6x DNA Loading Dye	Fermentas Inc., Hanover, MD, USA
Agencourt AMPure XP 60 mL Kit	Beckman Coulter, Munich, Germany
Boric acid	Carl Roth GmbH & Co. KG, Karlsruhe, Germany
Bovine Serum Albumine (BSA; 20 mg/ml)	Carl Roth GmbH & Co KG, Karlsruhe, Germany
Cetyl trimethylammonium bromide (CTAB)	Carl Roth GmbH & Co KG, Karlsruhe, Germany
Ethidium bromide (EtBr)	Fluka Chemie AG, Buchs, Switzerland
Chloroform	Carl Roth GmbH & Co KG, Karlsruhe, GermanyLactan
Chloroform/Isoamylalkohol (24:1 mixture)	Carl Roth GmbH & Co KG, Karlsruhe, Germany
Diethylpyrocarbonate (DEPC)	Sigma-Aldrich Chemie GmbH, Steinheim, Germany
dNTP Mix (2 mM each)	Fermentas Inc., Hanover, MD, USA
Ficoll® 400	Sigma-Aldrich Chemie GmbH, Steinheim, Germany
Gene Ruler™ 1 kb DNA ladder	Fermentas Inc., Hanover, MD, USA
Magnesium chloride (MgCl ₂) (25 mM)	Fermentas Inc., Hanover, MD, USA
Orange G	Carl Roth GmbH & Co KG, Karlsruhe, Germany
Phenol/Chloroform/Isoamyl-Alcohol (25:24:1 mixture, pH 5.2)	Fisher Scientific, Germany
Potassium dihydrogen phosphate KH ₂ PO ₄	Carl Roth GmbH & Co KG, Karlsruhe, Germany

Quant-iT™ PicoGreen® dsDNA Kit	Invitrogen Corporation, Carlsbad, CA, USA
Sodium acetate	Carl Roth GmbH & Co KG, Karlsruhe, Germany

F.2.2 Technical equipment

Table F.15. Technical equipment used

Instrument	Manufacturer
Agarose gel electrophoresis apparatus	Bio-Rad Laboratories GmbH, Munich, Germany
Sub-Cell GT	
Beadbeater Fast Prep FP 120	Savant Instruments Inc. Holbrook, NY
CCD camera AxioCam HRc	Carl Zeiss MicroImaging GmbH, Jena, Germany
Electrophoresis power supply (PowerPac Basic)	Bio-Rad Laboratories GmbH, Munich, Germany
Icycler Thermal cycler	Bio-Rad Laboratories GmbH, Munich, Germany
Microwave MD6460	Microstar
NanoDrop ND-1000 UV/Vis spectrophotometer	Thermo Fisher Scientific, Germany
UV sterilizing PCR workstation	PeqLab Biotechnologie GmbH, Erlangen, Germany
Transilluminator UST-C30M-8R, 312 nm	Biostep GmbH, Jahnsdorf, Germany

F.2.3 Buffers and solutions

Table F.16. CTAB extraction buffer. Ingredients were combined and pH was adjusted to 8,0.

Ingredient	Quantity
10% CTAB (wt/vol) in 0,7M NaCl	50 ml
240 mM KH ₂ PO ₄	50 ml

Table F.17. 10x TBE buffer

Ingredient	Concentration (mmol/l)	Quantity (g/l)
Tris	890	107,8
Boric Acid	890	55
EDTA disodium salt dihydrate	20	7,4
MQ		ad 1l

Table F.18. 1x TBE buffer

10x TBE	100 ml/l
MQ	ad 1000 ml

Table F.19. Orange G loading dye

Ficoll	6 g
Orange G	100 mg
PCR water	ad 50 ml

Ethidium bromide staining solution

10 mg/ml Ethidium bromide stock solution was diluted 1:10000 in MQ.

DEPC-treatment

To remove RNase and Dnase liquids were treated with 0.1% (v/v) Diethylpyrocarbonate (Blumberg, 1987), stirred overnight and finally autoclaved.

Following table lists all primers used for PCR. For bcPCR, primers were tagged with sequencing adapters for GS FLX Titanium chemistry. Linker sequences were used for forward primer (CC) and reverse primer (TA). The reverse primer includes a 8 base barcode for identification.

Table F.20. Primers used for bcPCR.

Name ^a	Specificity	Sequence (5' - 3') ^b	T _a [°C] ^c
1492*R	Most bacteria	NTACTTTGTTACGACT	52
909F	Most bacteria	ACTCAAAGGAATWGACGG	52
TiB-909F	Most bacteria	CTATGCGCCTTGCCAGCCCGCTCAGCCA CTCAAAGGAATWGACGG	52
Barcoded reverse primer	Most bacteria		52

^a F: Forward primer binds to complementary 16S-rRNA strand; R: Reverse primer binds to identical 16S-rRNA strand

^b abbreviations according to IUPAC:

K = G/T; N = A/G/C/T; W = A/T

^c Annealing-temperature of primer used for PCR

F.2.4 Extraction and Purification Procedure for RNA and DNA (adapted from Griffiths et al., 2000)

1. Cool down the centrifuge to 4 °C
2. Label one bead-beating tube (Lysis Matrix A) and three 1,5 ml tubes per sample.
3. Add 500 µl of CTAB extraction buffer and 500 µl phenol-chloroform-isoamyl alcohol to the sample and transfer to bead beating tube.
4. Bead-beat for 30 seconds at 5.5 m/s.
5. Let samples cool down on ice.
6. Centrifuge at 13,000 rpm for 5 minutes at 4 °C and transfer upper, aqueous phase into a new 1,5 ml tube.
7. Add a further 500 µl of CTAB extraction buffer and 500 µl phenol-chloroform-isoamyl alcohol to the bead beating tube and lyse for 30 seconds at 5,5 m/s in the bead beater.
8. Centrifuge at 13,000 rpm for 5 minutes at 4 °C and combine the aqueous phase with that previously collected.
9. Add 1 volume (1 ml) of chloroform-isoamyl alcohol and spin at 13,000 rpm for 5 minutes at 4 °C.
10. Transfer upper, aqueous phase into a new 1,5 ml tube
11. Add: 0,1 volume (50 µl) 3M sodium acetate and 0,6 volume ice-cold isopropanol (300 µl) and mix by inversion.
12. Precipitate nucleic acids for at least 2 hours at room temperature.

13. Centrifuge at 13,000 rpm for 5-10 minutes and remove supernatant.
14. Wash the pelleted nucleic acids in 500 µl of ice cold 70% ethanol, centrifuge at 14,000 rpm for 2-10 minutes and remove supernatant.
15. Dry nucleic acids at RT.
16. Resuspend the pellet in 50 µl of DEPC treated MQ and place on shaking incubator for 20 minutes at 30°C to facilitate dissolving of the pellet.
17. Calculate quantity of nucleic acids extracted using the NanoDrop spectrophotometer.
18. Store extracted nucleic acids at -80°C.

F.2.5 Amplification of 16S rRNA-genes via 2-step bcPCR (Berry et al., 2011)

Standard reaction mix (25 µl) - step 1

MgCl ₂	2 µl
Buffer (10 x)	2,5 µl
dNTP-mix	1 µl
Taq DNA polymerase	0,1 µl
Primer 909F (50 pmol/µl)	0,5 µl
Primer 1492*R (50 pmol/µl)	0,5 µl
BSA	0,125 µl
Template	0,5 µl
PCR water	ad 25 µl

Table F.21. Conditions for the amplification of 16S-rRNA gene fragments

PCR-step	Temp. [°C]	Time	Number of cycle
Denature	95	4 min	1
Denature	95	30s	20
Anneal	52	30s	
Elongation	72	1 min	
Finale Elongation	72	7 min	1

To avoid unequal pipetting, a mastermix was created by adding all components except for nucleic acids from sample and distributed to equal amounts to PCR tubes. After adding 1 µl of nucleic acids (50-100 ng/µl), tubes were mixed and reactions were started. A negative control was also included.

Standard reaction mix (50 µl) - step 2

MgCl ₂	2 µl
Buffer (10 x)	2,5 µl
dNTP-mix	2,5 µl
Taq DNA polymerase	0,1 µl
Primer F (100 pmol/µl)	0,25 µl
Primer R (100 pmol/µl)	0,25 µl
BSA	0,125 µl
Orange G loading dye	1,25 µl
PCR product from step 1	0,5 µl
MQ	ad 25 µl

Table F.22. Conditions for the amplification of 16S rRNA gene fragments

PCR-step	Temp. [°C]	Time	Number of cycle
Denature	95	4 min	1
Denature	95	30s	5
Anneal	52	30s	
Elongation	72	1 min	
Finale Elongation	72	7 min	1

A mastermix was created by adding all components except for nucleic acids from sample and individually labeled reverse primer and distributed to equal amounts to PCR tubes. After adding reverse primer, tubes were mixed and transferred to three additional tubes. 1 µl of PCR product from step 1 was added to three of these tubes and one remained as negative control. Tubes were mixed, reactions were started and controlled with agarose gel electrophoresis.

Agarose was weighed and mixed with 1x TBE-buffer to give a 2% solution and molten in a microwave and then poured into a gel slide (Sub-Cell GT UV-Transparent Gel Tray, 15 x 15 cm, Biorad) including a comb. After polymerization, gel was embedded in 1x TBE-buffer into gel-electrophoresis device (Sub-Cell GT, Biorad). Samples were pipetted into gel slots, GeneRuler™ 1 kb DNA Ladder 250–10000 was applied to outer slots of the gel and a voltage of 110V was applied. After 45 minutes, gel was stained with EtBr (Sigma-Aldrich) for 20 minutes and checked for amplified 16S-rRNA gene products with UV light from Transilluminator (UST-30M-8E, Biostep GmbH). Triplicates of PCR products were purified with Agencourt AMPure XP Kit according to manufactures instructions, pooled and

concentrated to 30 µl elution buffer. Quantification of amplified 16S-rRNA genes was performed with Quant-iT™ PicoGreen® dsDNA Kit. An amount of 40 ng per sample was transferred to a 1,5 ml tube, including a control plasmid. 5 µl from this mix were run on an 2% agarose gel at 110 V for 45 minutes, stained and digitalized. Amplicons were sequenced from the reverse side. Sequencing was performed on a GS FLX instrument using Titanium chemistry (454 Life Sciences) at the Norwegian High-Throughput Sequencing Centre (NSC).

Table F.23. Sample IDs with corresponding barcodes, tube labels and concentrations of purified PCR products from 1st pyrosequencing run.

Sequencing sample ID	Barcode ID	Tube label	Concentration (ng/µl)
AGR_1	332	AGR 38	19,26
AGR_1	40	AGR 39	37,81
AGR_1	92	AGR 40	42,35
AGR_WT1	73	AGR 41	18,56
AGR_WT2	132	AGR 42	32,33
AGR_WT3	353	AGR 43	33,09
G1_d0	28	G1	28,89
G2_d0	36	G2	32,66
G3_d0	86	G3	22,93
G10_d14	157	1	17,00
G11_d14	205	4	17,05
G12_d14	247	7	16,72
G19_d33	201	10	16,90
G20_d33	816	13	17,16
G21_d33	288	16	11,92
G27_d58	87	19	17,29
G28_d58	213	22	13,37
G29_d58	838	25	14,69
G30_d58	869	28	17,95
G31_d58	198	31	17,15
G32_d58	148	34	19,31
G33_d58	234	37	16,41
G34_d58	155	40	13,11
G34_d0	141	43	18,60
G35_d0	866	46	18,98
G36_d0	149	49	19,93

Sequencing sample ID	Barcode ID	Tube label	Concentration (ng/μl)
G43_d0	150	52	14,95
G44_d0	155	55	23,10
G45_d0	156	58	25,71
G46_d0	116	61	9,27
G47_d0	168	64	22,26
G45_d7	198	82	15,02
G46_d7	151	85	15,57
G47_d7	305	88	14,10
G34_d14	225	91	20,53
G35_d14	208	94	15,57
G36_d14	210	97	13,59
G43_d14	88	100	8,41
G44_d14	228	103	19,80
G45_d14	232	106	23,39
G46_d14	246	109	30,68
G47_d14	316	112	29,50
G34_d20	310	115	28,00
G35_d20	246	118	30,04
G36_d20	318	121	24,61
G43_d20	403	124	22,40
G44_d20	410	127	14,13
G45_d20	418	130	18,45
G46_d20	419	133	25,97
G47_d20	451	136	8,05
G34_d24	160	139	17,21
G35_d24	176	142	17,57
G36_d24	290	145	15,55
G44_d24	317	151	12,49
G45_d24	204	154	8,39
G46_d24	206	157	23,66
G47_d24	360	160	24,53
G34_d33	407	163	13,26
G35_d33	409	166	12,12
G36_d33	534	169	14,97
G43_d33	556	172	13,84

Sequencing sample ID	Barcode ID	Tube label	Concentration (ng/μl)
G44_d33	448	175	8,82
G45_d33	572	178	21,81
G46_d33	647	181	18,74
G47_d33	649	184	8,60
G34_d39	102	187	21,24
G36_d39	458	193	9,41
G43_d39	449	196	24,27
G44_d39	514	199	9,71
G45_d39	442	202	18,41
G46_d39	77	205	16,38
G47_d39	104	208	21,72
G34_d52	676	211	12,65
G35_d52	677	214	15,91
G36_d52	254	217	11,63
G43_d52	157	220	13,45
G44_d52	172	223	13,29
G45_d52	205	226	14,31
G46_d52	288	229	14,23
G47_d52	234	232	9,53
G44_d58	147	247	11,78
G45_d58	173	250	19,94
G47_d58	26	256	19,73
FT_R0	74	I	9,56
FT_R1	119	II	30,19
FT_R2	115	III	10,02
FT_D1	755	IV	37,61
FT_D2	879	V	37,63
plasmid_759	759	759	13,95

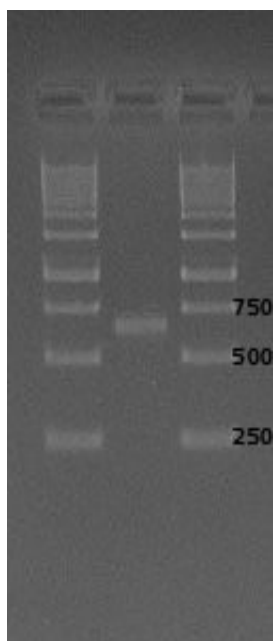


Figure F.1. Image of 2% agarose gel showing 16S-rRNA amplicons between 1kb GeneRuler (outer lanes).

Table F.24. Sample IDs with corresponding barcodes, experiment sample IDs and concentrations of purified PCR products from 2nd pyrosequencing run.

Sequencing sample ID	Barcode ID	Experimental sample ID	Concentration (ng/μl)
GATA1	92	I B	1,17
GATA2	132	II B	2,15
GATA3	88	III B	1,99
GATA4	160	I A	17,62
GATA5	168	II A	12,63
GATA6	806	III A	8,38
GATA7	812	IV B	1,25
GATA8	198	V B	16,55
GATA9	201	VI B	2,30
GATA10	204	IV A	14,93
GATA11	205	V A	13,33
GATA12	206	VI A	14,53
GATA13	232	VII B	14,04
GATA14	234	VIII B	4,34
GATA15	254	IV B	12,42
GATA16	288	VII A	2,42
GATA17	290	VIII A	14,82
GATA18	293	IV A	4,03

Sequencing sample ID	Barcode ID	Experimental sample ID	Concentration (ng/μl)
GATA19	301	X B	3,94
GATA20	332	XI B	18,11
GATA21	336	XII B	3,43
GATA22	353	X A	3,69
GATA23	360	XI A	15,18
GATA24	368	XII A	14,03
I1	208		1,51
I2	210		6,15
I3	213		6,71
I4	225		14,37
I5	228		12,59
I6	246		6,91
I7	247		13,54
I8	305		12,63
I9	310		12,03
I10	316		1,41
I11	317		12,80
I12	318		9,91
I13	403		4,52
I14	407		31,44
I15	409		5,35
I16	410		1,68
I17	418		18,31
I18	816		17,56
I19	838		14,67
I20	866		15,11
I21	869		15,95
I22	879		14,79
I23	419		12,60
I24	442		15,25
I25	448		15,89
I26	451		7,29
I27	458		13,76
I28	487		3,09
I29	499		18,24

Sequencing sample ID	Barcode ID	Experimental sample ID	Concentration (ng/μl)
I30	514		16,63
I31	534		19,46
I32	556		24,60
I33	572		14,00
I34	647		14,07
I35	649		12,73
I36	676		15,80
I37	677		29,25
I38	26		17,42
I39	28		22,11
I40	36		19,43
Tyk1	86		16,68
Tyk2	176		25,31
Tyk3	8		18,33
Tyk4	23		13,87
Tyk5	150		16,20
Tyk6	151		24,78
Tyk7	155		17,35
Tyk8	156		14,65
Tyk9	157		20,50
ATM1	102	5356 (.4)	12,44
ATM2	104	5390 (.2)	16,04
ATM3	115	5412 (.8)	13,81
ATM4	116	5350 (.6)	14,93
ATM5	119	5392 (.5)	13,84
ATM6	173	5415 (.3)	6,33
ATM7	701	1149 (.2)	4,99
ATM8	709	1255 (.6)	6,12
ATM9	755	1384 (.4)	1,98
ATM10	756	1148 (.1)	5,82
ATM11	40	A-1253	14,65
ATM12	64	1385 (.5)	4,42
ATM13	73	5403 (.1)	6,22
ATM14	74	5416 (.4)	14,38
ATM15	77	5478 (.5)	15,91

Sequencing sample ID	Barcode ID	Experimental sample ID	Concentration (ng/μl)
ATM16	172	866 (.6)	15,46
ATM17	166	1009 (.4)	18,92
ATM18	149	1037 (.5.8)	14,90
ATM19	141	A 1460 (.3)	14,24
ATM20	147	1462 (.6)	1,41
ATM21	148	Ab 1465 (.1)	14,01
ATM22	763	1122 (.5)	15,10
ATM23	805	5384 (.2)	2,26
plasmid_759	759		13,95



Figure F.2. Image of 2% agarose gel showing 16S-rRNA amplicons between 1kb GeneRuler (outer lanes).

G List of abbreviations

%	Percent
% (v/v)	volume/volume percentage
°C	Degree Celsius
ΔG	Gibbs energy
ε	Molar factor of extinction
ρ	Specific resistance
μ	Micro (10^{-6})
Ω	Ohm
Ω -m	Ohmmeter
Ω /sq	Sheet resistance
^{15}N	Stable nitrogen isotope
16S rRNA	rRNA from the small ribosomal subunit
A	Adenin
ABC	Ammoniumbicarbonate
a.u.	Arbitrary unit
APS	Ammonium peroxy-disulfate
ARB	Software package for phylogenetic analysis (from lat. <i>arbor</i> , “tree”)
bc	barcoded
bp	Basepairs
BSA	Bovine serum albumin
C	Cytosin
cDNA	Complementary DNA
CLSM	Confocal laser scanning microscopy
CTAB	Cetrimonium bromide
Cy3	5,5'-di-sulfo-1,1'-di-(X-carbopentynyl)- 3,3,3',3'-tetra-methylindol-Cy3.18-derivative N-hydroxysuccimidester

Cy5	5,5'-di-sulfo-1,1'-di-(X-carbopentynyl)- 3,3,3',3'-tetra-methylindol-Cy5.18-derivative
DAIME	Nhydroxysuccimidester Digital image analysis in microbial ecology
ddH ₂ O	Double distilled and filtered water
DEPC	Diethylpyrocarbonate
DIC	Differential interference contrast
DNA	Deoxyribonucleic acid
dNTP	Desoxynucleotide triphosphate
dsDNA	Double-stranded DNA
DSM	Deutsche Sammlung von Mikroorganismen
DSS	dextran sodium sulfate
DTT	Dithiothreitol
EDTA	Ethylenediamine-tetraaceticacid
<i>et al.</i>	<i>Et alteri</i> (lat., “and others”)
EtBr	Ethidium bromide
EtOH	Ethanol
F	Forward (used for primer labeling)
FA	Formamide
Fig.	Figure
FISH	Fluorescence <i>in situ</i> hybridization
FLUOS	5,(6)-Carboxyfluorescein-N- hydroxysuccimidester
g	Gram or gravitational acceleration
G	Guanine
GIMP	GNU image manipulation program
h	hour(s)
HCl	Hydrochloric acid
HPLC	High Pressure Liquid Chromatography
IBD	Inflammatory bowel disease
ID	identification

IL	Interleukines
IRMS	Isotope-ratio mass spectrometry
ITO	Indium tin oxide
IUPAC	International union of pure and applied chemistry
K	Guanine or thymine
kb	Kilobases
KbL	kilobase-ladder
kcal	kilo calories
kDa	Kilo Dalton ($1,66018 \times 10^{-21}$ g)
KH_2PO_4	Potassium dihydrogen phosphate
l	Liter
LMD	Laser micro dissection
log	Logarithmic
LR	London Resin
m	milli (10^{-3}), meter(s)
M	Molar, adenine or cytosine
MeOH	Methanol
MgCl_2	Magnesium chloride
min	minutes
mRNA	Messenger ribonucleic acid
n	Nano (10^{-9})
N	Adenine, guanine, cytosine or thymine
NaCl	Sodium chloride
NaH_2PO_4	Di-sodium hydrogen phosphate
Na_2HPO_4	Sodium dihydrogen phosphate
NanoSIMS	Nano secondary ion mass spectrometry
NaOH	Sodium hydroxide
$(\text{NH}_4)_2\text{SO}_4$	Ammonium sulfate
<i>nov.</i>	<i>nova</i> (lat., “new”)
nt	nucleotides

O/N	Over night
OTU	Operational taxonomic unit
p	pico (10^{-12})
PAA	Poly-acrylamide
PBS	Phosphate buffered saline
PCR	Polymerase chain reaction
PFA	Paraformaldehyde
pH	<i>potentia hydrogenii</i> (lat. “ability of hydrogen)”
R	Reverse (used for primer labeling), adenine or guanine
rpm	Rounds per minute
rRNA	Ribosomal ribonucleic acid
RT	Room temperature
SDS	Sodium dodecyl sulfate
Si	silicon
SIMS	Secondary ion mass spectrometry
sp.	species (singular)
spp.	species (plural)
T	thymine
T _a	Annealing temperature
Taq	Thermostable DNA-polymerase from <i>Thermus aquaticus</i>
TBE	Tris-boron acid-EDTA
T _d	Temperature of dissociation
TEMED	Tetramethylethylenediamine
TNF	Tumor necrosis factor
Tris	Tris-(hydroxymethyl)-aminomethane
U	Units
UV	Ultraviolet
V	Volts
W	Adenine or thymine

wt	Wild type
x	times
\bar{x}	Mean
Y	Cytosine or thymine

H References

- A.H. Franks, H.J. Harmsen, G.C. Raangs, G.J. Jansen, F. Schut, G.W. Welling (1998). Variations of bacterial populations in human feces measured by fluorescent in situ hybridization with group-specific 16S rRNA-targeted oligonucleotide probes. *Appl. Environ. Microbiol.* 64:3336–3345.
- Alm EW, Oerther DB, Larsen N, Stahl DA, Raskin L. (1996). The oligonucleotide probe database. *Appl Environ Microbiol.* 62:3557–3559.
- Amann, R. I., B. J. Binder, R. J. Olson, S. W. Chisholm, R. Devereux, and D. A. Stahl (1990). Combination of 16S rRNA-targeted oligonucleotide probes with flow cytometry for analyzing mixed microbial populations. *Appl. Environ. Microbiol.* 56:1919-1925.
- Amann, R., Ludwig, W., and Schleifer, K. (1995). Phylogenetic identification and in situ detection of individual microbial cells without cultivation. *Microbiol Rev* 59, 143-169.
- Aminov RI et al. (2006). Molecular diversity, cultivation, and improved detection by fluorescent in situ hybridization of a dominant group of human gut bacteria related to *Roseburia* spp. or *Eubacterium rectale*. *Appl Environ Microbiol* 72:6371–6376.
- Backhed, F., Ley, R. E., Sonnenburg, J. L., Peterson, D. A. & Gordon, J. I. (2005). Host–bacterial mutualism in the human intestine. *Science* 307, 1915–1920
- Bandyopadhyay SK, Motte CA, Kessler SP, Hascall VC, Hill DR, Strong SA (2008). Hyaluronan-mediated leukocyte adhesion and dextran sulfate sodium-induced colitis are attenuated in the absence of signal transducer and activator of transcription 1. *Am J Pathol* 173:1361–1368.

Behrens, S., Losekann, T., Pett-Ridge, J., Weber, P. K., Ng, W. O., Stevenson, B. S., Hutcheon, I. D., Relman, D. A., and Spormann, A. M. (2008). Linking microbial phylogeny to metabolic activity at the single-cell level by using enhanced element labeling-catalyzed reporter deposition fluorescence in situ hybridization (EL-FISH) and NanoSIMS. *Appl Environ Microbiol* 74, 3143-3150.

Berry D, Ben Mahfoudh K, Wagner M, Loy A (2011). Barcoded pyrosequencing primers used in multiplex amplicon sequencing bias amplification. *Appl. Environ. Microbiol.* 77: 7846-7849.

Berry et al. (2012). Phylotype-level 16S rRNA analysis reveals new bacterial indicators of health state in acute murine colitis. *The ISME Journal.*, in press.

Braun J, Wei B (2007). Body traffic: Ecology, genetics, and immunity in inflammatory bowel disease. *Annu Rev Pathol: Mech Dis* 2:401-429.

Daims H, Brühl A, Amann R, Schleifer KH, Wagner M (1999). The domain-specific probe EUB338 is insufficient for the detection of all Bacteria: development and evaluation of a more comprehensive probe set. *Syst Appl Microbiol.* 22:434-44.

Daims H, Lückner S, Wagner M. 2006. daime, a novel image analysis program for microbial ecology and biofilm research. *Environ. Microbiol.* 8:200-213.

Daims, H., Stoecker, K., and Wagner, M. (2005). Fluorescence in situ hybridization for the detection of prokaryotes. *Advanced Methods in Molecular Microbial Ecology*, S.C. Osborn AM, ed. (Abingdon, UK: Bios-Garland), pp. 213-239.

Davies, Julia and Ingemar Carlstedt (2000). Isolation of large gel-forming mucins. *Methods in Molecular Biology* 125:3-13.

Decker T, Müller M, Stockinger S (2005). The yin and yang of type I interferon activity in bacterial infection. *Nat Rev Immunol* 5:675-687.

DeLong, E., Wickham, G., and Pace, N. (1989). Phylogenetic stains: ribosomal RNA-based probes for the identification of single cells. *Science* 243, 1360-1363.

Derrien M, Collado MC, Ben-Amor K, Salminen S, de Vos WM (2008). The Mucin degrader *Akkermansia muciniphila* is an abundant resident of the human intestinal tract. *Appl Environ Microbiol.* 74:1646-8.

Dianda L, Hanby AM, Wright NA, Sebesteny A, Hayday AC, Owen MJ (1997). T cell receptor-alpha beta-deficient mice fail to develop colitis in the absence of a microbial environment. *Am J Pathol* 150:91-97.

Egan LJ, Sandborn WJ (2004). Advances in the treatment of Crohn's disease. *Gastroenterology* 126:1574–81.

Elson CO, Cong Y, McCracken VJ, Dimmitt RA, Lorenz RG, Weaver CT (2005). Experimental models of inflammatory bowel disease reveal innate, adaptive, and regulatory mechanisms of host dialogue with the microbiota. *Immunol. Rev.* 206:260–76.

Fry, J. (2000). Bacterial diversity and ‘unculturables’. *Microbiology Today* 27, 3.

Gibson, G. R., Cummings, J. H. & MacFarlane, G. T. (1991). Growth and activities of sulphate-reducing bacteria in gut contents of healthy subjects and patients with ulcerative colitis. *FEMS Microbiol Ecol* 86, 103–112.

Griffiths, R. I., Whiteley, A. S., O'Donnell, A. G. & Bailey, M. J. (2000). Rapid method for coextraction of DNA and RNA from natural environments for analysis of ribosomal DNA- and rRNA-based microbial community composition. *Applied and Environmental Microbiology* 66(12):5488–5491.

Harmsen, H.J.M., Elfferich, P., Schut, F., Welling, G.W. (1999). A 16S rRNA-targeted probe for detection of *Lactobacilli* and *Enterococci* in fecal samples by fluorescent in situ hybridization. *Microbiol. Ecol. Health Dis.* 11, 3–12.

- Harmsen H. J. M. et al. (2000b). Development of 16S rRNA-based probes for the *Coriobacterium* group and the *Atopobium* cluster and their application for enumeration of *Coriobacteriaceae* in human feces from volunteers of different age groups. *Appl. Environ. Microbiol.* 66:4523–4527.
- Harmsen, H.J., Raangs, G.C., He, T., Degener, J.E., and Welling, G.W. (2002). Extensive set of 16S rRNA-based probes for detection of bacteria in human feces. *Appl Environ Microbiol* 68:2982–2990.
- Hold, G. L., A. Schwiertz, R. I. Aminov, M. Blaut, and H. J. Flint. (2003). Oligonucleotide probes that detect quantitatively significant groups of butyrate-producing bacteria in human feces. *Appl. Environ. Microbiol.* 69:4320-4324.
- Johansson MEV, Gustafsson JK, Sjöberg KE, Petersson J, Holm L, Sjövall H et al (2010). Bacteria penetrate the inner mucus layer before inflammation in the dextran sulfate colitis model. *PLoS ONE* 5:e12238.
- Kimball, S., Mattis, P. & the GIMP Development Team (2010). GNU Image Manipulation Program.
- Kitakima S, Takuma S, Morimoto M (1999). Changes in colonic mucosal permeability in mouse colitis induced with dextran sulfate sodium. *Exp Anim* 48:137-14.
- Kühn R, Löhler J, Rennick D, Rajewsky K, Müller W (1993). Interleukin-10-deficient mice develop chronic enterocolitis. *Cell* 75:263-274.
- Kuypers, M. M., and Jorgensen, B. B. (2007). The future of single-cell environmental microbiology. *Environ Microbiol* 9, 6-7.
- Langendijk PS, Schut F, Jansen GJ, Raangs GC, Kamphuis GR, Wilkinson MH, Welling GW. (1995) Quantitative fluorescence in situ hybridization of *Bifidobacterium* spp. with genus-specific 16S rRNA-targeted probes and its application in fecal samples. *Appl Environ Microbiol.* 61(8):3069-75.

Lay, C. et al. (2005). Design and validation of 16S rRNA probes to enumerate members of the *Clostridium leptum* subgroup in human faecal microbiota. *Environmental Microbiology*, 7:933–946.

Lee IA, Bae EA, Hyun YJ, Kim DH. (2010). Dextran sulfate sodium and 2,4,6-trinitrobenzene sulfonic acid induce lipid peroxidation by the proliferation of intestinal gram-negative bacteria in mice. *J Inflamm (Lond)*. 7:7.

Li, T., Wu, T. D., Mazeas, L., Toffin, L., Guerquin-Kern, J. L., Leblon, G., and Bouchez T. (2008). Simultaneous analysis of microbial identity and function using NanoSIMS. *Environ Microbiol* 10, 580-588.

Loy A, Arnold R, Tischler P, Rattei T, Wagner M, Horn M. (2008) probeCheck--a central resource for evaluating oligonucleotide probe coverage and specificity. *Environ. Microbiol.* 10(10):2894-8.

Ludwig, W., Strunk, O., Klugbauer, S., Klugbauer, N., Weizenegger, M., Neumaier, J., Bachleitner, M., and Schleifer, K. H. (1998). Bacterial phylogeny based on comparative sequence analysis. *Electrophoresis* 19, 554-568.

Ludwig, W., Strunk, O., Westram, R., Richter, L., Meier, H., Yadhukumar, Buchner, A., Lai, T., Steppi, S., Jobb, G., et al. (2004). ARB: a software environment for sequence data. *Nucleic Acids Res* 32, 1363-1371.

Macdonald, T. T. & Monteleone, G. (2005). Immunity, inflammation, and allergy in the gut. *Science* 307, 1920–1955

Manz W., Amann R., Ludwig W., Vancanneyt M., Schleifer K. H. (1996). Application of a suite of 16S rRNA-specific oligonucleotide probes designed to investigate bacteria of the phylum *Cytophaga-Flavobacter-Bacteroides* in the natural environment. *Microbiology* 142(Pt. 5):1097–1106.

Meraz MA, White JM, Sheehan KCF, Bach EA, Rodig SJ, Dighe AS et al. (1996). Targeted disruption of the STAT1 gene in mice reveals unexpected physiologic specificity in the JAK-STAT signaling pathway. *Cell* 84:431-442.

Momose, Y., Park, S., Miyamoto, Y. and Itoh, K. (2011). Design of species-specific oligonucleotide probes for the detection of *Bacteroides* and *Parabacteroides* by fluorescence in situ hybridization and their application to the analysis of mouse caecal *Bacteroides*–*Parabacteroides* microbiota. *Journal of Applied Microbiology*, 111:176–184.

Mueller C, Macpherson AJ (2006). Layers of mutualism with commensal bacteria protect us from intestinal inflammation. *Gut* 55:276-284.

Musat, N., Halm, H., Winterholler, B., Hoppe, P., Peduzzi, S., Hillion, F., Horreard, F., Amann, R., Jorgensen, B. B., and Kuypers, M. M. (2008). A single-cell view on the ecophysiology of anaerobic phototrophic bacteria. *Proc Natl Acad Sci USA* 105, 17861-17866.

Nagalingam NA, Kao JY, Young VB (2011). Microbial ecology of the murine gut associated with the development of dextran sodium sulfate-induced colitis. *Inflamm Bowel Dis* 17: 917-926.

Nell S, Suerbaum S, Josenhans C (2010). The impact of the microbiota on the pathogenesis of IBD: lessons from mouse infection models. *Nat Rev Micro* 8:564-577.

Okayasu I, Hatakeyama S, Yamada M, Ohkusa T, Inagaki Y, Nakaya R (1990). A novel method in the induction of reliable experimental acute and chronic ulcerative colitis in mice. *Gastroenterology* 98:694-702.

Orphan, V. J., House, C. H., Hinrichs, K. U., McKeegan, K. D., and DeLong, E. F. (2001). Methane-consuming archaea revealed by directly coupled isotopic and phylogenetic analysis. *Science* 293, 484-487.

Pitcher, M. C. L. & Cummings, J. H. (1996). Hydrogen sulphide: a bacterial toxin in ulcerative colitis? *Gut* 39, 1–4.

Postgate, J. R. (1984a). The Sulphate-reducing Bacteria, 2nd ed. Cambridge: Cambridge University Press.

R. J. Xavier, D. K. Podolsky (2007). Unravelling the pathogenesis of inflammatory bowel disease. *Nature* 448, 427-434

Reiff C, Kelly D (2010). Inflammatory bowel disease, gut bacteria and probiotic therapy. *Int J Med Microbiol* 300:25-33.

Rigottier-Gois L, Rochet V, Garrec N, et al. Enumeration of *Bacteroides* species in human faeces by fluorescent in situ hybridisation combined with flow cytometry using 16S rRNA probes. *Syst Appl Microbiol*. 2003; 26:110–118.

Robertson BR, O'Rourke JL, Neilan BA, Vandamme P, On SL, Fox JG, Lee A. (2005) *Mucispirillum schaedleri* gen. nov., sp. nov., a spiral-shaped bacterium colonizing the mucus layer of the gastrointestinal tract of laboratory rodents. *Int J Syst Evol Microbiol*. 55(Pt 3):1199-204.

Romagnani P, Annunziato F, Baccari MC, Parronchi P (1997). T cells and cytokines in Crohn's disease. *Curr Opin Immunol*. 9(6):793-9.

Rossello-Mora, R., and Amann, R. (2001). The species concept for prokaryotes. *FEMS Microbiol Rev* 25, 39-67.

Roszak, D. B., and Colwell, R. R. (1987). Survival strategies of bacteria in the natural environment. *Microbiol Rev* 51, 365-379.

Sartor RB (2004). Therapeutic manipulation of the enteric microflora in inflammatory bowel diseases: antibiotics, probiotics, and prebiotics. *Gastroenterology* 126:1620–33.

Schleifer, K. H. (2004). Microbial diversity: facts, problems and prospects. *Syst Appl Microbiol* 27, 3-9.

Schwartz et al., (2000). Quantification of Different *Eubacterium* spp. in Human Fecal Samples with Species-Specific 16S rRNA-Targeted Oligonucleotide Probes. Appl. Environ. Microbiol. 66: 375-382.

Sghir A. et al. (2000). Quantification of bacterial groups within human fecal flora by oligonucleotide probe hybridization. Appl. Environ. Microbiol. 66:2263–2266.

Staley, J. T., and Konopka, A. (1985). Measurement of in situ activities of nonphotosynthetic microorganisms in aquatic and terrestrial habitats. Annu Rev Microbiol 39, 321-346.

Strober W, Fuss IJ, Blumberg RS (2002). The immunology of mucosal models of inflammation. Annu. Rev. Immunol. 20:495–549

Suau A et al.(2001). *Fusobacterium prausnitzii* and related species represent a dominant group within the human fecal flora. Syst Appl Microbiol 24:139–145.

Wagner, M. (2009). Single-cell ecophysiology of microbes as revealed by Raman microspectroscopy or secondary ion mass spectrometry imaging. Annu Rev Microbiol 63:411-429.

Wagner, M., Horn, M., and Daims, H. (2003). Fluorescence in situ hybridisation for the identification and characterisation of prokaryotes. Curr Opin Microbiol 6, 302-309.

Walker, A. W., S. H. Duncan, E. C. McWilliam Leitch, M. W. Child, and H. J. Flint. (2005). pH and peptide supply can radically alter bacterial populations and short-chain fatty acid ratios within microbial communities from the human colon. Appl. Environ. Microbiol. 71:3692-3700.

Wallner, G., Amann, R. and Beisker, W. (1993). Optimizing fluorescent in situ hybridization with rRNA-targeted oligonucleotide probes for flow cytometric identification of microorganisms. Cytometry, 14:136–143.

I Acknowledgement

My greatest thanks go to Dr. David Berry for his great and supportive guidance throughout my research career as diploma student. I'm thankful for the freedom he rendered me and for the skills he passed on. I sincerely thank him for all his help.

I also want to thank:

Dr. Alexander Loy for being a member of his group

Prof. Dr. Michael Wagner (Head of the Department) for the possibility to do my diploma thesis at the Department of Microbial Ecology (DOME)

Arno Schintlmeister (Core Facility NanoSIMS) for his patience answering all my questions regarding the NanoSIMS device and its technical background

Mag. Daniela Gruber (Core Facility Cell Imaging and Ultrastructure Research) for introducing me to the Ultracut Microtome and support during my work

Allen, Andreas, Bela, Christoph, Faris, Julia, Karim, Martina and Thomas S. for a very good working atmosphere and the fun especially at coffee breaks and BBQ-parties on the rooftop.

All the other members of DOME who shared their lab experiences and always had time for my questions. Especially Dr. Celine Lesaulnier, who gave me a helping hand when reagents were out of stock.

Adela for her strong support and encouragement.

This work was financially supported by the Austrian Federal Ministry of Science and Research (GEN-AU III InflammoBiota).

J Curriculum Vitae

Jochen Reichert

Personal data

Date of birth	July 27, 1986
Place of birth	Neunkirchen, Austria
Nationality	Austria

Education

1992 – 1996	Volksschule Neunkirchen
1996 – 2004	Bundesrealgymnasium Neunkirchen
2004 – 2005	Präsenzdienst
since 2005	Study of biology with focus on genetics and microbiology, University of Vienna, Vienna, Austria
since November 2010	Diploma thesis at the Department of Microbial Ecology, University of Vienna, Vienna, Austria